CHAPTER ONE

INTRODUCTION

1.1. Background of the Study

Tuberculosis (TB), a bacterial infection commonly expressed in the respiratory tract, is the leading infectious killer worldwide (Amy et al, 2008); it is estimated that one-third of the world's population is currently infected with TB, and it results in 3 million deaths every year (WHO, 2005). Human Immunodeficiency Virus (HIV) is a strong risk factor for developing active TB, and TB is the leading cause of death among HIV-positive individuals. Of 4.1 million AIDS deaths in 2004, 13% can be attributed to TB (WHO, 2005).

Tuberculosis (TB) mainly presents as a pulmonary disease caused by infection with Mycobacterium Tuberculosis (M-TB). The initial infection usually occurs in the lungs and in most cases is controlled by the immune system. Even after successful control of primary TB infection, some bacilli remain in a non- or slowing replicating state, termed latent TB infection (LTBI). Latently infected individuals have a 10% risk of developing the disease in their lifetime (WHO, 2012), which constitutes a huge global reservoir of infection and a continuous threat of disease transmission.

Tuberculosis (TB) is an airborne disease caused by the bacterium Mycobacterium Tuberculosis (M-TB). This causative agent of TB is one of the world's most devastating human pathogens. The contagious disease is transmitted through air and most commonly affects the lungs, but can also attack other parts of the body,

such as the brain, spine or kidneys, which is responsible for more than 75% of cases (De Souza, 2006).

Several reviews so far have been reported the incidences of TB cases, a particular report surveyed that out of 134 countries only 35 showed declination of cases of around 5% per year based on per capita rate (Lonnroth et al, 2009). This survey considered the data from 1998 to 2007. Different surveillance analysis and mathematical modeling studies recommended reduction of TB incidences per capita is around 1% per year, further suggesting diminution of cases by 2015 (Adeeb et al, 2013). It is being predicted that growth of the world population of approximately 2% per year may be an important reason for increment of TB cases (WHO, 2009). All these previous reports showing the presence of lacunae in the existing management approaches for TB and the inadequate effectiveness of public health systems, with special reference to underdeveloped countries. In spite of the availability of anti-TB drugs developed over the last five decades, one-third of the world's population retains a dormant or latent form of Mycobacterium Tuberculosis (Corbett et al, 2003).

The highest incidence of TB is in Sub-Saharan Africa, in part due to interaction with Human Immunodeficiency Virus (HIV) (Nunn et al, 2005; Corbett et al, 2006; Maartens and Wilkinson, 2007), which has fuelled dramatic rises in incidence of the disease in many countries. [Globally, TB is the proximate cause of many HIV-related deaths, particularly in Africa (Corbett et al, 2006)]. Even in many countries where its overall incidence is low, TB remains a problem. To compound the problem further, the deadly association with HIV makes the treatment of co-infected patients even more challenging (WHO, 2009; Nunes et al, 2011).

Much research has been and is still on, on the subject with a cure not yet in view. The choice to approach this issue via the vehicle of surface thermodynamics against the conventional clinical methods is a novel one. The role of surface properties in this biological process will be established.

In this study, M-TB is conceptualized as particle dispersed in a liquid (the sputum) and interacting with another particle (macrophage). The bacterium attaches itself on the surface of the macrophage cell before penetrating and attacking it. If the surface of the macrophage cell is such that it will repel the bacteria, access of the bacteria into the alveoli of the cell would have been denied. Thus the initial actions actually take place on the surface of the cell and of the bacteria.

It is a well-known fact that surface property determination of interacting particles lead to the further understanding of the mechanism of interactions. A common area of contact is established once two particles meet each other. In such process, a certain portion of each particle gets displaced through work. Work responsible for the displacement of a unit area is known as surface free energy. The consecutive impact on the surface is known as surface thermodynamic effects. To attain the equilibrium such impacts are changed in a slow pace. In this particular study similar concepts have been implemented to characterize the M-TB – macrophage interactions with the sputum as the intervening medium.

1.2. Pathogenesis of Tuberculosis

Infection occurs when a person inhales droplet nuclei containing tubercle bacilli that reach the alveoli of the lungs. These tubercle bacilli are ingested by alveolar macrophages; the majority of these bacilli are destroyed or inhibited.

A small number may multiply intracellular and are released when the macrophages die. If alive, these bacilli may spread by way of lymphatic channels or through the blood stream to more distant tissues or organs (including area of the body in which TB disease is most likely to develop: regional lymph nodes, apex of the lung, kidneys, brain, and bone). This process of dissemination primes the immune system for a systemic response.

1.3. Statement of Problem

The World Health Organization (WHO) declared tuberculosis (TB) as a global emergency in 1993. Unfortunately, the efforts made by the impede TB Strategy were not enough to impede the occurrence of 1.3 million deaths in 2009 (WHO, 2010). However, WHO estimates that the number of cases per capita peaked at 2004 and is slowly falling (WHO, 2009). Nonetheless, the battle against TB is far from being over, since Mycobacterium tuberculosis (the main causative agent of TB) proved to be highly adaptive (Kumar and Rao, 2011) and capable of evading the current strategies for treatment of about half million cases of multi-drug-resistant TB (MDR-TB) that were reported in 2007, including cases of extensively drug-resistant TB (XDR-TB) (WHO, 2009), and the more recently reported totally drug-resistant strains (TDR-TB) (Nunes et al, 2011; Velayati et al, 2009; Velayati et al, 2009).

Mycobacterium TB is among the world's most deadly infectious diseases despite the long-standing availability of some effective treatment. The steady emergence of multi-drug resistant (MDR), extremely drug-resistant (XDR) and totally drug-resistant strains (TDR) forms of TB is a cause of concern. Globally MDR-TB accounts for roughly 3.6% of all TB cases, but accounts for up to 28% of TB cases

in some regions (De Souza, 2006; Gonzalez-Juarrero et al, 2001). The emergence of MDR, XDR and TDR TB is very worrying due to the increasing difficulty of treating these forms of TB and rendering even the frontline drugs inactive.

In addition, drugs such as Rifampicin have high levels of adverse effects making them prone to patient incompliance. Another important problem with most of the anti-mycobacterials is their inability to act upon latent forms of the bacillus. To compound the problems further, the complex (vicious) interactions between the HIV and TB makes the treatment of co-infected patients even more challenging (Nunes et al, 2011; Gonzalez-Juarrero et al, 2001).

It is against this backdrop that this study explores a novel and rare approach using interfacial free energy approach to seek a way forward in the research on the topic of mycobacterium tuberculosis human sputum interaction.

1.4. Aim and Objectives

This research work is aimed at employing the concept of surface thermodynamics to evaluate the effects of the bacterium on HIV infected blood with a view to avoiding bacteria penetration.

The following objectives were pursued;

- To determine the M-TB infection level in the blood.
- To determine the HIV infection status of the blood samples.
- To correlate the HIV infection status with M-TB infection using surface thermodynamics energetics.

- To determine the change in free energies of adhesion for both infected sputum and uninfected Sputum.
- To model the level of the HIV infection with the level of M-TB prevalence.

1.5. Significance of the Study

Surface energies approach is a very important thermodynamics tool used in determining the absolute and combined Hamaker coefficients of M-TB/HIV-Human sputum interaction processes. The Lifshiftz derivation for van der Waals forces is used to model the interaction and the surface energies and surface free energies of adhesion obtained by this method will be used to predict the nature of surface interactions between two solid particles suspended in a liquid medium. When the absolute combined Hamaker coefficient is positive, the attractive van der Waals forces between the M-TB/HIV-Macrophage prevail. In addition, when absolute combined Hamaker is negative, the van der Waals forces become repulsive and separation is predicted in the system. Therefore, any intermediary or condition that will render the absolute combined Hamaker coefficient negative will be recommended to the pharmaceutical industries as choice solution to the treatment of M-TB/HIV infection from surface thermodynamics point of view. Under this condition of separation, the bacteria will not be ingested by the macrophages and so will not have the opportunity to overcome the immune system and multiply.

1.6. Scope of the Study

The scope of the work is limited to twenty samples each of TB infected and uninfected sputum and twenty M-TB/HIV sputum obtained from Anambra State University Teaching Hospital Awka. The absorbance will be measured on these sputum samples and the results will be used to determine the various interfacial energies. The absorbance data will also be used to estimate the Hamaker coefficient and hence predict the interaction between the M-TB/HIV and its host.

This is intended to be achieved by the application of surface thermodynamics using the concept of Hamaker. The scope of the work is limited to specifying the relevance of van der Waals forces to the fusion of the M-TB/HIV with the host and how such fusion process could be quantified and prevented. Hamaker Coefficients derived from absorbance data required for the computation of the Lifshitz formula. The next approach would be to suggest a formulation that would aid in preventing contact between the M-TB/HIV and the host, and hence prevent their interactions.

However, reasonable suggestions can be made to integrate the clinical approach to the surface thermodynamic in providing solution to M-TB/HIV infections association.

Sourcing for additives to achieve this aim is beyond the scope of this work. Other approach for the determination of Hamaker coefficients, e.g. by contact angle data, will not be considered. These will serve as suggested areas for further research.

CHAPTER TWO

LITERATURE REVIEW

A good number of research works on surface thermodynamics have been done in the past. A couple of these works will be briefly referred to and deductions that would give a sound grip to this research extracted. In concluding the literature review, a summary of the proposed study, combinations of approaches used, benefits as well as its knowledge gap are established.

2.1. Mycobacterium Tuberculosis and Transmission of Tuberculosis

Tuberculosis is an airborne disease caused by the bacterium Mycobacterium tuberculosis (M-TB) (figure 2.1). Mycobacterium tuberculosis and seven very closely related mycobacterial species (M. bovis, M. africanum, M. microti, M. caprae, M. pinnipedii, M. canetti and M. mungi) together comprise what is known as the Mycobacterium tuberculosis complex. Most, but not all, of these species have been found to cause disease in humans. The majority of TB cases are caused by Mycobacterium tuberculosis. Mycobacterium tuberculosis organisms are also called tubercle bacilli (American Thoracic Society, 2000).

A small number of tubercle bacilli enter the bloodstream and spread throughout the body. The tubercle bacilli may reach any part of the body; including areas where TB disease is more likely to develop (such as the brain, larynx, lymph node, lung, spine, bone, or kidney) (figure 2.3c).

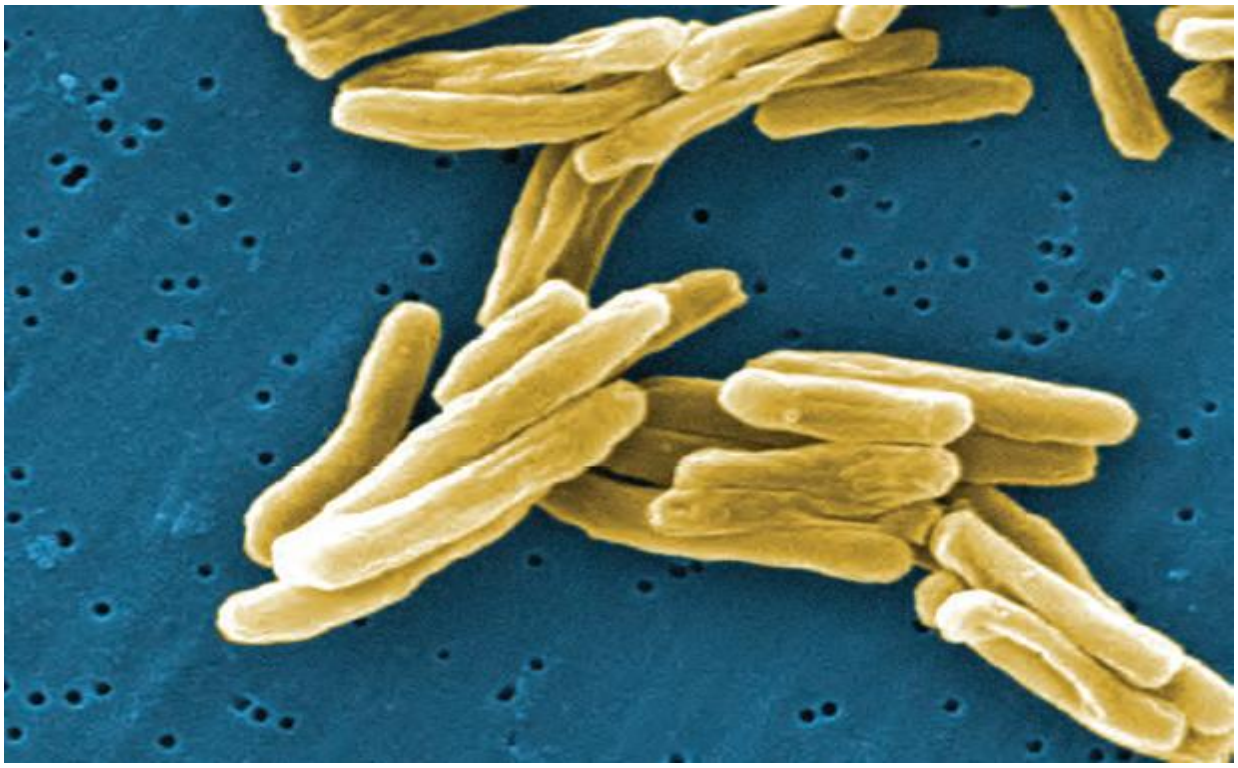

Fig. 2.1: Mycobacterium Tuberculosis *(American Thoracic Society, 2000)*

Mycobacterium tuberculosis is carried in airborne particles, called droplet nuclei, of 1 – 5 microns in diameter. Infectious droplet nuclei are generated when persons who have pulmonary or laryngeal TB disease cough, sneeze, shout, or sing. Depending on the environment, these tiny particles can remain suspended in the air for several hours. Mycobacterium tuberculosis is transmitted through the air, not by surface contact. Transmission occurs when a person inhales droplet nuclei containing M-TB, and the droplet nuclei traverse the mouth or nasal passages, upper respiratory tract, and bronchi to reach the Aveoli of the lungs (American Thoracic Society, 2007) (see figure 2.3).

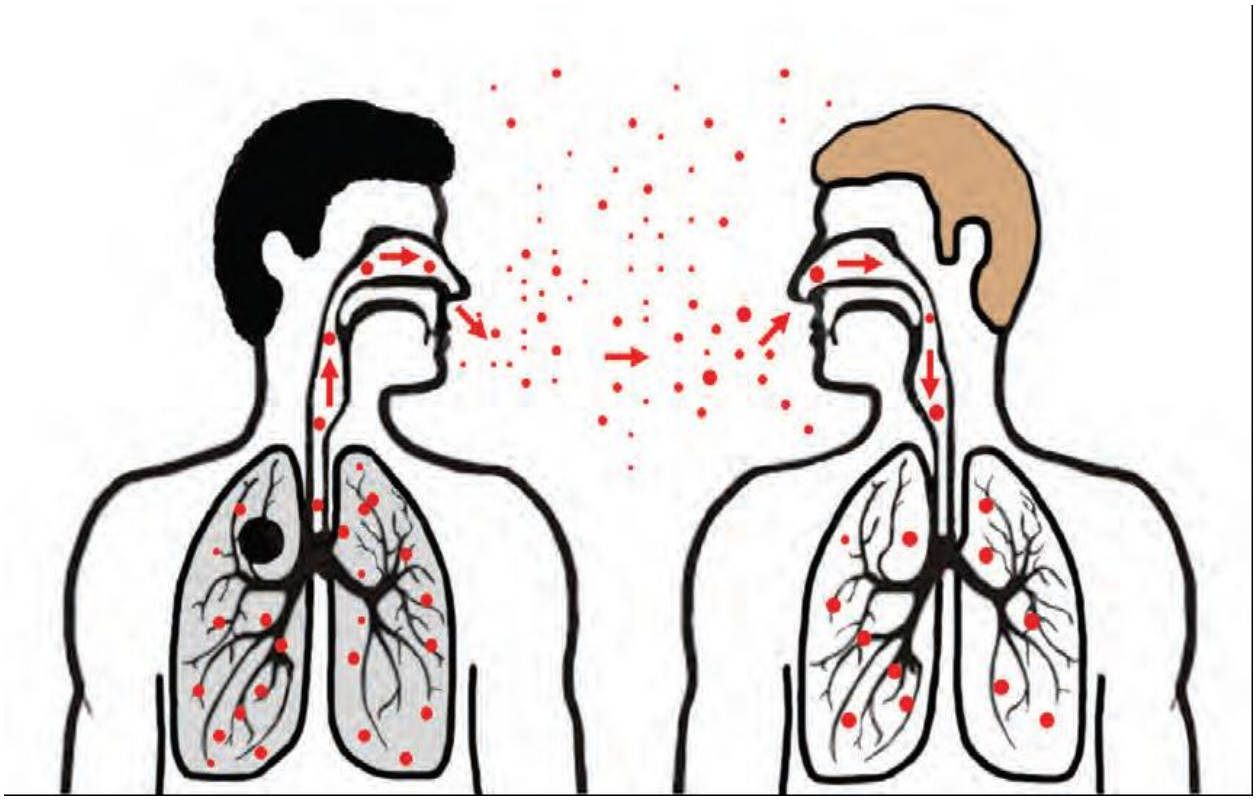

Fig.2.2: Transmission of Tuberculosis *(American Thoracic Society, 2000)*

(a) Droplet nuclei containing tubercle bacilli are inhaled, enter the lungs, and travel to the alveoli.

(b) Tubercle bacilli multiply in the alveoli.

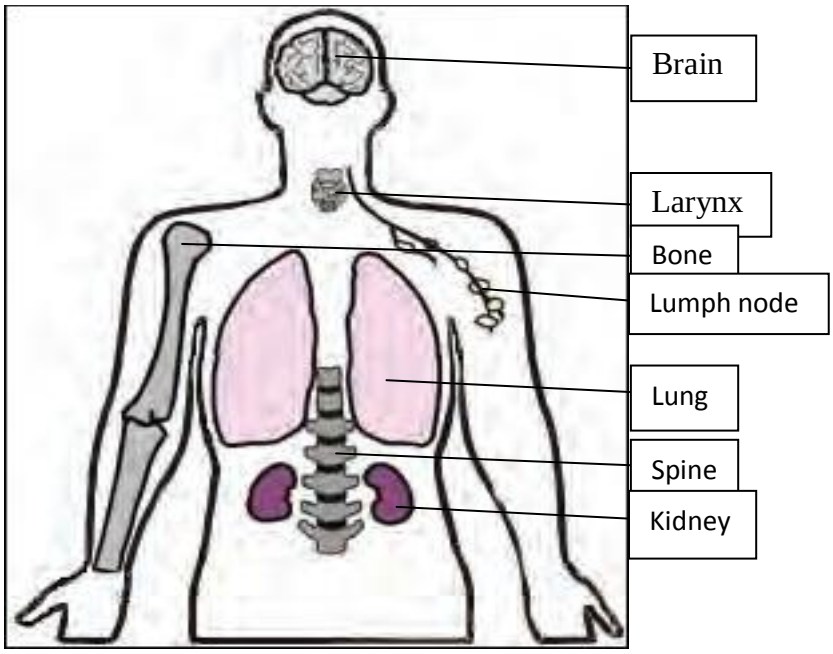

(c) A small number of tubercle bacilli enter the bloodstream and spread throughout the body. The tubercle bacilli may reach any part of the body, including areas where TB disease is more likely to develop (such as the brain, larynx, lymph node, lung, spine, bone, or kidney).

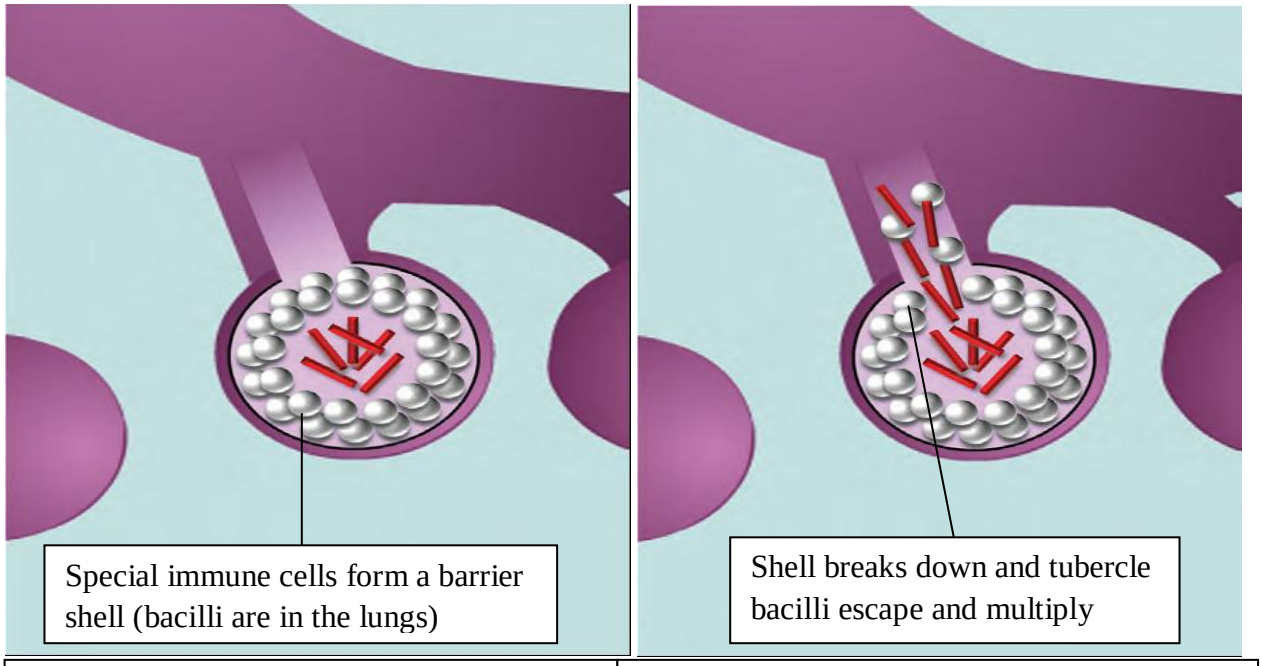

(d) Within 2 to 8 weeks, special immune cells called macrophages ingest and surround the tubercle bacilli. The cells form a barrier shell, called a granuloma, that keeps the bacilli contained and under control (LTBI)	(e) If the immune system cannot keep the tubercle bacilli under control, the bacilli begin to multiply rapidly (TB disease). This process can occur in different areas in the body, such as the lungs, kidneys, brain, or bone (see Fig.1.3 C).

Fig. 2.3(a-e): Pathogenesis of LTBI and TB *(American Thoracic Society, 2007)*

There are four factors that determine the probability of transmission of M. tuberculosis (American Thoracic Society, 2007) (see table 2.1).

Table 2.1: Factors that Determine the Probability of Transmission of M-TB
(American Thoracic Society, 2007)

S/N	FACTOR	DESCRIPTION
1	Susceptibility	Susceptibility (Immune status) of the exposed individual.
2	Infectiousness	Infectiousness of the person with TB disease is directly related to the number of tubercle bacilli that he or she expels into the air. Persons who expel many tubercle bacilli are more infectious than patients who expel few or no bacilli.
3	Environmental	Environmental factors that affect the concentration of M-TB organisms.
4	Exposure	Proximity, frequency, and duration of exposure.

2.1.1. Latent Tuberculosis Infection (LTBI)

Persons with LTBI have M-TB in their bodies, but do not have TB disease and cannot spread the infection to other people. A person with LTBI is not regarded as having a case of TB. The process of LTBI begins when extracellular bacilli are ingested by macrophages and presented to other white blood cells. This triggers the immune response in which white blood cells kill or encapsulate most of the bacilli, leading to the formation of a granuloma. At this point, LTBI has been established. LTBI may be detected by using the tuberculin skin test (TST) or an interferon-gamma release assay (IGRA). It can take 2 to 8 weeks after the initial TB infection for the body's immune system to be able to react to tuberculin and for the infection to be detected by the TST or IGRA. Within weeks after infection, the immune

system is usually able to halt the multiplication of the tubercle bacilli, preventing further progression.

2.1.2. Tuberculosis Disease

In some people, the tubercle bacilli overcome the immune system and multiply, resulting in progression from LTBI to TB disease.

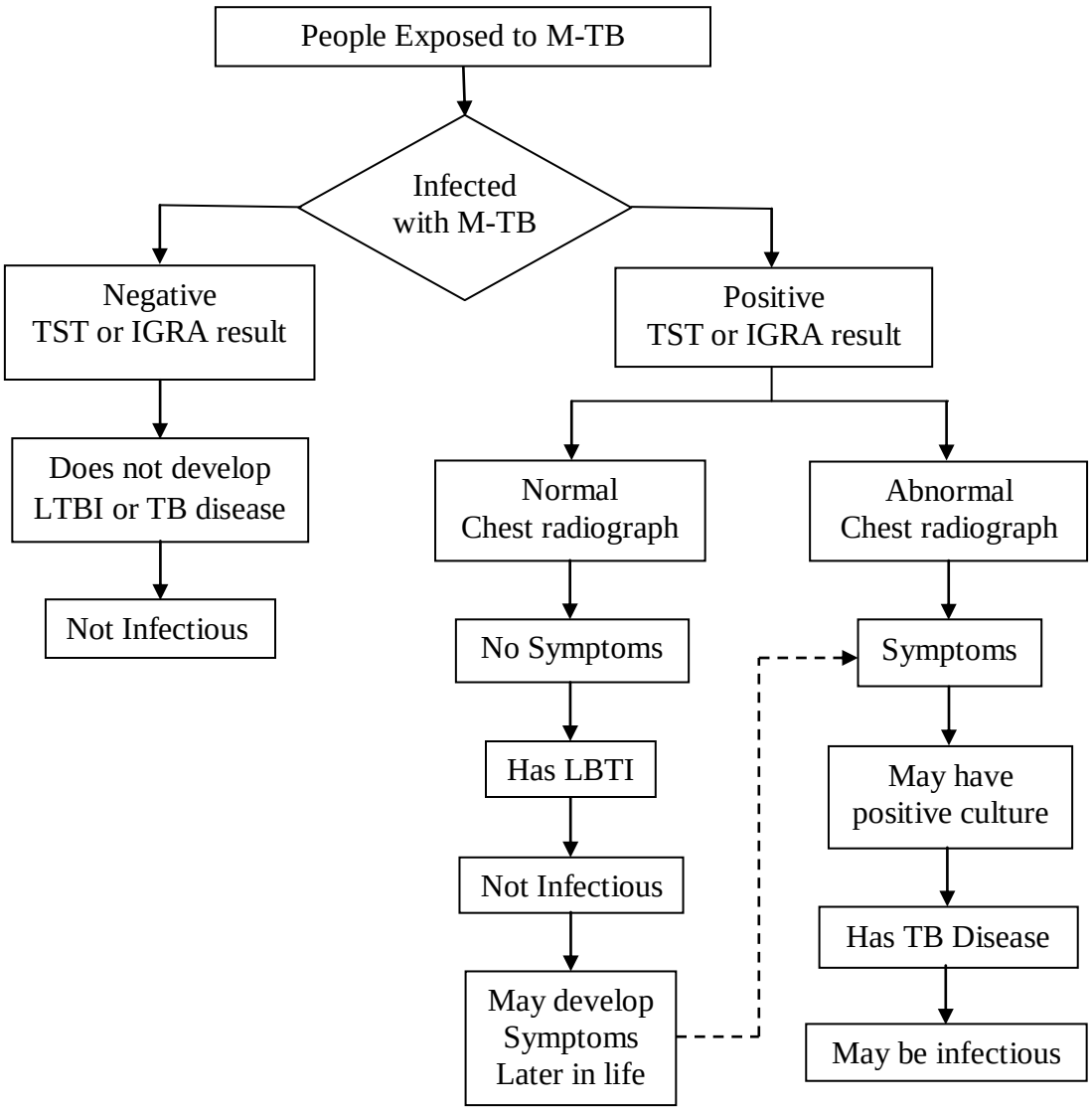

Fig. 2.4: Progression of Tuberculosis *(American Thoracic Society, 2007)*

Persons who have TB disease are usually infectious and may spread the bacteria to other people. The progression from LTBI to TB disease may occur at any time, from soon to many years later. Body fluid or tissue from the disease site should be collected for smear and culture. Positive culture for M-TB confirms the diagnosis of TB disease.

2.2. Immunopathology and M-TB Infection

Mycobacterium TB normally enters the host through the mucosal surface usually via the lung after inhalation of infectious droplets from an infected individual, occasionally via the gut after ingestion of infected material (e.g. Milk – a common route for the TB complex member, Mycobacterium bovis). Either way, the bacteria can be taken up by phagocytic cells that monitor these surfaces, and if not swiftly killed, can invade the host inside these cells. Some heavily M-TB exposed individuals show no signs of infection: no pathology, no symptoms and no apparent adaptive immune response. It is possible that in these cases, the innate immune response has eliminated the pathogen at the earliest stage (see figure 2.5).

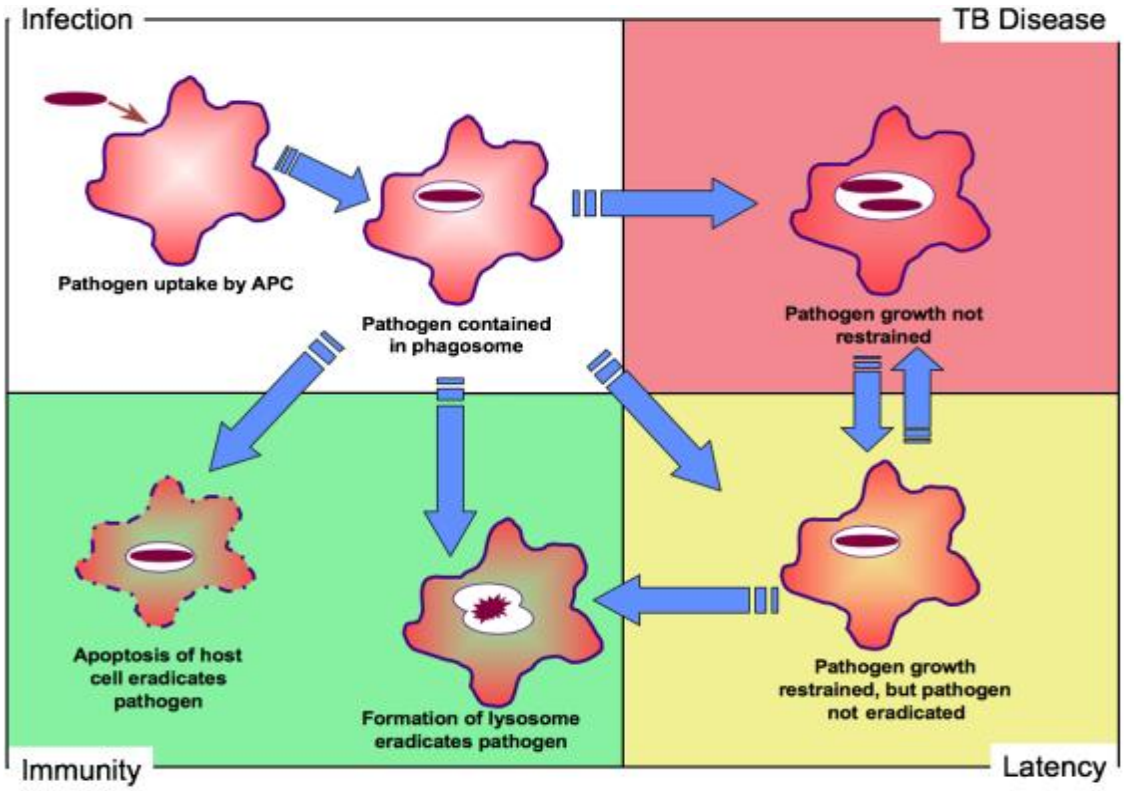

Fig.2.5: A Simple Schematic of the Outcomes of Mycobacterium Tuberculosis Infection at the level of the Infected Host Cell – normally a Macrophage
(Gonzalez-Juarrero et al, 2001)

More commonly, however, ingestion of the bacteria by an antigen presenting cell (APC) rapidly induces an inflammatory response. Cytokine and Chemokine release triggers the swift accumulation of a variety of immune cells and, with time, the formation of a granuloma, characterized by a relatively small number of infected phagocytes, surrounded by activated monocyte/macrophages and, further out, activated lymphocytes (Gonzalez-Juarrero et al, 2001; Dietrich and Doherty, 2009). If the infection is successfully contained at this stage, the granuloma shrinks and may eventually disappear, leaving a small scar or calcification and the patient's T-cells become responsive to M-TB-derived antigens. If, however, the immune response does not successfully control the bacterial replication, the granulomas increase in size and cellularity. Eventually, cell death in the granuloma

leads to necrosis. In this case, if the granuloma is close to the surface of the lung, the tissue destruction caused by necrosis can breach the mucosal surface and the granuloma contents leak into the lumen of the lung – a process referred to as cavitation. This gives rise to the prototypic symptom of TB – a persistent cough with blood in the sputum. At this point, the patient is highly infectious, spreading the bacteria by aerosol.

Tissue destruction in TB is not mediated by the activities of the bacteria alone – it is primarily immunopathological in nature and the crucial point to understand is that an inflammatory immune response is critical for the survival of both the host and the bacteria. It thus appears that M. tuberculosis actively stimulates– and then subverts this response.

2.3. The Immune Response to TB

2.3.1. Humoral Immunity

Immunity due to the formation of circulating antibodies plays a marginal role in TB, as the mycobacteria are resistant to the direct effect of antibodies and their products. However, the existence of these antibodies is the focus of research into new methods of serological diagnosis of TB.

2.3.2. Cellular Immunity

After phagocytosis of tubercle bacilli by the macrophages antigens are liberated from the bacilli (Ait-Khaled and Enarson, 2005; Marchal, 1993; Daniel, 1994). The antigens activate nonspecific lymphocytes, which become specific CD4 and CD8 lymphocytes. These specific lymphocytes are central to TB immunity. Their fundamental role is TB control is demonstrated in studies of HIV-infected

individuals. These individuals have a reduced number of specific circulating lymphocytes, in particular CD4 lymphocytes, which diminish as their disease develops. This is why they are more likely to develop TB following infection.

2.4. Epidemiology of Tuberculosis

Tuberculosis is an infectious disease and progression of TB within the body of a susceptible individual with no history of TB starts with infection with M-TB. The disease can remain latent, become active, or it can progress from latent TB to active TB either by endogenous reactivation or exogenous reinfection. Another way of acquiring TB is through co-infection of TB with other diseases. TB can be treated; however, non compliance to treatment causes drug resistant TB to develop in the individual.

2.4.1. Latent TB Infection and active TB Infection

After infection with M-TB, the symptoms of TB are not immediately observed. An individual is said to have latent TB if such one is infected with M-TB, but not infectious. The latent period is the period from the point of infection to the beginning of the state of infectiousness. When latent TB progresses to active TB, the infectious period starts and the symptoms of TB show up with a delay. An individual with active Tb is both infected and infectious; therefore the individual can spread the disease.

2.4.2. Endogenous reactivation and Exogenous re-infection

The progression from latent TB to active TB occurs in two ways; endogenous reactivation and exogenous re-infection. Endogenous reactivation is the activation of latent TB with M-TB which resides inside the body and had infected the

individual earlier. Exogenous re-infection in which the new M-TB makes the individual infectious, thereby causing the active TB infection. Such infections by more than one type of M-TB pathogen are called “mixed infectious”.

2.4.3. Treatment

Control of TB is managed by two types of treatment. The treatment of latent TB is called “Chemoprophylaxis” and the treatment of active TB is called “Therapentics”. Treatment of TB lasts long; therefore control strategies have been developed for compliance to TB treatment. DOTs (Directly observed treatment, short-course) is a treatment program used for compliance with treatment of drug-sensitive TB. Another control program is DOTs-plus, which is developed for compliance with treatment of drug-resistant TB. A good public health treatment strategy combines different control strategies to control all types of TB infectious.

2.4.4. Drug Resistance

If TB treatment is ineffective or if the patient does not comply to treatment, M-TB may become resistant to first line anti-TB drugs. Drug resistance can either be acquired during treatment or transmitted from individuals infected with drug-resistant strains. An individual develops acquired drug-resistant TB (ADR-TB) due to treatment failure. Spread of TB via individuals infected with drug resistant TB causes the newly-infected individuals to develop resistance always initials an epidemic of drug-resistant TB, but if the drug-resistant pathogen is transmissible, the risk of primary drug resistance increases over time.

2.4.5. Co-infection

Co-infection is the infection of a host by at least two different types of pathogens. TB and HIV dynamics have a correlation, as HIV weakens the immune system of the host, which creates a proper medium for M-TB to infect the host. Therefore, in areas with high HIV prevalence, TB is one of the main causes of death.

2.4.6. HIV-related TB

HIV Infection and Risk of TB: HIV increases a person's susceptibility to infection with M-TB. In a person infected with M-TB, HIV is a potent cause of progression of TB infection to disease. Consider an individual infected with M-TB, the effect of HIV infection on lifetime risk of developing TB is about 50% positive.

Consequences of M-TB/HIV Co-infection: Compared to an individual who is not infected with HIV, an infected individual has a 10 times increased risk of developing TB. TB notifications have increased in populations where both HIV infection and M-TB infection are common (e.g. some parts of Sub-Saharan Africa have seen a tripling in the number of notifications over the past decade). HIV seroprevalence in these TB patients is upto 70%. In Sub-Saharan Africa, one third or more of HIV-infected people may develop TB.

Patterns of HIV-related TB: As HIV infection progresses, CD4+ lymphocytes decline in number and function. The immune system is less able to prevent the growth and local spread of M-TB.

2.5. Incidence and Prevalence

Tuberculosis incidence and prevalence are central to the rate of TB transmission. TB incidence is the rate of appearance of new TB cases per unit time. TB prevalence is the proportion of infected individuals at one point in time, or over a short time period. The measurement of incidence and prevalence is often based on stratification of the population by a variety of factors, such as age, ethnicity, etc.

2.6. Effects of HIV-1 Infection on Latent Tuberculosis

The impact that HIV-1 infection has on persons with latent tuberculosis was examined in (Bauer et al., 2008) and a mathematical model of an adaptive immune response in the lung which considers relevant immune effectors such as macrophages, various sub-populations of T-cells and key cytokines to predict which mechanisms are important to HIV-1infection induced reactivation of tuberculosis. The model shows that persons latently infected with TB who are subsequently co-infected with HIV-1 will suffer reactive TB. The mechanisms that contribute to this are essentially related to a completely different cytokine environment at the onset of HIV-1 infection due to the presence of M-TB. The model shows that macrophage plays an important role during co-infection and decrease in macrophage counts are coupled to a decline in $CD4^+$ T-cells and increased viral loads. These mechanisms are also coupled to lower recruitment of T-cells and macrophages, comprising protective immunity in the lung and eventually leading to TB reactivation. Their results point to potential targets for drug and vaccine therapies.

The above model was purely on immune response in the lungs and mechanisms. De Riener et al., (2007) explained epidemiologic study of TB and they showed that HIV infection increases the risk for reactivation of latent infection and for exogenous infection. Toosi et al, (2001) assessed plasma viral load in HIV-1 infected patients with pulmonary TB (HIV/TB) and non-TB symptomatic HIV-1 infected patients (HIV). Toosi et al, (2001) noted in their work that HIV-1 load was higher in HIV/TB compared with HIV at higher CD4 counts (>500/μl) ($P<0.01$), but not at lower CD4 counts (<500μl). Therefore during active TB, HIV-1 transcriptional activity is increased in both the cellular and accellular (serum) compartments of the blood. Toosi et al, (2001) also assessed the expression of cytokines in cellular from HIV/TB and HIV subjects. Their results show that the pathogenesis of TB during HIV-1 infection includes both reactivation of prior M-TB infection, and progressive primary M-TB infection. TB in early HIV-1 disease resembles reactivation disease, and thus is most amenable to preventive therapy.

Nonlinear mathematical model to study the effect of tuberculosis on the spread of HIV infection was presented by (Naresh et al., 2009). In their study, the model exhibits for equilibrium namely, a disease free, HIV free, TB free and an endemic equilibrium. The model was studied qualitatively using stability theory of nonlinear differential equations and computer simulation. Naresh et al., (2009) found a threshold parameter R_o which is if less than one, the disease free equilibrium is locally asymptotically stable otherwise for $R_o > 1$, at least one of the infections will be present in the population. The model showed that the positive endemic equilibrium is always locally stable but it may become globally stable under certain conditions showing that the disease becomes endemic. In their study, Naresh et al, (2009) found that as the number of TB infective decreases due to recovery, the number of HIV infective also decreases and endemic equilibrium

tends to TB free equilibrium. It is also observed that number of AIDS individuals decreased if TB is not associated with HIV infection.

2.7. Mycobacterial Infections in HIV Patients

Human Immunodeficiency Virus type 1 (HIV-1) is one of the leading global health problem caused by an infectious agent. According to a recent World Health Organization (WHO) report there were approximately 34 million people living with HIV in 2010 (WHO, 2011). There were also 2.7 million new cases and 1.8 million AIDS deaths in 2010. WHO reported that HIV patients experience increasing immunodeficiency due to loss of $CD4^+$ T helper cells and are prone to opportunistic infections by a range of pathogens. The majority of complications are caused by co-infections with mycobacterial. WHO estimated that more than 10 million HIV infected people are co-infected with M-TB, the causative agent of tuberculosis. WHO, (2012) suggested that co-infected individuals are 21 to 34 items more likely to develop active TB disease than people without HIV. About 25% of death among people living with HIV is attributed to TB (WHO, 2012).

After infection with HIV, $CD4_+$ T cell numbers slowly decline over time. During this period, $CD4^+$ T cell counts of patients are regularly monitored and in case $CD4^+$ T cell counts fall below a certain threshold, highly active antiretroviral therapy (HAART) is initiated. Even though antiretroviral treatment is associated with significant reduction on the incidence of M-TB (Badri et al, 2002), the risk still remains higher in treated patients compared to HIV uninfected individuals (Girardi et al, 2004). Moreover, unlike other opportunistic pathogens M-TB causes disease early in the course of HIV infection in patients with relatively normal CD4 count (Sonnenberg et al, 2005). This suggests that there is a qualitative defect in

immune response to M-TB, independent of the total CD4 count. This defect could be on cell of inmate or adaptive immunity.

Sonnerberg et al., (2005) suggest that as CD4 T-cells are crucial to control of mycobacterial infections, analyzing the effect of underlying HIV-1 infection on function of CD4 T cells may lead to a better understanding of the mechanism of increased susceptibility of HIV patients to M-TB.

2.8. Effects of HIV on the M-TB Granuloma

Collin and JoAnne, (2011) reported that the increase in pathology associated with HIV-M-TB coinfection is caused by a functional disruption of the local immune response within the granuloma. These disruptions presumably decreases, the ability of the granuloma to contain M-TB, leading to increased bacterial growth with more mycobacterial dissemination and severe pathology. Bezuidenhout et al, (2009); Lawn et al, (2002); Safi et al, (2003) divided the cause of the disruption into general and overlapping processes including (i) and increase in the viral load within involved tissue, leading to (ii) a decrease in the total number of CD4T-cells, along with (iii) a disruption of macrophage function and (iv) a perturbation of M-TB specific T-cell function that lead to functional and detrimental changes within granulomas.

2.9. HIV-Mycobacterium TB Pathology

Sonnerberg et al., (2005); Whelen, et al., (2000); Glynn et al., (2008) established that HIV impairs the ability to control M-TB infection. Clinical studies provide compelling evidence that HIV leads to an increased risk of developing TB shortly after HIV infection. Glynn et al., (2008); Sonnerberg et al., (2005) proposed that

among miners in South Africa, HIV^+ individuals were 2 to 3 times more likely to develop TB than HIV miners within 2 years of HIV seroconversion. It was observed that after 11 years, half of the HIV^+ miners developed TB. Although HIV^+ individuals in these studies are more prone to developing TB, half of the cases of TB were attributed to time not HIV due to the high incidence rate of TB among South African miners. Whalen et al., (2000) concluded that not only are HIV^+ individuals at greater risk of acquiring M-TB and developing active TB, they have an increased risk of death due to TB.

2.10. Mycobacterium Tuberculosis Models Review

The majority of previous studies have used deterministic compartment models (Blower et al, 1996; Blower and Gerberding, 1998; Murray and Salomon, 1998a; Murray and Salomon, 1998b; Dye et al, 1998; Currie et al, 2003; Currie et al, 2005; Williams et al, 2005). Deterministic compartment models are when the population is divided into different epidemiological states and the movements between the states are represented by a system of differential equations. These previous compartment models have focused on modeling TB at the population level. The studies concentrated on the effect of interventions at a large scale and although many of them addressed the implications of reducing transmission, none of them was able to look at the actual mechanism behind it. These studies have been vital in understanding and quantifying TB disease progression in populations and will be used to inform our model. However, it is felt that a discrete event simulation is more appropriate for investigating interventions at the household level and enables the more intricate details of transmission to be understood.

The importance of household versus random transmission has previously been studied using a deterministic compartment model developed to look at the

importance of cluster size in TB disease dynamics (Aparicio et al, 2000; Song et al, 2002). Whilst this analysis was useful in understanding the impact of the evolution of TB virulence on TB dynamics, some aspects of the modeling were unrealistic and critically, the population structure was ignored. The study also did not incorporate the effect of HIV.

Discrete event simulation to model TB was used by (Murray, 2002). The model was used to investigate the clustering of different strains of TB. The use of this technique was successful and modeling TB at the individual level proved to be a powerful tool.

From the work of (White and Garnett, 2010), despite the infectious agent that causes tuberculosis having been discovered in 1882, many aspects of the natural history and transmission dynamics of TB were still not fully understood. This was reflected in differences in the structure of mathematical models of TB, which in turn produced differences in the predicted impacts of interventions. Gaining a greater understanding of TB transmission dynamics required further empirical laboratory and field work. It also requires mathematical modeling and interaction between them. Modeling could be used to quantify uncertainty due to different gaps in their knowledge to help identify research priorities. Fortunately, the present moment was an exciting time for TB epidemiology, with rapid progress being made in applying new mathematical modeling techniques, new tools for TB diagnosis and genetic analysis and a growing interest in developing more effective public health interventions.

The spread of tuberculosis through one-strain and two-strain models was addressed by (Claude et al., 2011). A basic model that incorporated fast and slow progression, effective chemoprophylaxis and therapeutic treatment was first presented and the system exhibited the traditional behaviour. They proved that if the basic reproduction ratio R_o =1, then the disease-free equilibrium is globally asymptomatically stable on the nonnegative out-hunts. However, if Ro >1 an endemic equilibrium exists and is globally asymptomatically stable. Based on the first model, the second model dealt with the problem of drug resistance as a competition between multiple types of strains of mycobacterium tuberculosis: those that were sensitive to anti-tuberculosis drugs and those that were resistant. Their objectives were to characterize the role of multi-drug-resistance in the transmission of tuberculosis. The coexistence and stability of the associated equilibrium was discussed.

According to (Caroline et al, 2006), TB was a leading cause of infectious mortality. Although anti-biotic treatment was available and there was vaccine, tuberculosis levels were rising in many areas of the world. They used mathematical models to study tuberculosis in the past and had influenced public policy. The spread of HIV and the emergence of drug-resistant TB strains motivated the use of mathematical models today. Here, they reviewed and compared the mathematical models of tuberculosis dynamics in the literature. They presented two models of their own: a spatial stochastic individual-based model and a set of delay differential equations encapsulating the same biological assumptions. They compared two different assumptions about partial immunity and explored the effect of preventive treatment. They argued that seemingly subtle differences in model assumptions could have significant effects on biological conclusions.

The efficacy of recommended tuberculosis infection control measures was evaluated by (Kwame et al, 2013). A deterministic mathematical model for airborne contagion was used and examined the percentage of purified protein derivative conversions under various exposure conditions; environmental control cannot eliminate the risk for TB transmission during high risk procedures. However, respiratory protective devices, and particularly high efficiency particulate air masks, may provide nearly complete protection if used with air filtration or ultraviolet irradiation. Nevertheless, the efficiency of those control measures deceased as the infectivity of the source case increased. Therefore, administrative control measures were the most effective because they substantially reduced the rate of infection.

The spread of tuberculosis through a two-patch epidemiological system $SE_1 \ldots E_nI$ which incorporated migrations from one patch to another just by susceptible individuals was studied by (Jean et al., 2012). Their model was considered with bilinear incidence and migration between two patches, where infected and infectious individuals cannot migrate from one patch to another due to medical reasons. They discussed the existence and uniqueness of the associated endemic equilibria. Quadratic forms and lyapunor functions was used to show that when the basic reproduction ratio is less than one, the disease-free equilibrium (DFE) is globally asymptotically stable and when it is greater than one there exists in each case a unique endemic equilibrium which was globally asymptotically stable. Numerical simulation results were provided to illustrate the theoretical results.

Mathematical models to establish the conditions on the size of the area occupied required minimizing and thereafter eradicating tuberculosis was formulated by (Sematimba et al, 2005). Both numerical and qualitative analyses of the model

were done and the effect of variation in the area size and recruitment rate on the different epidemiological groups was investigated. Their results of the analysis showed that there exists a stable disease-free equilibrium point provided that the characteristic area was greater than the product of the probability of survival from the latent stage to the infectious stage and the number of latent infections produced by a typical infectious individual during his/her mean infectious period. Their study recommended that the characteristic area per individual should be at least 0.25 square kilometers in order to minimize the tuberculosis incidence.

A mathematical model of the dynamic behaviour of tuberculosis disease in the upper East Region of the Northern part of Ghana was reviewed by (Adetunde, 2009). The equilibrium points of the model system where found and their stability was investigated. His model exhibited two equilibria, namely, the disease-free equilibrium and the endemic equilibrium. Stability theory and computer simulation was used, and observed that population determines the infection rate of tuberculosis, hence the higher the population density, the greater the risk of instability of the disease free equilibrium.

The use of different mathematical tools to study biological processes is necessary to capture effects occurring at different scales. Grammack et al, (2005) studied as an example the immune response to infection with the bacteria mycobacterium tuberculosis, the causative agent of tuberculosis. The immune responses were both global as well as local in nature was presented. Four different mathematical tools to explore the global immune response as well as the more local one and compared and contrasted results obtained using those methods was used. Applying a range of approaches from continuous deterministic models to discrete stochastic ones allowed them to make predictions and suggested hypotheses about the underlying

biology that might otherwise go unnoticed. The tools developed and applied were also applicable in other settings such as tumor modeling (Grammack et al, 2005).

The strengths and limitations of using homogeneous mixing and heterogeneous mixing epidemic models were explored in the context of the transmission dynamics of tuberculosis (Aparicio and Carlos, 2009). Their focus was on three types of models: a standard incidence homogenous mixing model, a non-homogeneous mixing model that incorporates "household" contacts, and an age-structured model. The models were parameterized using demographic and epidemiological data and the patterns generated from those models were compared. Furthermore, the effects of population growth, stochasticity, clustering of contacts, and age structure on disease dynamics were explored. That framework was used to assess the possible causes for the observed historical decline of tuberculosis notifications.

The study looked at the estimation of the economic burden and household welfare impact of tuberculosis (TB) in the Western Region of Ghana. Studies into the economic burden of TB in Ghana have been limited. WHO's (2002a) guidelines on cost and cost effectiveness of TB management were followed in the estimation of cost of TB from the patient/household and health provider perspectives. Human capital method was applied in the estimation. Wells-Riley model and multiple regression technique were employed in the estimation of the probability of transmission within households and the household welfare impact of TB. Results established that tuberculosis causes a significant deterioration in household income and welfare. The study also found that TB imposes various catastrophic economic costs on affected households and utilizes considerable resources within the public health system. It is recommended that safety nets or income insurance be

established for households affected by TB to help them cope with high economic burden as well as helping patient's fully complete treatment (Blankson, 2012).

According to (Cao et al., 2013), tuberculosis is a serious public health issue in developing countries. Early prediction of TB epidemic is very important for its control and intervention. To develop an appropriate model for predicting TB epidemics and analyze its seasonality in China was aimed. Data of monthly TB incidence cases from January 2005 to December 2011 were obtained from the Ministry of Health, China. A seasonal autoregressive integrated moving average (SARIMA) model and a hybrid model which combined the SARIMA model and a generalized regression neutral network model to fit the collected data from 2005 to 2010 was used. Simulation performance parameters of mean square error (MSES), mean absolute error (MAE) and mean absolute percentage (MAPE) were used to compare the goodness-of-fit between these two models. Data from 2011 TB incidence data was used to validate the chosen model. From their results, although both two models could reasonably forecast the incidence of TB, the hybrid model demonstrated better goodness-of-fit than the SARIMA model. For the hybrid model, the MSE, MAE and MAPE were 38969150, 3406.593 and 0.030, respectively. For the SARIMA model, the corresponding figures were 161835310, 8781.971 and 0.076, respectively. The seasonal trend of TB incidence is predicted to have lower monthly incidence in January and February and higher incidence from March to June. They conclude that the hybrid model showed better TB incidence forecasting than the SARIMA model. There is an obvious seasonal trend of TB incidence in China that differed from other countries.

2.11. Mechanism of Immunological Interaction of HIV and TB

Infection with HIV enhances the susceptibility to MTB infection. Because the occurrence of these two diseases is heavily dependent on the immune system, their interactions are more complex than previously understood. Previously, (Chagan-Yasutan et al, 2009) studied the plasma levels of two matricellular proteins such as galectin-9 (GAL-9) and osteopontin (OPN) in AIDS patients complicated with various opportunistic infections. The levels of both molecules were high in all the patients but only the level of GAL-9 decreased and that of OPN remained high after Highly Active Antiretroviral Therapy (HAART). Also, it was noted that the GAL-9 level was exceptionally high in acute HIV infected individuals. The cellular receptor for GAL-9 is the T-cell immunoglobulin domain and mucin domain 3 (Tim-3) and Tim-3 is expressed on Th1 cells. Mycobacterium tuberculosis-infected macrophages express GAL-9 and the Tim-3 GAL-9 interaction leads to macrophage activation and stimulates the bactericidal activity by inducing caspase-1–dependent interleukin-1β (IL-1β) secretion. Therefore, Th1 cell surface molecule Tim-3 may have evolved to inhibit the growth of intracellular pathogens via its ligand GAL-9, which is also known to inhibit the expansion of effector Th1 cells (Jayaraman et al, 2010). Therefore, only one case of MTB associated with acute HIV was reported (Crowley et al, 2011).

In contrast, chronic HIV infected individuals succumb to various opportunistic infections and pulmonary TB is known to occur when CD4+ T cell numbers are still high, indicating that the immune system plays a role in the development of pulmonary TB. Similarly, T cell epitopes of different strains representative of global diversity are highly conserved in MTB (Comas et al, 2010). Due to the conserved epitopes, the host can maintain MTB for a long time as latent infection

and can transmit it to the next generation. It is also suspected that CD4+ T cells have an essential role in tissue damage that results in cavity formation, which enhances aerosol infection. In HIV endemic areas, the situation becomes more complex if the CD4+ T cells numbers increase after HAART and then recovery of the immune system is variable.

2.12. **Low CD4 Counts in Various Human Infections**

In 1983, about one year before HIV was first mentioned as a possible cause of AIDS, a study was published showing severely reduced CD4 counts in 146 consecutive people with serious acute infections who were admitted to their hospital in New Mexico (Williams et al, 1983). The infections included pneumonia, acute pyelonephritis, abscesses, infected wounds, cellulitis, deep tissue infections, and sepsis. This reveals that 31 of 45 (69%) had CD4 counts less than 500 cells/mm^3, 19 of 45 (42%) had counts below 300, 13 of 45 (29%) had counts below 200, 6 of 45 (13%) had 100 or less, and 2 of 45 (4%) had values less than 50. The average CD4 count for all the people with pneumonia was 574. They also provide tables with clinical information and CD4 counts for 9 patients with soft tissue infections (STI) and 12 patients with sepsis/deep infections, all of whom had multiple T-cell abnormalities.

It is also remarkable that 30% of people with pneumonia, which is a very common illness in people diagnosed HIV-positive, had CD4 counts below 200.

2.12.1. Low CD4 Counts in Pulmonary Tuberculosis

In 1985 a group of researchers in Indonesia examined the lymphocyte subsets in 26 patients newly diagnosed with pulmonary tuberculosis (TB) (Beek et al, 1985).

They undertook the study because of a previous report of lowered CD4 counts in HIV-positive patients with TB in which the authors assumed that the lowered CD4 counts were due to HIV. They found that in HIV-negative TB patients; CD4 counts were also significantly lowered, with an average of 748, compared to 1,043 in healthy controls. They also found significantly lowered CD4/CD8 ratios. Although the effects seen here were not as dramatic as in the studies reviewed previously, with only 5 of 26 patients having CD4 counts less than 500, the authors still felt their findings were highly significant to people diagnosed HIV-positive. The authors also commented on some similar findings in leprosy, as well as in HIV-negative hemophiliacs.

2.12.2. Low CD4 Counts in Malaria

In 1999 a letter was published documenting severely lowered CD4 counts in African patients with malaria (Chirenda, 1999). The author examined the CD4 count in 78 patients with malaria who were HIV-positive, and 19 who were HIV-negative. He was surprised to find that more HIV-negative malaria cases had severely lowered CD4 counts than did the HIV-positive cases, on average, with 8 of 19 (42%) HIV-negative cases being below 200, while only 31 of 78 (40%) HIV-positive cases had CD4 counts below 200. Seven HIV-negative malaria cases had CD4 counts below 100. In addition, 6 HIV-positive patients had normal CD4 counts, and the author states, "One may want to hypothesize that malaria reduces the CD4 count more than HIV infection".

2.12.3. Low CD4 Counts in Mononucleosis

Mononucleosis is caused by cytomegalovirus (CMV) or Epstein-Barr virus (EBV), and usually results in prolonged cold and flu symptoms, swollen lymph nodes, and

fatigue. In 1981 a group of researchers looked at CD4 and CD8 counts in ten consecutive patients with acute CMV mononucleosis, and compared their counts with those of ten healthy volunteers (Carney et al, 1981). The CD4 counts were measured in nine of the ten patients, and the three with the lowest CD4 counts had 194, 202 and 255 cells/mm^3. The authors also found that the T-lymphocytes of people with mononucleosis responded poorly to antigens, showing depressed function.

Five years later, a different set of researchers measured various lymphocyte subsets in acute EBV mononucleosis (Junker et al, 1986). They took 17 consecutive patients who had recently been diagnosed, gave them an immunization designed to activate their B lymphocytes, and then took samples of blood. The immunization makes this study different from any of the other studies to be examined here. They did not find a statistically significant lowering of CD4 counts, but they did find significantly lowered CD4/CD8 ratios, with the ratios falling below 1 as is reported to occur in people diagnosed HIV-positive. The authors concluded that "these studies demonstrate that infection with EBV affects both B and T lymphocytes and causes a broad based transient immune deficiency".

2.12.4. Low CD4 Counts in Sepsis

In 1986, a group of researchers from Osaka, Japan published a study where they examined various lymphocyte subsets in 9 consecutive patients admitted to the ICU with sepsis (Nishijima et al, 1986). They examined their blood at weekly intervals for four weeks. The CD4 counts in these patients were markedly reduced, with averages being below 500 and staying there for the entire 4 week study period. They also found T-cell function to be diminished, especially in patients

who did not survive, although there was no significant difference in CD4 counts between those that died and those that survived.

2.13. HIV-Blood Interactions: CD4+ Lymphocytes Dynamics

Hraba and Dolezal, (2009) presented a mathematical model of CD4+ lymphocyte dynamics in HIV infection. The model incorporated a feedback mechanism regulating the production of T-lymphocytes and simulated the dynamics of CD8+ lymphocytes, whose production was assumed to be closely linked to that of CD4+ cells. Thus, because CD4+ lymphocyte counts are a good prognostic indicator of HIV infection, the model was used to simulate such therapeutic interactions as chemotherapy and active and passive immunization. The model also simulated the therapeutic administration of anti-CD8 antibodies; this intervention was assumed to activate T-cell production by activating a feedback mechanism blocked by the high number of CD8+ lymphocytes present in HIV-infected persons. This model concentrated on CD4+ lymphocytes because the depletion of the T-cell subpopulation and the parallel decrease in the helper activity of T-lymphocytes seemed to be major immune system defect caused by HIV infection.

The above model was purely on maintenance of T-cell population in HIV infections. Alderman, (1988) suggested that the depletion of CD4+lymphocytes might activate some homeostatic mechanism that would increase their production. This assumed that the homeostatic mechanism increased the production of both CD4+ and CD8+ lymphocytes and did not discriminate between the two T-cell subpopulations.

In their study, Bragardo and Buonifiglio, (1997) showed that HIV-1 glycoprotein120 induced CD4+ association with several molecules on the surface of CD4+ lymphocytes. One of the molecules was CD38, which is involved in lymphocyte/endothelium interactions. They therefore examined the possibility that glycoprotein120 binding altered the CD4+ T-cell interaction with vascular endothelium in vitro and in vivo. They were therefore able to confirm that glycoprotein120 induced CD4+ association with CD38 in peripheral blood CD4+ T-cells.

While most people know about the reports of lowered CD4 levels in people diagnosed HIV-positive, which continue to receive widespread press coverage, other reports concerning lowered CD4 counts in people who are HIV-negative have been widely ignored. These reports show that CD4+ counts commonly fall very low, especially if a person suffers from certain conditions. These conditions include a variety of viral illnesses, bacterial infections, parasitic infections, sepsis, septic shock, multiple organ system failure, tuberculosis, coccidioidomycosis, burns, trauma, transfusions, malnutrition, over-exercising, pregnancy, normal daily variation, psychological stress, and social isolation. In addition to lowered CD4 counts, these conditions result in other immunosuppressive changes that are also identical to those seen in people diagnosed HIV-positive, including reduced CD4/CD8 ratios, reduced lymphocyte function, energy, atrophy of lymphoid organs, and general suppression of cell-mediated immunity.

2.14. HIV - Blood Interaction: Thermodynamic Approach

Achebe et al, (2012) measured absorbance using ultraviolet visible spectrophotometer for twenty samples of HIV infected and uninfected blood. The Hamaker constants $A_{11,}$ $A_{22,}$ A_{33} and the combined Hamaker coefficients A_{132} were obtained using the values of the dielectric constant together with the Lifshitz equation. The harmonized Hamaker coefficients A_{132har} and the absolute Hamaker coefficient, A_{132abs} (a mean of all the values of the various Hamaker coefficients) for the infected blood samples were then calculated. The value of A_{132abs} = $0.2587x10^{-21}$Joule (i.e. $0.2587x10^{-14}$erg) was obtained for HIV-infected blood (Achebe and Omenyi, 2013; Achebe, 2014); Achebe and Omenyi, 2013). This value lies within the range of values derived by various researchers for other biological systems. Another significance of this result is the positive sense of the absolute Hamaker coefficient which implies net positive van der Waals forces indicating an attraction between the virus and the lymphocyte. This in effect suggests that infection has occurred thus confirming the role of this principle in HIV-blood interactions. A lower value of $A_{131abs} = 0.1026x10^{-21}$ Joule obtained for the uninfected blood samples is also an indicator that a zero or negative absolute combined Hamaker coefficient is attainable. As a first step to this, a mathematical derivation for $A_{33} \geq 0.9763x10^{-21}$Joule which satisfies this condition for a negative A_{132abs} was obtained (Achebe et al, 2012).

Ozoihu, (2014) measured contact angle on HIV infected blood and uninfected blood samples using the three probe liquids (water, glycerine and diiodomethane). The surface free energies were determined from contact angle data. The CD4+ cell counts were also measured using partec flow Cytometry instrument. The change in interfacial free energy of adhension ΔF^{adh} and Hamaker coefficient A_{132} for

infected T4 cells were found to be -23.50mJ/m^2 and 0.227x10^{-16}mJ/m^2 (≈0.227x10^{-23}J) respectively using Neumann model at low energy (hydrophobic) surface of 31.81x10^{-16}mJ/m^2. The Hamaker coefficient for uninfected T4 cell was found to be 0.176x10^{-16}mJ/m^2 (≈0.176x10^{-23}J). the positive value of Hamaker coefficient shows that attraction exist between HIV and T4 cells but lower value of A_{132} for uninfected T4 cells indicated less attraction. This in effect suggests that contact angles values of infected blood are generally higher than uninfected blood and tends to increase with decrease in CD4+ count for infected blood. These results however agreed with the work of (Achebe et al, 2012) that gave 0.2587x10^{-21}J for infected blood and 0.1026x10^{-21}J for uninfected blood. The negative Hamaker coefficient (-0.6637x10^{-19}mJ/m^2) indicated that isolation of the virus is possible. Ozoihu, (2014) suggested that finding the agents that will reduce the surface tension of serum to obtain a negative value of Hamaker coefficient will be the next step in formulating a drug to be recommended to the pharmaceutical industries for eradication of HIV infection.

2.15. The Role of Surface Thermodynamics in Thromboresistance of Biomaterials

Neumann et al, (1975) in their work considered the applicability of thermodynamics to thrombus formation induced by biomaterial implants with special interest on the attachment and subsequent adhesion of platelets to various substrates. The proper thermodynamic potential for the process of platelet attachment is the Helmholtz free energy (Defay et al, 1966). The introduction of thermodynamic or at least quasi thermodynamic quantities to this subject from the earlier qualitative concepts of “hydrophilic” and “hydrophobic” surfaces was done by (Baier, 1972; Lyman et al, 1965). Their works applied the critical surface

tension of wetting γ_c (Zisman, 1964) and a surface free energy quantity γ_{so} (solid surface tension against a vacuum). They correlated these parameters empirically with factors relevant to thrombogenesis like clotting time, platelet adhesion, and extent and type of thrombus formed.

2.16. Empirical Correlations between Surface Tension and Quantities Related to Thromboresistance

Lyman et al, (1965) found empirical correlation between γ_c (observed prior to protein adsorption) of bare polymer surface and clotting time as well as platelet adsorption whereas (Baier, 1972) found a correlation between γ_c and thrombus formation (clotting). The conventional γ_c values of polymers, particularly those measured by (Zisman, 1964) agree closely with the γ_{sv} obtained from the equation of state. This development admits the correlations as relevant while the conclusions drawn from contact angle data of carbon or adsorbed protein layers are somewhat suspect.

Unfortunately, Lyman's and Baier's results do not tell us which curve is applicable. A biomaterial of a higher surface tension of about 40ergs/cm^2 (4.0×10^{-2}J/m^2) might absorb protein to a smaller extent than that of a surface tension of say, 25ergs/cm^2 (2.5×10^{-2}J/m^2) and hence will effectively have a smaller resultant surface tension than the latter. It is therefore along these lines that an explanation of apparent contradictions between the empirical findings of (Lyman et al, 1965) and of (Baier, 1972) may be found.

2.17. Molecular Interpretation of Surface Free Energy/Surface Tension

The surface free energy(γ_{sv}) of a solid (Good and Stromberg, 1979) is defined as the change in the total surface free energy(G) per unit change in surface (A) at constant temperature (T), pressure (P) and mole (N):

$$\gamma_{SV} = \left(\partial G / \partial A\right)_{T,P,n} \tag{2.1}$$

For liquids, the surface area can be changed under the above conditions. For solids however, surface area cannot, in general, be changed without affecting its chemical potential. Therefore, in changing the area, work needs to be done against the elastic forces in the solid. In a given experiment involving stretching of solid surfaces, it is often difficult to delineate the effect of bulk and surface mechanics. The research carried out by Langmuir, Zisman and Adams stimulated other surface scientists (Good and Stromberg, 1979; Girifalco and Good, 1957; Fowkes, 1964; Owens and Wendt, 1969; Kaeible, 1970; Wu, 1982) to investigate ways to determine directly the surface free energies of solid from contact angles. Gibbs, (1969) commented that the surface energies of solids cannot be derived from contact angles because there is virtually no way of estimating the interfacial free energy of solid and liquid. However, the simplification of Young's equation was actually possible as a result of (Dupre, 1869) equation; combining the work of adhesion at the liquid interface with the surface and interfacial tensions of the solid-vapor, solid-liquid and liquid-vapor interfaces:

$$W_{SL} = \gamma_{SV} + \gamma_{LV} - \gamma_{SL} \tag{2.2}$$

The (Dupre, 1869) equation (2.2) amounts to a conservation of total energy in a reversible process of adhesion and cohesion of two phases.

This analysis involves the interfacial free energies between the three phases and is given by Young's equation:

$$\gamma_{SV} - \gamma_{SL} = \gamma_{LV} \cos\theta \qquad (2.3)$$

The combination of Young equation (2.3) and Dupre equation (2.2) results in equation (2.4):

$$W_{SL} = \gamma_{LV}(1 + \cos\theta) \qquad (2.4)$$

In this way the unknowns (γ_{SV} and γ_{SL}) of the original Young's equation can be reduced to only the term, W_{SL}. The left-hand side of equation (2.4) is actually a deformation term; it may be viewed as the strain energy of the liquid drop per unit area. Unlike solids, the strain energy is contributed by surface tension alone. The next major simplification of Young – Dupre equation (2.4) was due to (Good and Girifalco, 1957), who proposed analogous to the Berthelot, (1898) combining rule of intermolecular interaction, that the work of adhesion can be expressed as geometric mean of the surface tensions of the pure components; γ_{SV} and γ_{LV}:

$$W_{SL} = 2\Phi(\gamma_{SV}\gamma_{LV})^{0.5} \qquad (2.5)$$

Where Φ: is a correction factor for intermolecular interaction, Φ is equal to unity if the intermolecular forces acting across the surface are similar; such is the case with a hydrocarbon liquid interacting with a hydrocarbon solid. Φ is less than unity when the intermolecular interactions that constitute cohesive and adhesive forces do not match, such as the case with a hydrogen – bonding liquid interacting with a pure hydrocarbon surface. Good and Girifalco, (1957) expressed Φ in terms of the molecular level parameters of surfaces such as polarizability, ionization energy and dipole moments. The combination of Good and Girifalco equation (2.5) and the Young – Dupre equation (2.4) results in fundamental equation:

$$\gamma_{LV}(1 + \cos\theta) = \left(\gamma_{SV}\gamma_{LV}\right)^{0.5} \qquad (2.6)$$

When the primary forces constituting the cohesive and adhesive interactions of dispersive type, equation (2.6) reduces to equation (2.7):

$$\gamma_{SV} = \gamma_{LV}(1 + Cos\Phi)^2/4 \qquad (2.7)$$

According to equation (2.7), cosθ will be unity only when $\Phi^2\gamma_{sv}$ is equal to γ_{LV}. Thus one obtains a relationship between γ_c and γ_{sv} as $\gamma_c = \Phi^2\gamma_{sv}$. The critical surface tension γ_c of wetting is equal to the surface free energy only when the interaction parameter Φ is equal to unity. The computation of Φ depends upon the detailed knowledge of the chemical constitution of the solid and liquid as well as the model used to compute it.

Fowkes, (1964) provided a method of analyzing the energetics of the surfaces from the contact angles which does not require detailed knowledge of the surface compositions of solid. He considered that the total surface tension of a solid or a liquid can be decomposed into components corresponding to the specific types of intermolecular interactions:

$$\gamma = \gamma^d + \gamma^p + \gamma^i + ... \qquad (2.8)$$

The division of the surface tension into components allowed the work of adhesion to be expressed (Owens and Wendt, 1969; Kaeible, 1970):

$$W_{12} = 2\sqrt{\gamma_1^d}\gamma_2^d + 2\sqrt{\gamma_1^p}\gamma_2^p + 2\sqrt{\gamma_1^i}\gamma_2^i \qquad (2.9)$$

The surface tension components of the solid are determined by combining equation (2.4) and equation (2.9):

$$\gamma_{LV}(1+\cos\theta) = 2\sqrt{\gamma_1^d}\gamma_2^d + 2\sqrt{\gamma_1^p}\gamma_2^p + 2\sqrt{\gamma_1^i}\gamma_2^i \qquad (2.10)$$

Wu, (1982) used harmonic – mean combining rule of the surface tension components to approximate Young's equation:

$$\gamma_{LV}(1+\cos\theta)=4\gamma_{LV}^{d}\gamma_{SV}^{d}\Big/\left(\gamma_{LV}^{d}+\gamma_{SV}^{d}\right)+4\gamma_{LV}^{p}\gamma_{SV}^{p}\Big/\left(\gamma_{LV}^{p}+\gamma_{SV}^{p}\right) \qquad (2.11)$$

2.18. Microscopic Approach to Surface Interfacial Interactions

Good and Girifalco, (1957) earlier used pair wise additive to compute interaction energies across condensed phases. The energy of interaction between two semi-infinite flat slabs is given by:

$$G_{12}=\int_{v_1} dv_1 \int_{v_2} n_1 n_2 g_{12} dv_2 \qquad (2.12)$$

Where $dv_1 and\ dv_2$ are the volume elements of bodies 1 and 2 with respect to v_1 and v_2; n_1 and n_2 are the number densities of the oscillators in bodies 1 and 2, and g_{12} is the interaction energy between two oscillators of bodies 1 and 2.

The interaction energy between two flat slabs was calculated rigorously by (Good and Girifalco, 1957) by considering the Debye, Keesom and London forces. The heuristic derivation of the Good – Girifalco equation (2.5) using (McLachlan, 1963) equation according to which g_{12} can be expressed as:

$$g_{12}=-\left(\frac{6kT}{R^6}\right)\sum_{n=o}^{\infty}\propto_1(i\omega_n)\propto_2(i\omega_n) \qquad (2.13)$$

Where $(i\omega_n)$ is the polarizability of the oscillator expressed along the complex frequency axis $i\omega_n$. For g_{12}, the overall interaction energy can be written as:

$$G_{12}=-A_{12}/(12\pi l^2) \qquad (2.14)$$

Where A_{12} is the Hamaker constant and l is the separation distance, A_{12} is obtained using equation (2.15):

$$A_{12} = 6\pi^2 n_1 n_2^{kT} \sum_{n=0}^{\infty} \alpha_1(i\omega_n)\alpha_2(i\omega_n) \qquad (2.15)$$

The polarizability appearing in the summation can be decomposed into two terms: one arising from zero frequency (d.c photon) interaction and the other from the higher frequency interaction:

$$\alpha_1(i\omega_n) = \left(\mu^2/3kT\right)/\left(1+\omega_n/\omega_{rot}\right) + \alpha_e(0)/\left[1+\left(\omega_n/\omega_e\right)^2\right] \qquad (2.16)$$

Where μ is the dipole moment, ω_{rot} is the rotational frequency of the dipole, $_e(0)$ is the electronic polarizability and ω_e is the electronic excitation frequency.

The zero frequency of Eq. (2.15) can be written as:

$$A_{12}\mathrm{I}_{n=o} = \pi^2 n_1 n_2\left[\left(\mu^2\mu_2^2/3kT\right) + \left\{\mu_1^2\alpha_{e2}(0) + \mu_2^2\alpha_{e1}(0)\right\} + 3kT\alpha_{e1}(0)\alpha_{e2}(0)\right] \quad (2.17)$$

The fist term of the equation (2.16) is due to the classical dipole – dipole interaction, the second term is due to a dipole – induced dipole, and the third term is due to the (Casimir–Poldar, 1948) interaction. The Casimir–Polder interaction is due to electrically neutral atoms or molecules in unexcited state. This formula agrees with the calculations in quantum electrodynamics for the interaction of two atoms at large distances. The higher frequency component of the Hamaker constant can be written as:

$$A_{12}\mathrm{I}_{n\rangle 0} = (3/2)\pi^2 n_1 n_2 h\omega_{e1}\omega_{e2}(0)\alpha_{e2}(0)/\left(\omega_{e1}+\omega_{e2}\right) \qquad (2.18)$$

2.19. Macroscopic Theory of Lifshitz

Lifshitz, (1961) used a macroscopic model, where the interaction energy between two surfaces is calculated from the fourier transform of the normal component of the electromagnetic stress tensor. In a simplified form, the Hamaker constant of

interaction at short distance can be expressed according to Lifshitz's theory as follows:

$$A_{12} = 1.5kT\sum_{n=0}^{\infty}\sum_{j=1}^{\infty}\left(\left\{\left[\left(\in_1(i\omega n)-1\right)/\left(\in_1(i\omega n)+1\right)\right]\left[\left(\in_2(i\omega n)-1\right)/\left(\in_2(i\omega n)+1\right)\right]\right\}^j / j^3 \quad (2.19)$$

Here, $\in_1(i\omega n)$ is the dielectric susceptibility of the material m(m$\in$) expressed along the complex frequency axis $i\omega n$.

Lifshitz's theory of interaction provides protocol to calculate the interaction energy between condensed phases in terms of the dielectric susceptibility of the materials which are continuum properties that is valid for large separation distance. The continuum approach of Lifshitz does not rigorously apply to wetting and adhesion where the separation distance is comparable with molecular sizes. The required corrections are of second order for dispersion forces. Fowkes, (1964); Fowkes and In, (1983); Isrealachvili, (1974); Hough and White, (1987) as well as (van Oss et al, 1988; Chaudhury, 1984) calculated the Hamaker constant of a number of non-polar liquids and solids, and found that the dispersion component of the surface tension and Hamaker constants form a ratio which is approximately constant for a number of different materials. The Lifshitz's theory has been used to estimate just how much of the interfacial interactions of the polar liquids are contributed by the dipolar interactions.

2.20. Role of Surface Free Energy in the Adhesion under Liquid: Stability of Particles Suspension

Neumann et al, (1983) devised several methods to estimate the surface free energy of solid, which are based on adhesion under liquid media. The central theme of this method is based on the following equation:

$$\Delta F_{132} = \gamma_{12} - \gamma_{13} - \gamma_{23} \quad (2.20)$$

Where; ΔF_{132} denotes the free energy of adhesion of two surfaces 1 and 2 in liquid 3. In principle, the free energy of adhesion can take any value from negative to positive, depending upon the relative magnitude of the interfacial tension of the three interfaces. When 1and 2 denote the same particles, equation (2.21) reduces to:

$$\Delta F_{131} = -2\gamma_{13} \qquad (2.21)$$

In Neumann's studies, it has been assumed that the interfacial tension between a solid and liquid can only be positive or zero. If the interfacial tension is positive, the particles will coagulate spontaneously to an unstable suspension. This kind of situation arises for hydrophobic particles suspended in a hydrophilic liquid, such as water. If now, the surface tension of the liquid is slowly decreased by adding a low surface tension liquid to the first, a situation may arise when γ_{13} becomes zero. In that case, there is no driving force for the particles to adhere, and a stable suspension results. The surface tension of the liquid mixture at which this occurs was taken by (Neumann et al, 1983) as the surface free energy of the particle (Sandanger et al, 2009; Bolger and Michael, 1969). They used this technique to determine the surface tensions of several polymer particles, including biological and bacteria.

2.21. Repulsive van der Waals Interactions: Their Role in Various Seperation Methods

Hamaker, (1936) in his classical papers stated that "If two particles are embedded in a fluid and the London-van der Waals force between particles and fluid is greater than between the particles themselves, it might be though that the resultant action will be repulsion rather than an attraction". Owing to a peculiar property of

the London–van der Waals forces, the resultant force is generally attractive even when the particles are surrounded by fluid. This is a matter of considerable interest which warrants a detailed discussion.

Viser, (1981) in a review on Hamaker constants stated explicitly: "When two materials are immersed in a liquid medium and the interactions of each of these materials with that of the liquid medium is larger than the interaction between these materials themselves spontaneous separation can occur due to dispersion forces only". Fowkes, (1983) demonstrated the existence of such a repulsive interaction with poly-(tetrafluoroethylene)-glycol-iron oxide.

Omenyi et al, (1980) have shown theoretically and experimentally that the sign of the net van der Waals interaction between two different solid bodies or between two different dissolved macromolecules in liquids, often is negative (i.e. they repel one another) even if they are electrically neutral and even when they are immersed in polar liquids. They also went further to test the methodology arising from these considerations on the dissociations of antigen-antibody bonds of the van der Waals-type and on the elution of proteins from hydrophobic chromatography columns (van Oss et al, 1972). The results of both studies confirmed the validity of the theory and the entire practicality of the ensuing experimental procedures (van Oss et al, 1975).

Clearly, the new capability to change the attraction between different (even neutral) solids submerged in liquids, and/or dissolved macromolecules into repulsion, has considerable implications for a variety of novel as well as traditional separation methods. The theory involved is basically same as has been introduced earlier. The assumption here for simplicity is the interaction between two different

solids (or dissolved) bodies 1 and 2 in a liquid 3 and may be represented as an interaction between semi-infinite slabs.

Considering the Hamaker expression for the free energy for that case:

$$\Delta F(d) = \left[-\frac{A_{132}}{12\pi d^2} \right] \tag{2.22}$$

Assuming a minimum separation distance d_0, and that equation (2.22) is still valid for such a small separation distance, the Hamaker coefficient can be expressed thus:

$$A_{132} = -12\pi d_0^{\,2} \Delta F(d_0) \tag{2.23}$$

The Hamaker coefficient A_{132} for the interaction between two different bodies in a liquid can be calculated from equation (2.23) once the free energy of adhesion between the two bodies is known for which:

$$\Delta F_{132}^{adh} = \gamma_{12} - \gamma_{13} - \gamma_{23} \tag{2.24}$$

The values of $\gamma_{12,}$ $\gamma_{13,}$ and γ_{23} can be obtained using the equation of state approach.

To explain the concept of Hamaker Constants, use is made of the van der Waals explanation of the derivations of the ideal gas law:

$$PV = RT \tag{2.25}$$

It was discovered that the kinetic energy of the molecules which strike the container wall is less than that of the bulk molecules. This effect was explained by the fact that the surface molecules are attracted by the bulk molecules even when the molecules have no permanent dipoles. It then follows that molecules can attract each other by some kind of cohesive force (van der Waals, 1873). These forces

have come to be known as van der Waals forces. van der Waals introduced the following corrections to equation (2.25):

$$\left[P + \frac{a}{V^2}\right](V - b) = RT \qquad (2.26)$$

The correction term to the pressure, $\left(\frac{a}{V^2}\right)$ indicates that the kinetic energy of the molecules which strike the container wall is less than that of the bulk molecules. This signifies the earlier mentioned attraction between the surface molecules and the bulk molecules.

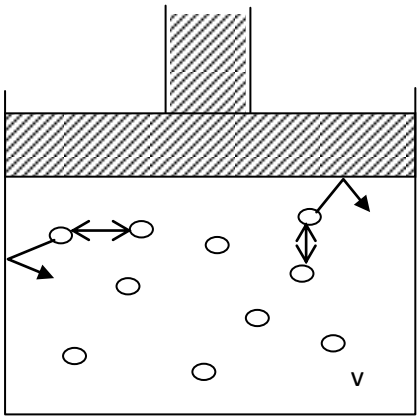

Fig. 2.6: Attraction of Surface Molecules by Bulk Molecules in a Container of Volume V *(Visser, 1981)*

After the development of the theory of quantum mechanics, London quantified the van der Waals statement for molecules without a dipole and so molecular attraction forces began to be known as London/van der Waals forces (London, 1930). London stated that the mutual attraction energy, V_A of two molecules in a vacuum can be given by the equation:

$$V_A = -\frac{3}{4} h\upsilon_0 \left[\frac{\alpha^2}{H^6}\right] = -\left[\frac{\beta_{11}}{H^6}\right] \qquad (2.27)$$

Where; h = Planck's constant, υ_o = the characteristic frequency of the molecule, α = the polarizability of the molecule, H = their separation

The interaction of two identical molecules of a material 1 is shown in figure (2.7).

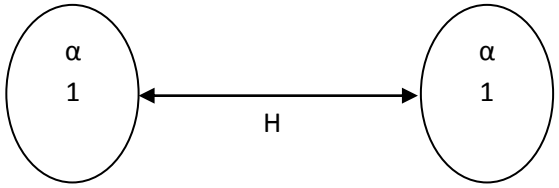

Fig. 2.7: Interaction of Two Identical Molecules of Materials, 1 and Polarizability, α, at a Separation, H *(Visser, 1981)*

Hamaker made an essential step in 1937 from the mutual attraction of two molecules. He deduced that assemblies of molecules as in a solid body must attract other assemblies. The interaction energy can be obtained by the summation of all the interaction energies of all molecules present as in figure (2.8).

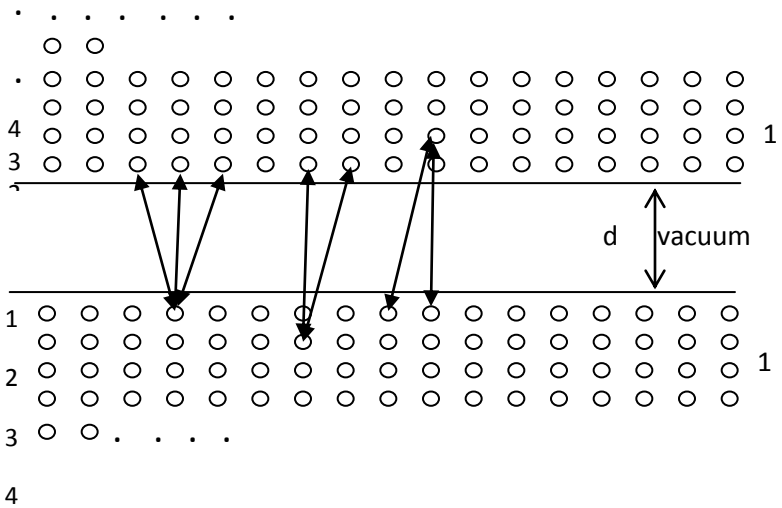

Fig. 2.8: Interaction of Two Semi-infinite Solid Bodies, 1 at a Separation, d in Vacuum *(Visser, 1981)*

The assemblies of molecules as in a solid body have interaction energy as the summation of all the interaction energies of all the molecules present and the van der Waals pressure, P_{vdw} as follows:

$$P_{vdw} = \left[\frac{A_{11}}{6\pi d^3} \right] \tag{2.28}$$

For a sphere of radius, R and a semi-infinite body at a maximum separation distance, d the van der Waals force of attraction, F_{vdw} is given as:

$$F_{vdw} = \left[\frac{A_{11} R}{6d^2} \right] \tag{2.29}$$

Where A_{11} = Hamaker constant

$$A_{11} = \pi^2 q_1^{\,2} \beta_{11} \tag{2.30}$$

Where q_1 = number of atoms per cm^3, and β_{11} = London-van der Waals constant

Given two dissimilar condensed bodies of given geometry with a separation distance, d, the corresponding van der Waals force between them can be determined.

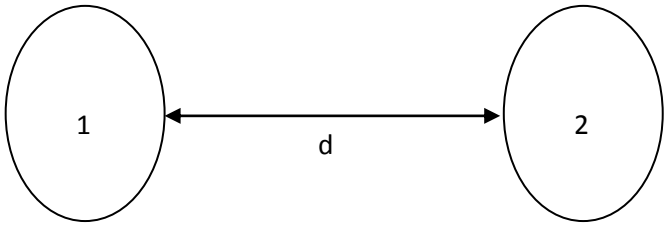

Fig. 2.9: Interaction of Two Non-identical Molecules, 1 and 2, at a Separation, d.

The van der Waals force between the molecule, 1 and the molecule, 2 is given by the relations:

$$F_{vdw} = -\left[\frac{A_{12} R_{12}}{6d^2} \right] \tag{2.31}$$

Where; $A_{11} = \pi^2 q_1^{\,2} \beta_{11}$ = Hamaker constant for molecule 1, $A_{22} = \pi^2 q_2^{\,2} \beta_{22}$ = Hamaker constant for molecule 2, and $A_{12} = \pi^2 q_{12}^{\,2} \beta_{12}$ = Hamaker constant for both materials.

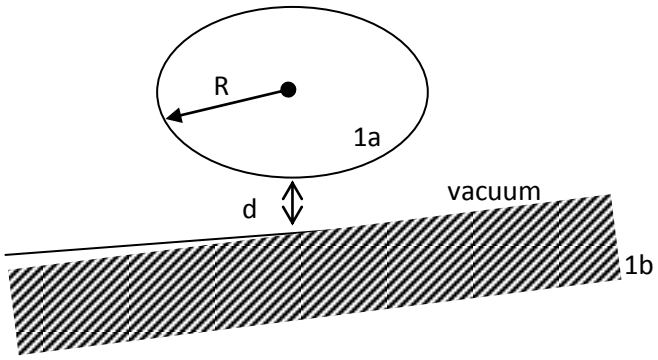

Fig. 2.10: Interaction of a Sphere of Radius, R at a Separation, d from a Solid Surface of the same Material, 1 in Vacuum *(Visser, 1981)*

According to Hamaker, the constant A_{11} equals:

$$A_{11} = \pi^2 q_1^{\,2} \beta_{11} \qquad (2.32)$$

Where q_1 is the number of atoms per cm^3 and β_{11} is the London/van der Waals constant for interaction between two molecules. Values for β can be obtained in approximation from the ionization potential of the molecules of interest, and so the Hamaker Constant can be calculated. The corresponding van der Waals force between two condensed bodies of given geometry can be calculated provided their separation distance is known.

Alternatively, A_{132} can be determined by the use of equation (2.33):

$$A_{132} = A_{12} + A_{33} - A_{13} - A_{23} \qquad (2.33)$$

For this approach A_{12}, A_{13} and A_{23} are obtained from:

$$A_{ij} = 12\pi d_0^{\,2} \Delta F_{ij}(d_0) \qquad (2.34)$$

And A_{33} can be derived from the free energy of cohesion:

$$\Delta F_{ij}^{coh} = -2\gamma_{iv} \qquad (2.35)$$

A positive value of A_{132} implies that the net van der Waals interaction between particles 1 and 2 immersed in liquid 3 is attractive, while a negative value means that the net van der Waals forces is repulsive

Actually, it can be easily shown (Viser, 1981) that A_{132} (considering equation (2.33) always is negative when:

$$A_{11} > A_{33} > A_{22} \qquad (2.36)$$

Or when:

$$A_{11} < A_{33} < A_{22} \qquad (2.37)$$

Which (compares equation 2.22) is the same as stating that A_{132} will always be negative when:

$$\Delta F_{11} > \Delta F_{33} > \Delta F_{22} \qquad (2.38)$$

or when:

$$\Delta F_{11} < \Delta F_{33} < \Delta F_{22} \qquad (2.39)$$

or

$$\gamma_{1v} > \gamma_{3v} > \gamma_{2v} \qquad (2.40)$$

or when:

$$\gamma_{1v} < \gamma_{3} < \gamma_{2v} \qquad (2.41)$$

However if the absolute value of A_{132} becomes closer to zero than $\approx \pm 3.5 \times 10^{-15}$ergs ($3.5 \times 10^{-22}$J), an exact prediction of attraction or repulsion based on whether A_{132} is positive or negative may no longer be reliable (van Oss et al, 1975).This then calls for different separation methods.

Hamaker's approach to the interaction between condensed bodies from molecular properties called microscopic approach has limitations. This is true against the backdrop of its neglect of the screening effect of the molecules which are on the surface of two interacting bodies as regards the underlying molecules. Therefore, Hamaker's approach is regarded as an over simplification.

Langbein, (1969) has shown that as a consequence of the screening effect, in the interaction between two flat plates at a separation distance d, the predominant contribution to the interaction by van der Waals forces comes from those parts of the interacting bodies, which are in a layer of a thickness equal to the separation distance d between the two plates.

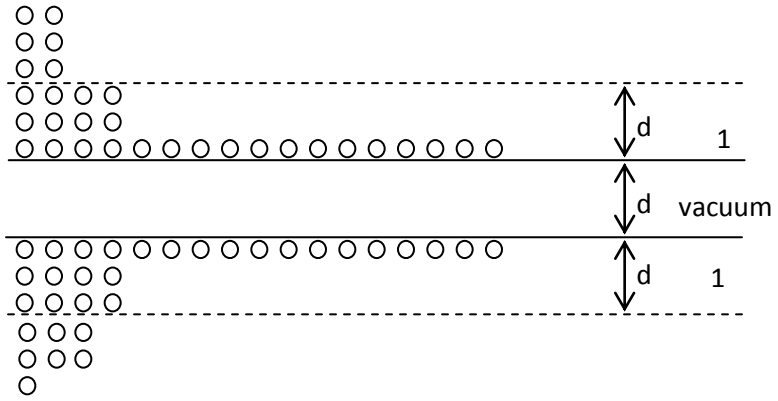

Fig. 2.11: Schematic Demonstration of the Screening Effect for the Interaction of Two Solid Bodies, 1, at a Separation, d, in Vacuum *(Visser, 1981)*

This demonstrates the importance of surface layers like the outer membrane of a cell, or the presence of an adsorbed layer on the overall interaction between two materials at short separations. It also demonstrates the need for the characterization of the surface of a body into its adhesional behaviour.

The limitations of Hamaker's approach led (Lifshitz et al, 1961) to develop an alternative derivation of van der Waals forces between solid bodies. The interaction between solids on the basis of their macroscopic properties considers the screening and other effects in their calculations. Thus the Hamaker Coefficient A_{132} becomes:

$$A_{132} = \frac{3}{4}\pi\hbar\int_0^\infty \left[\frac{\varepsilon_1(i\zeta)-\varepsilon_3(i\zeta)}{\varepsilon_1(i\zeta)+\varepsilon_3(i\zeta)}\right]\left[\frac{\varepsilon_2(i\zeta)-\varepsilon_3(i\zeta)}{\varepsilon_2(i\zeta)+\varepsilon_3(i\zeta)}\right]d\zeta \qquad (2.42)$$

Where, $\varepsilon_1(i\zeta)$ is the dielectric constant of material j, along the imaginary i, frequency axis ($i\zeta$) which can be obtained from the imaginary part $\varepsilon_1''(\omega)$ of the dielectric constant $\varepsilon_1(\omega)$.

This equation was further approximated by (Ninham and Parsegian, 1970; Isrealachvili, 1972; Nir et al, 1972; and Visser, 1975) since it is rather difficult to use.

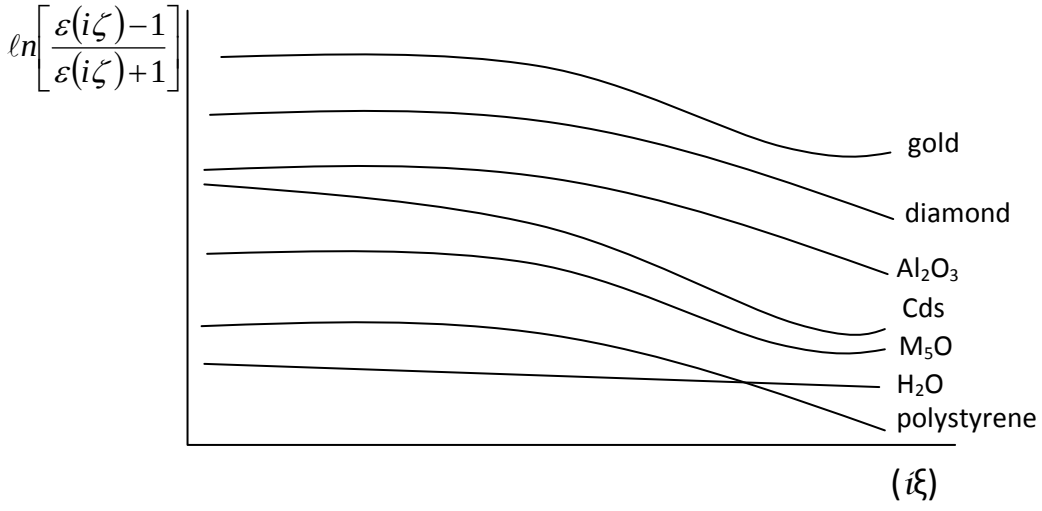

Fig. 2.12: Plot of ln{[ε (iζ) – 1]/[ε (iζ) + 1]} as a function of (iζ) for various materials *(Visser, 1981)*

The "physical" meaning of equation (2.42), was demonstrated by (Krupp, 1967) in showing that the factor $\ell n\left[\frac{\varepsilon(i\zeta)-1}{\varepsilon(i\zeta)+1}\right]$ as a function of (iζ) can be represented by a curve of the same shape.

For a group of materials like polymers, the curves are identical while starting at a different position at zero frequency. Applying the absorption data of polystyrene, the value of A_{11} becomes:

$$A_{11} = 2.5\left[\frac{\varepsilon_{10}-1}{\varepsilon_{10}+1}\right]^2 = 2.5\left[\frac{n_1^{\,2}-1}{n_1^{\,2}+1}\right]^2 \qquad (2.43)$$

Where ε_{10} is the dielectric constant and n_1 the refractive index of the polymer at zero frequency, both being bulk material properties which can easily be obtained.

A further deduction for a case of proper choice of materials for which the Lifshitz-Hamaker Constant will be negative was investigated. For the hypothetical combinations of material as in table (2.2) below negative values could be calculated using optical data of the materials and the corresponding computer programme provided by Dr. Krupp and his co-workers (Krupp, 1967).

Table 2.2: **Combinations of Materials for which Negative Lifshitz-van der Waals Coefficient A_{132} is found** *(Hamaker, 1937)*

System	A_{132} /eV
Si/Al_2O_3	- 0.19
Ge/Cds/olystyrene	- 0.28
Cu/MgO/KCl	- 0.17
Au/Si/KCl	- 0.81
Au/Polystyrene/H_2O	- 0.14

The table (2.2) consists in systems that the individual Lifshtiz-Hamaker constants obey equation (2.37). This implies that in the macroscopic theory of van der Waals forces there are situations where the van der Waals force of three different materials can be negative. This therefore demonstrates that the concept of negative van der Waals force is physically sound.

2.21.1. Separation of Antigens and Antibodies

Antigen-antibody bonds are principally Coulombic (electrostatic) and/or van der Waals-London bonds (van Oss and Grossberg, 1979). Some antigen-antibody systems interact solely by van der Waals interactions (Grossberg and Pressman, 1962) while others do so through a combination of Coulombic and van der Waals bonds. The combination method is always more operative due to the small separation distances between antigenic determinant and antibody active site (van Oss and Neuan, 1977). Hapten3-azopyridine (P_3) when coupled to rabbit serum albumin (P_3A) precipitates quite well with rabbit anti-P_3 (which is elicited with P_3 coupled to bovine gamma globulin) (Grossberg and Pressman, 1962).

Thus the precipitating P_3A-anti-P_3 system was extensively studied, as an exclusively van der Waals-London interaction system and compared with a typical combined van der Waals and Coulombic precipitating system namely bovine serum albumin-goat anti-bovine serum albumin (BSA-anti-BSA) (Neuman et al, 1974).

The following discoveries were made: P_3A-anti-P_3 precipitates can be dissociated at neutral pH at $\gamma \approx$ 50dynes/cm ($5x10^{-2}$N/m). The prevention of P_3A-anti-P_3 precipitate formation is attained at $\approx$ 62dynes/cm ($6.2x10^{-2}$N/m). Lower surface tension is needed for the complete dissociation of P_3A-anti-P_3 precipitates than for the prevention of their formation because once an antigen-antibody precipitate is formed; part of the interstitial liquid between antigenic determinant and antibody-active site is expelled. This condition tends to strengthen the antigen-antibody bond, so that it requires more energy to dissociate such a bond, once formed, than to prevent its formation (Neuman et al, 1974).

Precipitates of the combined Coulombic-van der Waals-London system BSA-anti-BSA could not be dissociated at neutral pH at surface tensions of the liquid medium below even 48 dynes/cm ($4.8x10^{-2}$N/m). Likewise, the precipitation of BSA-anti-BSA at neutral pH could not be prevented at surface tensions of the medium below 52dynes/cm ($5.2x10^{-2}$N/m). Also, at the surface tension of water and pH values as low as 3 or as high as 9.5, BSA-anti-BSA precipitates could not be dissociated. Only lowering the surface tension of the liquid to $\approx$ 50dynes/cm ($5x10^{-2}$N/m) and lowering the pH at 4.0 or raising it to 9.5, would result in dissociation of BSA-anti-BSA (Neuman et al, 1974). By electrophoresis it could be demonstrated that in mixed systems as these, the dissociation of antigen-antibody complexes by this method is quite complete (van Oss et al, 1979).

The surface tension of the liquid medium can conveniently be lowered by the addition to the buffer of ethylene glycol, dimethyl sulfoxide or propanol. Concentrations of propanol ≈ 0.25 to 0.50% which lowers the surface tension of water to respectively 59 and 52 dynes/cm ($5.9x10^{-2}$N/m and $5.2x10^{-2}$N/m) generally suffice. Propionic acid is popular and efficacious in the dissociation of antigen-antibody bonds as its low concentrations readily lower the pH of water to below 4.0 and its surface tension below 44 dynes/cm ($4.4x10^{-2}$N/m). Citric acid, acetic acid and acid glycine act in the same manner.

P_3A-anti-P_3 complexes dissociated with ethylene glycol solutions will re-precipitate upon removal of the ethylene glycol by dialysis (Neuman et al, 1974). With the P_3A-anti-P_3 system the γ_{1V} of the antibody-active site probably is close to ≈ 65dynes/cm ($6.5x10^{-2}$N/m) and γ_{2V} of the antigenic determinant as low as ≈ 40dynes/cm ($4x10^{-2}$N/m).

The deductions here is that in immunochemical systems also, van der Waals interactions can be given a net negative value (i.e. they can be changed from attractive to repulsive interactions) by lowering the surface tension of the liquid medium to a value intermediate between those of the two different interacting sites. This approach to the dissociation of antigen-antibody bonds has a considerable impact on a variety of analytical and preparative immunochemical procedures; it opens new possibilities in the determination of antigen-antibody ratios in circulating antigen-antibody complexes from animals or patients with immune complex disease (van Oss et al, 1979), the quantitative elution of blood group antibodies from erythrocytes (van Oss et al, 1979), the study of the influence of various salts on the dissociation of coulombic antigen-antibody bonds under

conditions of zero (or slightly negative) van der Waals attraction ((van Oss et al, 1979), and finally, in the improvement of the methods used in immuno-adsorption as earlier discussed in affinity chromatography.

2.21.2. Separation of Proteins by Hydrophobic Chromatography

Polymeric biological substances, such as protein and polysaccharides have their surface tensions lower than water which is their natural solvent. They will be less attracted to the hydrophobic "low energy" surfaces in water due to a net positive van der Waals interaction. The biopolymers can be made to adhere to the hydrophobic surfaces as a result of van der Waals interactions. They can also be made repulsive by lowering the surface tension of water to a value below that of a polymer and thus causing it to elute. This mechanism of separation method is called hydrophobic chromatography (van Oss et al, 1972).This research had earlier revealed that elution of protein from hydrophobic surfaces could be enhanced by the addition of organic solvent such as ethylene glycol (van Oss et al, 1979; Doellgant and Fishman, 1974).

Phenyl-sepharose as well as octyl- sepharose had also been used in hydrophobic chromatography of proteins (Stjernstrom et al, 1977). A study was made of the elution of proteins from whole human serum, after adsorption onto phenyl-sepharose, and from the concentrations (and thus the surface tensions) of ethylene glycol corresponding to the maximum concentration of each of the eluted protein fractions (van Oss et al, 1979). The free energy of detachment ΔF_{132} and the values of combined Hamaker coefficients for each eluted protein were calculated (table 2.3).

Table 2.3: Hydrophobic Chromatography on Phenyl-Sepharose of Whole Human Serum *(London, 1930)*

Eluted Protein	γ_{1V} **Protein (dynes/cm)**	γ_{3V} **of eluant (dynes/cm)**	ΔF_{132} **Protein (ergs/cm^2)**	A_{132} **Protein (x10^{-14}ergs)**
α_2 macroglobin	70.6	67.3	+ 3.5	- 4.3
Serum albumin	70.2	64.0	+ 5.4	-6.6
α_2 HS glycoprotein	68.1	59.0	+ 5.6	-6.8
β_{1C}- β_{1A} (C3)	67.8	56.0	+ 5.8	-7.1
Immunoglobulin G	67.2	54.0	+ 5.6	-6.8
Transferrin	66.8	53.0	+ 5.3	-6.5

** Assuming the separation distance $d_0 \approx 1.8$Å

The γ_{2V} of the adsorbent (phenyl-sepharose) = 40.9 dynes/cm (4.09x10^{-2}N/m).

The six proteins came off the column in the order of their decreasing surface tension γ_{1V} as the surface tension γ_{3V} of the eluant solution decreased. The free energies of detachment ΔF_{132} values were all positive which favoured detachment. The Hamaker Coefficients A_{132} were all negative which imply a net van der Waals repulsion and higher values are in comparison with those obtained in earlier treated phenomena.

This reveals that hydrophobic chromatography in which solutes (and/or particles) are attached to the adsorbent surface occurs principally by van der Waals attraction. Here the surface tension of the liquid medium is higher than those of the solutes (and/or particles) and the adsorbent. Elution thus occurs when the van der Waals attraction is changed into a repulsion by lowering the surface tension of the

liquid to a value intermediate between that of the solutes (and/or particles) and the adsorbent.

Also, solutes may be attached to the adsorbent when the surface tension of the liquid is lower than that of both solutes and the adsorbent. In this case, elution can occur by increasing the surface tension of the liquid to a value in between the surface tensions of the solutes and the adsorbent.

In polar liquids, like water, electrostatic interactions are inevitable. A means of partially eliminating this effect is by the addition of salt. However, too high a salt concentration in the elution step should be avoided since most salts can create an increase in the surface tension.

2.21.3. Separation of Polymer in Solution by Phase Separation

Many studies have been published on the phase separation of polymer solutions (van der Esker and Vrij, 1976). The same treatment used in the interpretation of engulfment versus rejection of particles by a solidification front was applied to the prediction of compatibility or separation of polymer pairs in solution (Omenyi, 1978). A negative Hamaker coefficient A_{132} for the interaction of two different polymers 1 and 2 in the solvent 3 implies repulsion between the two types of polymer molecules. As A_{131} and A_{232} are always, like molecules will always attract each other. Thus, a negative A_{132} favors phase separation.

Evidently, in all cases where the combined Hamaker coefficient A_{132} is unmistakable positive, the polymer pairs exert a van der Waals attraction on each other, in their respective solvents, and are compatible. Clearly, polymer

compatibility or separation in ternary systems also conforms well to the theory developed by van der Waals. Attraction allows compatibility or separation of polymer pairs dissolved in a given common solvent, whilst a negative (repulsive) net van der Waals interaction results in polymer separation.

2.21.4. Separation of Particles by Advancing Solidification Fronts

The engulfing, or rejection, of solid particles suspended in a melt, by advancing solidification front can be of great importance in science and engineering as a separation method. Various surface thermodynamics as well as fluid dynamics, treatment of particle engulfment or rejection phenomena at solid- liquid interfaces have been published (Omenyi et al, 1980; van Oss et al, 1975). In biology, the engulfment of bacteria by phagocytes is major defensive mechanism against infective invaders, whilst the ability of bacteria to be rejected by phagocytes is the principal mechanism by which many pathogenic bacteria achieve virulence (Omenyi et al, 1980; Omenyi, 1978). The advancing solidification front method has also been proposed as a procedure for separating particles according to size (Kua and Wilcox, 1973). Particles with diameters varying between 0.2 and 0.01mm, consisting of acetal, nylon-6,nylon-6,6,nylon-12, nylon-6,10, nylon-6,12,polystyrene particles, Teflon, and siliconized glass were used. However, the surface tensions of solid particles and Hamaker coefficient A_{132} determined by contact angle method (using equation of states) for particle 1,suspended in liquid naphthalene 3, and with solidified naphthalene 2, was found with the help of equations (2.29) and (2.30). Table 2.4 compares the combined Hamaker coefficient A_{132} found for various particles, with an advancing solidification front, with an advancing naphthalene solidification front with their engulfment, or rejection by the solidification melt.

Table 2.4: Hamaker Coefficient A_{132} at 80°C, Compared with Rejection or Engulfment of Various Particles by an Advancing Solidification Front of Naphthalene *(Vroman and Adams, 1967)*

Nature of particle	A_{132} in 10-14 ergs	Particle behavior
Acetal	-3.27	Rejection
Nylon-6	-2.81	Rejection
Nylon-6,6	-2.67	Rejection
Nylon-12	-1.97	Rejection
Nylon-6,10	-0.92	Rejection
Nylon-6,12	+ 0.35	Engulfment
Polystylene	+ 2.01	Engulfment
Teflon	+ 6.43	Engulfment
Siliconed glass	+ 8.28	Engulfment

2.22. Relationship between Hamaker Coefficients and Free Energy of Adhesion ΔF^{adh}

For all given combinations, it is possible to express ΔF^{adh} in terms of van der Waals energies. For instance, for a flat plate/flat plate geometry:

$$\Delta F_{12}^{adh}(d_1) = -\left[\frac{A_{12}}{12\pi d_1^{\,2}}\right] \tag{2.44}$$

$$\Delta F_{132}^{adh}(d_0) = -\left[\frac{A_{132}}{12\pi d_0^{\,2}}\right] \tag{2.45}$$

The surface tension approach has proved valid against the backdrop of surface tensions being directly accessible to experimental investigations and do not include the dispersion or van der Waals contribution to the interaction only. On the basis of

these results and in line with (van Oss et al, 1979), the bulk van der Waals interaction term A_{132} would rather be referred to as the Hamaker coefficient rather than the Hamaker Constant. It is only the case of a material interacting with itself through a vacuum is the Hamaker constant A_{11} a constant, with its own specific equilibrium interfacial separation distance. Some indications as to equilibrium separation distances can be obtained from calculations on noble gases where only van der Waals forces are operating and as published by Abramzon. Distances between the electron clouds of helium, neon, xenon, argon and krypton are given as 2.36, 1.65, 2.05, 1.82 and 2.59Å respectively, indicating that the interfacial separation distance can indeed be a variable, that its magnitude is lower than originally proposed by (Krupp, 1967) as 4Å but in line with the values obtained in the calculations of van Oss of 1.82Å. Thus the following deductions were made by (Visser, 1981); (i) the occurrence of van der Waals repulsion for component systems can be demonstrated experimentally as well as theoretically, (ii) the use of the term Hamaker constant is limited and should be replaced by Hamaker coefficient, (iii) interfacial separation distances between solid bodies are variable depending on the materials involved, in particular immersion of a system in a liquid can alter the equilibrium position between the adherents, (iv) surface tension data are the most useful tool to predict conditions for three-component systems to be repulsive leading to phase separation.

Based on Hamaker's classical paper on the London-van der Waals attraction between spherical particles, the concept of negative Hamaker coefficients was introduced and the conditions for attaining negative values were given (Visser, 1981). This concept is also valid with respect to the Lifshitz macroscopic theory of interaction between solid bodies. The van der Waals forces can be expressed in terms of a geometrical term and a material dependent contribution. Hamaker

succeeded in expressing the material part in terms of molecular properties of the materials involved. A detailed study of van der Waals forces revealed that in the case of a three- component system, the corresponding Hamaker Coefficient A_{132} could attain a negative value given the conditions stated:

$$A_{11} < A_{33} < A_{22} \text{ or } A_{11} > A_{33} > A_{22} \quad (2.46)$$

Where; A_{11}, A_{22} and A_{33} are the individual Hamaker Constants of components 1, 2 and 3 respectively.

The implication of this is that two adhering bodies 1 and 2 of different composition will separate spontaneously upon immersion in a liquid 3 provided the conditions given by equation (2.46) are fulfilled.

2.23. Adhesion of Platelet to a Homogeneous Solid Surface

Neumann et al, (1975) adopted a simplified approach using a situation in which the platelet is adsorbed out of a suspension in saline on to a smooth homogeneous solid surface. This avoided the detailed and rather complicated real life case where the surface of biomaterials are actually rough and heterogeneous and the incidence of adsorption of proteins from the plasma. They set up a simple experiment where a study of the attachment of a platelet P, originally suspended in a liquid L to a smooth and homogeneous solid surface S was conducted. This process thus generated a new platelet/substrate PS interface while eliminating the initial platelet/liquid PL and substrate/liquid SL interfaces. The work done per unit area in annihilating or generating these various interfaces is the interfacial tension γ_{ps}, γ_{pl} or γ_{sl}. The overall work done per unit area in the platelet attachment is then given by the change in the Helmholtz free energy, ΔF^{adh}:

$$\Delta F^{adh} = \gamma_{ps} - \gamma_{pl} - \gamma_{sl} \qquad (2.47)$$

If ΔF^{adh} is negative, then the contact between platelet and substrate will be permanent. On the other hand, if ΔF^{adh} is positive, then a contact will not result in adhesion.

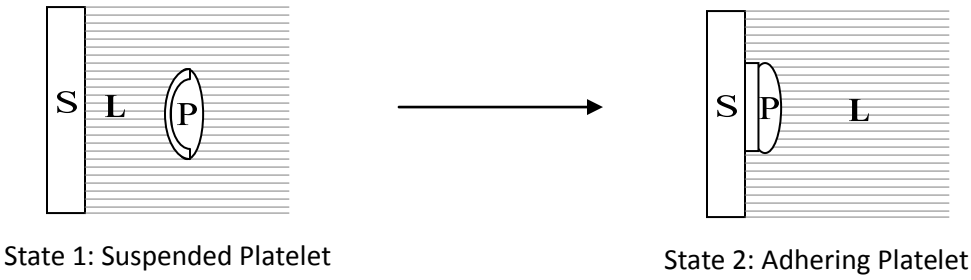

Fig.2.13: Process of Platelet Adhesion to a Surface (P: Platelet, L: Suspending Liquid, S: Substrate) *(Neuman et al, 1975)*

A thermodynamic prediction about platelet adhesion was made by obtaining numerical values for the surface tensions γ_{ps}, γ_{sl} through quantitative interpretation of contact angles. The solid/liquid interfacial tensions can be expressed in terms of the solid/vapor and liquid/vapor interfacial tensions as follows (Omenyi et al, 1980):

$$\gamma_{sl} = f(\gamma_{sv}, \gamma_{lv}) \qquad (2.48)$$

An explicit expression for this relation is given by Neumann equation (2.49):

$$\gamma_{sl} = \left[\frac{\left(\gamma_{sv}^{1/2} - \gamma_{lv}^{1/2}\right)^2}{1 - 0.015(\gamma_{sv}\gamma_{lv})^{1/2}} \right] \qquad (2.49)$$

Introducing the Young contact angle to this equation results in Young's equation.

$$\gamma_{sv} - \gamma_{sl} = \gamma_{lv} \cos \Theta_Y \qquad (2.50)$$

Where Θ_Y is the Young contact angle and defined as follows:

$$Cos\theta_Y = \left[\frac{(0.015\gamma_{sv} - 2.00)(\gamma_{sv}\gamma_{lv})^{1/2} + \gamma_{lv}}{\gamma_{lv}\{0.015(\gamma_{sv}\gamma_{lv})^{1/2} - 1\}} \right] \qquad (2.51)$$

Equation (2.51) enables the derivation of γ_{sv} from a single pair of data (γ_{lv}, Cos Θ_Y) since the surface tension γ_{lv} and the contact angle Θ_Y are readily measured. This is important in the investigation of biological systems, where contacting of the substrate by any liquid other than water (or isotonic saline) may result in changes of the substrate. Having obtained the value of γ_{sv} from equation. (2.51) the value of the corresponding γ_{sl} is calculated from Young's equation [i.e. equation (2.50)]. Alternatively, using equation (2.47), γ_{sl} may be obtained from γ_{lv} and contact angle data on platelets [where the index P replaces S in equations (2.48) to (2.51)]. Hence applying equation (2.49), γ_{lv} is replaced by γ_{pv} to obtain the interfacial tension γ_{ps} between platelet and substrate. The ΔF^{adh} value can be obtained from contact angles and liquid surface tensions γ_{lv}. This thermodynamic approach has been successfully applied to in vitro phagocytosis of various bacteria by human neutrophilis. The thermodynamics of phagocytosis is somewhat more complicated than that for the adhesion of platelets to substrates. Phagocytosis will occur when the free energy changes and all the various steps involved in the engulfment are negative. Thermodynamic predictions of phagocytosis have not only been borne out by in vitro phagocytosis experiments, but have also been corroborated by in vitro bacterial pathogenicity determinations (Gillman and van Oss, 1971; Neumann et al, 1974). It follows that since the theory of surface thermodynamics has been successfully applied to a biological process involving cellular adhesion, it is likely that platelet adhesion can be similarly understood (Neumann et al, 1975).

2.24. Adhesion of Platelet in the Absence of Proteins

van Oss et al, (1972) noted in their work that contact angle data for various liquids in contact with biomaterials have been available a longtime before 1972 while contact angle values for platelets in contact with isotonic saline became available only shortly before the year in question (Girifalco and Good, 1957). Using values of $\Theta_Y = 16.3^o$ and $\gamma_{lv} = 72.8 ergs/cm^2$ ($7.28x10^{-2} J/m^2$) they obtained from equation (2.31) a value of $\gamma_{pv} = 70.0 ergs/cm^2$ ($7.0x10^{-2} J/m^2$). ΔF^{adh} was calculated as a function of γ_{sv} (the surface tension of biomaterials) and whether high or low γ_{sv} values were more conducive to platelet adhesion was determined. A plot of ΔF^{adh} against γ_{sv} for two different values of γ_{lv} was made as in figure 2.14. Curve A is for $\gamma_{lv} = 72.8 ergs/cm^2$ i.e. $7.28x10^{-2} J/m^2$ (the surface tension of water or isotonic saline) while curve B for $\gamma_{lv} = 63.4 ergs/cm^2$ i.e. $6.34x10^{-2} J/m^2$ (the surface tension of glycerol). Curve A is typical for the condition where $\gamma_{lv} > \gamma_{pv}$ and curve B for the situation where $\gamma_{lv} < \gamma_{pv}$

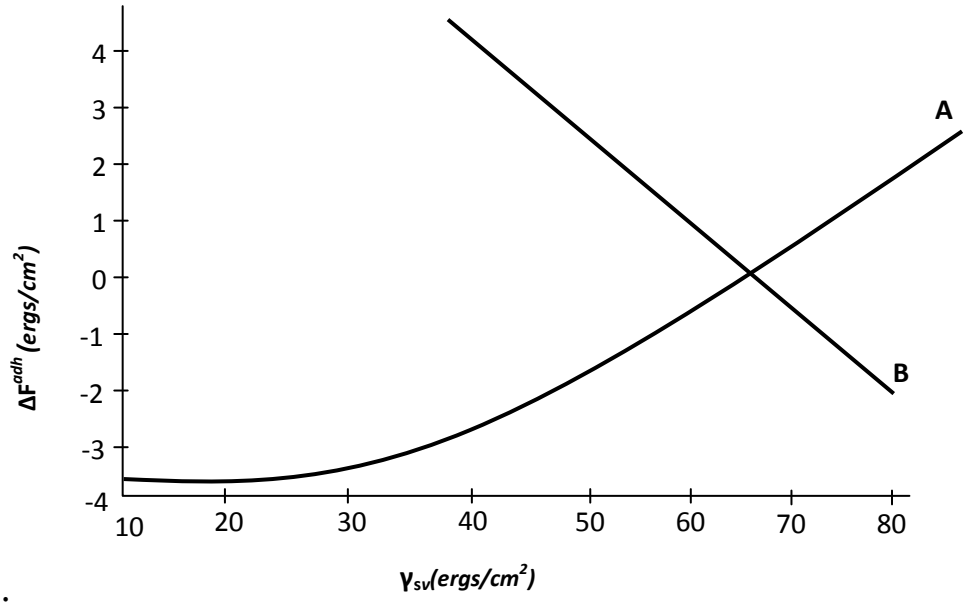

Fig.2.14: Dependence of ΔF^{adh} on γ_{sv} (A: $\gamma_{lv} > \gamma_{pv}$, B: $\gamma_{lv} < \gamma_{pv}$) *(Neumann et al, 1975)*

Deductions from thermodynamics of phagocytosis show that free energy differences well below 1.0erg/cm^2 (1.0x10^{-3}J/m^2) favour cellular adhesion and transport processes (Neuman et al, 1975). In some special cases however $\gamma_{lv} = \gamma_{pv}$ and $\Delta F^{adh} = 0$ independent of γ_{sv}. The thermodynamic model on which figure (2.13) was based predicts that where $\gamma_{lv} > \gamma_{pv}$ platelet adhesion (i.e. negative ΔF^{adh}) will increase with decreasing γ_{sv}, and where $\gamma_{lv} < \gamma_{pv}$ platelet adhesion will decrease with decreasing γ_{sv}.

2.25. Adhesion of Platelet in the Presence of Proteins and Non-ideal Surfaces

After a biomaterial is brought in contact with blood, a layer of protein rapidly builds up on the surface of the solid (Vronman and Adams, 1967). This in consequence changes the surface tension γ_{sv} of the solid. Values for the high and low energy patches on the solid surface could be obtained from the resulting contact angles, however, equation (2.47) would no longer represent the free energy of platelet adhesion unambiguously. If the surfaces are rough, with lateral dimensions of rugosities or crevices above approximately 1000Å, contact angle hysteresis will be produced, distinct from that due to heterogeneity (Neumann et al, 1971). The advancing and receding contact angles measured on rough surfaces are not Young contact angles and are not inserted into Young's equation nor into the equation of state relationships. Neumann et al, (1971) in their work for these reasons could only estimate the surface tensions of solids from contact angle measurements on rough surfaces. The reason lies in the fact that the presence of proteins could cause complications in the surface tension of platelets i.e. absorption of proteins could affect γ_{pv}. On a rough surface, difficulties may arise from nucleation or entrapment of gas or air bubbles. Platelets are more readily absorbed at the blood-gas interface and in larger numbers than on most biomaterials. The

number of platelets adhering to a biomaterial could therefore be more a function of the number of surface imperfections than a function of the surface thermodynamic properties of the biomaterial (Neuman et al, 1975). The following conclusions could thus be derived from the studies made;

- Theoretical and experimental means are available for a thermodynamic analysis of attachment of platelets from a suspension in saline on to smooth and homogeneous solid surfaces.

- The thermodynamic analysis shows that the relative magnitude of the surface tension of the platelets and the liquid in which they are suspended are of critical importance. A decrease in platelet adhesion results when the surface tension of the liquid is greater than the surface tension of the platelets while an increase in platelet adhesion is as a result of the surface tension of the liquid being less than that of the platelets, with of course increasing γ_{sv}.

- The presence of plasma proteins, roughness, and heterogeneity of the biomaterial introduce considerable difficulties. The roughness of the biomaterials induces considerable platelet adhesion by means of stabilization of gas pockets.

2.26. Repulsive Van der Waals Interaction between Particles

Neumann et al, (1983) studied the repulsive van der Waals interactions between two dissimilar materials in liquid as predicted by Lifshitz theory. They studied this phenomenon with a number of polymeric particles in naphthalene and found that the particles are either rejected or show engulfment by the solidification front. Engulfment of the particles depends on the speed of solidification. At lower speed,

particles are rejected while at higher speed, the particles are engulfed due to hydrodynamic drag forces. Using dimensional analysis, (Neumann et al, 1983) developed equation (2.52):

$$\Delta F^{adh} = 2.64X10^{5} \frac{\rho_L^{0.847} T^{0.280} k_p^{0.720}}{\mu^{0.127} \left(\rho_p C_p\right)^{0.441}} D^{0.407} V_c^{0.847} \qquad (2.52)$$

Equation (2.52) provides a novel to estimate the free energy of adhesion ΔF from the advancing solidification front. The free energy of adhesion can further be decomposed according to equation (2.53):

$$\Delta F^{adh} = \gamma_{PS} - \gamma_{PL} - \gamma_{SL} \qquad (2.52)$$

Neumann used equation (2.52) to determine the surface free energy of several polymer particles (table 2.5).

Table 2.5: Surface Tension Values of Several Polymers Obtained from Advancing Solidification

Particle material	**Surface free energy (mJ/m^2)**
Acetal	44.3
Nylon – 12	40.6
Nylon- 6,12	34.0
PVC	32.7
PMMA	35.3

This technique was found to be applicable not only to various polymers but with biological cells at the interface. The interfacial tension between two surfaces can be written:

$$\gamma_{12} = \gamma_{12}^{LW} + \gamma_{12}^{AB} \qquad (2.54)$$

Equation (2.54) can be reduced as:

$$\gamma_{12} = \left(\sqrt{\gamma_1^{LW}} - \sqrt{\gamma_2^{LW}} \right)^2 + \left(\gamma_1^{AB} + \gamma_2^{AB} - W_{12}^{AB} \right) \qquad (2.55)$$

The LW component of the interfacial tension is always positive, whereas the AB component of the interaction can have a negative value, since neither acid nor a base interacting with each other are self-associative. In this case the AB component of the interfacial tension is negative.

Chuadhury, (1984) stated that a negative interfacial tension implies that the interface will disintegrate accompanied by chaotic and dissipation transport unless there are other mechanisms to stabilize the surface.

2.27. Intermolecular Interactions/Van der Waals Interaction

J.D van der Waals, when studying in 1873 the deviation of a real gas behavior from the ideal gas law, proposed the idea that there exist non- covalent and non-electrostatic interactions (apolar interactions) between neutral atoms and molecules. These electrodynamics intermolecular forces collectively called van der Waals forces originated from three distinct interactions, Keesom, Debye and London. While these three kinds of interactions have distinct origins, they have in common the fact that their interaction energies decay rapidly with the sixth power of their inter-atomic or molecular distance

Namely:

$$W(r)keesom = -\frac{U_1^2 U_2^2}{3(4\pi\varepsilon_0)^2 kT r^6} \quad (2.56)$$

$$W(r)Debye = -\frac{\alpha U^2}{(4\pi\varepsilon_0)^2 r^6} \quad (2.57)$$

$$W(r)London = -\frac{3h\nu\alpha^2}{(4\pi\varepsilon_0)^2 r^6} \quad (2.58)$$

Equations (2.56 - 2.58) are referred to as interaction in vacuum. Of the three interactions, Keesom and Debye interactions require that molecules have permanent dipole moments and are therefore not present in all materials. The already small Keesom interaction is virtually completely screened out, especially in aqueous media which contain electrolytes. London, (1930) treated the interacting two atomic systems as dynamic and attributed van der Waals to the dispersion effect. The dispersion effect is the interaction between the instantaneous dipoles formed in the atoms by their orbiting electrons. London dispersion forces are the dominant and the most forces in much system. The dispersion forces play a role in a host of important phenomena such as adhesion, surface tension, wetting, physical adsorption, the flocculation of particle, the properties of gases, liquids and thin films, the strength of solids and others. The energy of interaction between atoms i and j separated by a distance H is given as:

$$E = -\frac{\lambda_{ij}}{H^6} \quad (2.59)$$

Where $\lambda_{ij;}$ is the London constant, whose value depends on the atomic numbers of the two interacting atoms. Equation (2.59) is valid only at distances less than the wavelength of the major electronic adsorption band for the gas due to the transition

from the ground state to an excited electronic state. At separations greater than this, retardation effects become of importance and the attractive energy is inversely proportional to H. Retardation effects are caused by the fact that the electromagnetic field has to travel father at greater separations. By the time the field influences the neighboring atom, the original atomic dipole has changed its orientation. This effect causes the interaction to be slightly out of phase. The attraction energy is still attractive but has been reduced.

Van der Waals forces exist not only between individual atoms and molecules but also between particles. Hamaker used the additivity concept proposed by (London, 1930) to determine the equations for the van der Waals forces between particles. The additivity concept allows the force to be calculated based on the interaction between individual atoms making up the particles. The non- retarded energy between two particles, 1 and 2, of volumes v_1 and v_2 containing q_1 and q_2 atoms per cm^3 is shown in equation (2.60):

$$E = -\frac{\int v_1 d v_1 \int v_2 d v_2 q_1 q_2 \lambda_{1,2}}{H^6} \qquad (2.60)$$

The van der Waal force will be given by:

$$F_{VDW} = \frac{\partial E}{\partial H} \qquad (2.61)$$

Equation (2.60) combined with equation (2.61) has been solved for the van der Waals force equations between bodies of regular geometric form (London, 1930).

Case 1: For two spheres of radii R_1 and R:

$$F_{VDW} = \frac{AR}{12H^2} \qquad (2.62)$$

Where R equals the reduced radius:

$$R = \frac{2R_1 R_2}{R_1 + R_2} \tag{2.63}$$

and A is called Hamaker's coefficient (or constant) and equals (for Hamaker's development):

$$A = \pi^2 q_1 q_2 \lambda_{1,2} \tag{2.64}$$

Case 2: For a sphere of radius R and a plane surface:

$$F_{VDW} = \frac{AR}{6H^2} \tag{2.65}$$

Case 3: For two plane surfaces, the solution of equations (2.59) and (2.60) is expressed as a pressure, p, or van der Waals force per unit area of contact:

$$F_{VDW} = \frac{\partial F_{VDW}}{\partial A} = \frac{A}{6\pi H^3} \tag{2.66}$$

Equations (2.55), (2.56) and (2.57) describe non- retarded van der Waals forces for perfectly smooth surfaces. The approach of Hamaker assumes complete additivity of forces between individual atoms and is called the microscopic approach to van der Waals forces.

Lifshitz, (1961) developed the macroscopic theory (also called the modern or continuum theory) of van der Waals forces between and within continuous materials. He argued that the concept of additivity was unsatisfactory when applied to closely packed atoms in a condensed body. He attributed the non- addititvity to the thermodynamic fluctuations always present in the interior of a material medium.

2.28. Lifshitz - van der Waals Interaction

The surface tension γi ie the surface free energy per unit area of a liquid in vaccum is equal to one half the free energy of cohesion (ΔG_{ii}) and opposite in sign:

$$\gamma_i = -\frac{1}{2}\Delta\gamma_{ii} \qquad (2.67)$$

For solids, equation (2.58) is equally true but solids differ from liquids in that $\Delta\gamma_{ii}$ is not their free energy of cohesion, but just the free energy available for interacting with liquids. Fowkes proposed that surface free energy of materials could be considered to be the sum of the components resulting from each class of intermolecular interaction:

$$\gamma_i = \frac{\sum\gamma_{ij}}{j} \qquad (2.68)$$

Where; the γ_j term represent the specific contributors eg hydrogen bonding, dipolar, dispersion etc.

Using the Liftshitz approach for van der Waals interaction in condensed media, (Chaudhury, 1984) experimentally demonstrated that dispersion (London), induction (Debye) and dipole (Keesom**)** contributions to the Lifshitz-van der Waals or (apolar) components of the surface tensionγ^{LW} are additive:

$$\gamma^{LW} = \gamma^{L} + \gamma^{D} + \gamma^{K} \qquad (2.69)$$

Thus, it follows that on a macroscopic level, the three types of van der Waals interactions; (Keesom, debye and London) can be treated together as the total of apolar, or Lifshitz- van der Waals (LW) interaction. The interfacial tension γ_{12} between two different materials 1 and 2 is one of the most important concepts in colloidal and surface science as it leads directly to a quantitative expression for the

free energy of inter-particle or intermolecular interaction in condensed phase system. Interfacial tensions between two reasonably immiscible liquids can be measured, but interfacial tensions between solid and liquid and between solid and solids cannot be determined directly. It thus becomes important to arrive at these interfacial tensions γ_{12} via the surface tension γ_1 and γ_2 of the interacting materials 1and 2. Good and Grifalco and Fowkes demonstrated experimentally that if only dispersion interaction forces are available between two condensed phase materials e.g a solid and a liquid, the interfacial tension between them is given by the following equations:

$$\gamma_{12}^{LW} = \left(\gamma_1^{LW} - \gamma_2^{LW}\right)^2 \tag{2.70}$$

or,

$$\gamma_{12}^{LW} = \gamma_1^{LW} + \gamma_2^{LW} - 2\sqrt{\gamma_1^{LW}}\,\gamma_2^{LW} \tag{2.71}$$

If we recall equation (2.67), the polar component of the free energy of cohesion of material 1 is:

$$\gamma_{ii}^{LW} = -2\gamma_1^{LW} \tag{2.72}$$

The free energy of interaction between materials 1 and 2 in vacuum is related to the surface tension by the Dupre equation:

$$\Delta\gamma_{12}^{LW} = \gamma_{12}^{LW} - \gamma_1^{LW} - \gamma_2^{LW} \tag{2.73}$$

Substituting equation (2.71) into equation (2.72):

$$\Delta\gamma_{12}^{lw} = -2\sqrt{\gamma_1^{LW}}\,\gamma_2^{LW} \tag{2.74}$$

This equation states that the atoms at an interface are pulled by those in the neighboring phase. Since the Lifshitz-van der Waals forces are universal and

always available at the surface. Equation (2.74) also suggests that the energy of interaction is negative, ie the interaction energy between two purely polar condensed phases is always attractive. Similarly, the interaction energy between molecules of particles of material 1 immersed in a liquid 2 is:

$$\Delta\gamma_{121}^{LW} = -2\gamma_{12}^{LW} \tag{2.75}$$

The two different objects (1and 2) immersed in a liquid 3 are related to the interfacial tensions by:

$$\Delta\gamma_{132}^{LW} = \gamma_{12}^{LW} - \gamma_{13}^{LW} - \gamma_{23}^{LW} \tag{2.76}$$

Using equation (2.71) and (2.73) to expand the interfacial surface tensions in equation (2.76) gives:

$$\Delta\gamma_{132}^{LW} = -2\gamma_{3}^{LW} - 2\sqrt{\gamma_{1}^{LW}}\,\gamma_{2}^{LW} + 2\sqrt{\gamma_{1}^{LW}}\,\gamma_{3}^{LW} + 2\sqrt{\gamma_{2}^{LW}}\,\gamma_{3}^{LW} \tag{2.77}$$

Since from equation (2.74), it follows from equation (2.77):

$$\Delta\gamma_{132}^{LW} = \Delta\gamma_{33}^{LW} + \Delta\gamma_{12}^{LW} - \Delta\gamma_{13}^{LW} - \Delta\gamma_{23}^{LW} \tag{2.78}$$

This is the confirmation of the Hamaker combining rule obtained via a purely surface thermodynamic treatment.

2.29. Concept of Hamaker Coefficient

Hamaker's classical paper on van der Waals – London interactions (Hamaker, 1937) stated that a condition could arise under which the sign of the van der Waals interaction between two different uncharged bodies, surrounded by a liquid, might be negative, ie that such bodies would repel each other. This means that, if two particles are embedded in a fluid and the London-van der Waals force between particles and fluid is greater than between the particles themselves, it might be

thought that the resultant action will be a repulsion rather than attraction. Viser, (1981) found that when two materials are immersed in a liquid medium, and the interaction of each of these materials with that of the liquid medium is larger than the interaction between these materials themselves with the liquid; spontaneous separation can occur due to dispersion forces only. Omenyi et al, (1980) had shown theoretically and experimentally that the sign of the net van der Waals interaction between two different solid bodies or between two different dissolved macromolecules, in liquid, often is negative, (i.e. they repel one another), even when they are electrically neutral, and when they are immersed in apolar liquid. However, this new possibility of changing the attraction between different (even neutral) solids submerged in liquids, or dissolved macromolecules into repulsion can be regarded as a traditional separation method.

2.30. Thermodynamic Considerations in Particles Separations

Omenyi et al, (1980) stated the condition for particle engulfment is that the net change in free energy, ΔF_{NET}, for the process of particle engulfing is less than zero, ie, if

$\Delta F_{NET} \langle 0$, There will be particle engulfment, and if it is larger than zero.ie, if

$\Delta F_{NET} \rangle 0$, There will be particle rejection.

From the thermodynamic model given below, ΔF_{NET} for the process the engulfment of a sphere of unit surface area is given by:

$$\Delta F_{NET} = \Delta F_b + \Delta F_c \qquad (2.79)$$

The free energy of engulfing of a particle by the solid phase now reduces to:

$$\Delta F_{NET} = \gamma_{PS} - \gamma_{PL} \quad (2.80)$$

And the free energy of adhesion of a particle, originally suspended in the liquid, to the solid/liquid interface is:

$$\Delta F^{adh} = \gamma_{PS} - \gamma_{PL} - \gamma_{SL} \quad (2.81)$$

Where; γ_{ij} is the interfacial free energy.

Adhesion is expected when the free energy change from above equations is negative. If it is positive, repulsion is predicted (table 2.6). An experimental verification of this thermodynamic prediction was carried out using the experimental rig on Teflon, Polystyrene, Nylon, Siliconed glass and Acetal particles in biphenyl and naphthalene matrices. An agreement was obtained between actual observation and theory (table 2.6).

Table 2.6: Change in Free Energy and Thermodynamics Predictions
(Omenyi et al, 1980)

Matrice materials	**ΔFNET (mJ/m^2)**	**Prediction**
Biphenyl/silicone glass	-3.4	Engulfing
Biphenyl/Teflon	-2.6	Engulfing
Biphenyl/polystyrene	-0.1	Engulfing
Biphenyl/nylon	+2.5	Rejecting
Biphenyl/acetal	+2.7	Rejecting
Naphthalene/silicone glass	-3.5	Engulfing
Naphthalene/Teflon	-2.7	Engulfing
Naphthalene/polystyrene	-0.4	Engulfing
Naphthalene/nylon	+2.1	Rejecting
Naphthalene/acetal	+2.3	Rejecting

For the situation at which there is particles rejection is operative, the particle remain at the advancing solid – liquid interface. But with increasing rates of solidification, however, a viscous drag force is generated which opposes the thermodynamic repulsive force. When the two effects become equal, engulfment occurs.

2.31. Hydrophobic Chromatography of Cells

Since the early 1960's the property of polymorphonuclear granulocytes (PMN's) to adhere preferentially to nylon fibres has been utilized for the removal of these particular leukocytes from human blood. This is prior to transfusion of the blood to patients with anti-leukocyte antibodies who are prone to manifest a transfusion reaction (Greenwalt et al, 1962). The same property of PMN's has been used by (Djerassi et al, 1972) to adsorb these cells from the blood and subsequently to elute them and transfuse the isolated and concentrated PMN's into leukopenic patients. PMN's will only adhere well to hydrophobic surfaces when they remain endowed with multiple pseudopodia with a small radius of curvature. This feature allows them to overcome the electrostatic repulsion that would otherwise prevent a sufficiently close approach between cells and adsorbent to permit adhesion to ensue (van Oss et al, 1972; Higby, 1979; Miller, 1977). However, elution of PMN's from hydrophobic surfaces without damaging the cells is a difficult problem (Higby, 1979).

The elution of adherent cells can be much facilitated by lowering the surface tension of the liquid medium. Lymphoid cells contain subgroups of cells that adhere preferentially to hydrophobic surfaces (Miller, 1977). As long as phagocytic cells (macrophages, monocytes or PMN's) may be intermixed with the

lymphocytes, there is a likelihood that these will prove to be adherent cells (Golub, 1977).

The least toxic surface tension lowering agent appears to be dimethyl sulfoxide (DMSO), which has been successfully used as a cryprotectant with a variety of blood cells, e.g. erythrocytes, platelets (Sumida, 1973), lymphocytes (du Bois et al, 1976), and PMN's (Lionetti et al, 1975). It is however very essential to add the DMSO to the cells in an extremely gradual manner, in order to prevent osmotic damage (van Oss et al, 1972).

A study by (Omenyi and Synder, 1982) used electrostatic-van der Waals interaction mechanisms to explain the stability of erythrocyte suspensions layered on D_20 cushion in droplet sedimentation process. By lowering the surface tension of D_20 ($\approx 65 ergs/cm^2$ or $6.5x10^{-2} J/m^2$) by addition of varying concentrations of Dimethyl Sulfoxide (DMSO), the van der Waals attraction between cells was reduced to zero. The surface tension results of some biological cells, obtained by this technique as compared with those obtained by freezing front technique together with the combined Hamaker coefficients (to be discussed later) are given in table (2.7).

Table 2.7: Comparison of Surface Tension Data of Biological Cells Obtained from some Techniques (Omenyi, 1978)

Material	Surface Tension at Maximum DMSO Concentration γ_{iv} (ergs/cm^2)		Combined Hamaker Coefficients A_{131} (x10^{-15} ergs)
	Droplet Sedimentation	Freezing Front	
Chicken	65.2	65.1	5.08
Turkey	65.7	65.4	4.35
Canine	64.4	64.2	6.38
Horse	65.4	64.5	4.78
Human	64.3	64.1	6.55

(* corrected to 25^{o}C)

The findings by (Omenyi, 1978) could be summarized;

- An electrostatic repulsion-van der Waals mechanism was used successfully to study the stability of fixed erythrocyte suspensions layered on a D_2O cushion.
- The surface tension of the suspending liquid medium and hence the energy of attraction is lowered by the addition of DMSO to the liquid medium.
- The surface tensions of all the erythrocytes were found to be close to 65ergs/cm^2 (6.5x10^{-2}J/m^2) differing from each other by less than 2ergs/cm^2 (2x10^{-3}J/m^2).
- The technique of the determination of maximum stability with respect to droplet sedimentation may serve as an alternative method for the study of surface tensions of biological particles.

- The combined Hamaker coefficients, A_{131}, were found to be between $4.35x10^{-15}$ergs and $6.55x10^{-15}$ergs ($4.35x10^{-22}$J and $6.55x10^{-22}$J) for all the cells studied.

2.32. Experimental Evidence for Van der Waals Repulsion

After (Visser, 1981) had predicted that under certain conditions van der Waals forces could be repulsive, (Visser, 1981) noticed that (Fowkes,1967) had done the same for the system PTFE/glycerol/iron oxide on the basis of surface tension data of the materials involved. Smith, (2007) on the other hand conducted some special flocculation studies on mixtures of PTFE and graphite particles in water. On the basis of their surface tension data of 18.6, 110 and 72.8 respectively, a negative value for A_{132} could be predicted. It was discovered that no mutual flocculation could be detected whereas from the point of view of collision between the particles there was no reason for a selective flocculation. Thus the PTFE and graphite particles must repel each other. The first values of Hamaker constants having a negative sign were published by (Schulze and Cichos,1972) for the system of air bubbles on a quartz surface in water, where A_{132} was found to be $-1.1x10^{-13}$erg ($-1.1x10^{-20}$Joule) and by (Deryagin et al, 1972) for a system of air/tetradecane/quartz where A_{132} was derived to be $-0.76x10^{-13}$erg ($-0.76x10^{-20}$Joule). They also gave experimental evidence for negative Hamaker constants for the system oil/water/organic solvent (decane, benzene, xylene). Wittmann et al, (1971) had earlier indicated that the extremely low Hamaker constant for quartz could give rise to negative values for a large number of combinations with other materials when water was acting as a third medium. They also confirmed this and in particular for combinations with air and calculated negative values according to the procedure of Ninham and Parsegian, (1970) simplification of Lifshitz theory

for an n-hexane film on water to be $-2.18x10^{-14}$ergs ($-2.18x10^{-21}$Joule) and for an n-heptane film on water to be $-0.23x10^{-14}$ergs ($-0.23x10^{-21}$Joule). This is in accordance with experiments regarding spreading lens formation of these liquids on water. The particle engulfment or rejection measurements at solidification fronts of (van Oss et al, 1979) and the phase separation studies of polymer solutions by the same author were the first experiments to demonstrate systematically that van der Waals repulsion had to be accepted as a genuine phenomenon in colloid chemistry.

2.33. Phagocytosis of Bacteria

The majority of previous studies are based on phagoctosis of bacteria engulfment. Absolom et al, (1982) studied the phagocytosis of bacteria by platelets using surface thermodynamics aspect. They investigated engulfment of four species of bacteria by pig platelets under well defined *in vitro* conditions from a surface thermodynamics aspect. They used a simple thermodynamic model to predict that bacterial ingestion should increase with increasing bacterial surface tension if the surface tension of the liquid medium in which the platelets and bacteria are suspended is lower than the surface tension of the platelets themselves. They also predicted an opposite behavior if the surface tension of the liquid medium is higher than that of the platelets. Absolom et al, (1982) validated these predictions using phagocytosis experiments, where the platelets and bacteria (opsonized and nonopsonized) was suspended in aqueous media of different surface tensions achieved through the addition of varying amounts of dimethyl sulfoxide. They used thermodynamics prediction to showed that bacterial engulfment should become independent of the surface tension of the ingested bacteria when the surface tensions of the platelets and that of the suspending medium are equal gives

rise to an experimental value of the surface tension of platelets of 67.6 ergs/cm^2, in excellent agreement with the value obtained via an equation—of-state approach from contact angles measured on layers of platelets. In addition, they examined the maximum value of the free energy of engulfment for any particular bacterium—platelet system that occurs when the surface tension of the liquid equals that of the bacteria. They observed that the level of engulfment should be a minimum under such conditions thus permitting the surface tension determination of the bacteria. Absolom et al, (1982) employed Experimental determinations of the minima for the four bacterial species to gives rise to bacterial surface tensions which conform very closely to the values they obtained from contact angle measurements on layers of bacteria. In conclusion, they predicted that platelet phagocytosis of bacteria provides an independent alternative method for determining the surface tension of both platelets and bacteria. They suggested that platelet interaction with bacteria is nonspecific in the sense that the phagocytosis does not appear to be modulated by immunoglobulin receptors.

Van oss et al, (1975); and Neumann et al, (1983) reported that phagocytic engulfment occurred more readily as the material became more hydrophobic whilst platelets adhered more readly to hydrophilic than hydrophobic surfaces. Van oss et al, (1975), presented a simple, but compelling, correlation between the contact angle measured on the surface of bacteria, and the average number of bacteria phagocytised per neutrophil. Neumann et al, (1983) investigated the adhesion of leucocytes and platelets to a range of polymer surface. The theory showed that the adhesion between a biological cell and a solid can be expected to developd upon the surface properties of the cell, the solid, and the liquid in which they are suspended. It is predicted that for high surface tension liquids, the tendency for cell adhesion will decrease with increased surface energy of the solid, whilst in low

surface tension fluids the opposite will be true. Absolom et al, (1982) also investigated the surface thermodynamics of phagocytosis, this time of bacteria by platelets, using the same model described by Van oss et al, (1975). The treatment of bacteria cells by the body can be expected to be similar to that seen with any drug delivery system which is recognized as foreign, and thus this work has directed relevance to targeted drug delivery.

2.34. Summary

The study of the literature has shown that from the available knowledge, there has been little or no attempt made to explain the Mycobacterium Tuberculosis (M-TB) - Macrophage interactions from the surface thermodynamics point of view. Related works are in the phagocytosis of bacteria platelets advanced by (Neumann et al, 1983; van Oss et al, 1975; and Absolom et al, 1982), from surface thermodynamics point of view. Their works considered the relationship between free energy of engulfment and number of bacteria ingested.

In this work, free energy for the condition where no adhesion should occur is to be predicted from the concept of negative Hamaker coefficient obtained from absorbance methods. It is also desired to determine quantitatively the interaction between the M-TB T-cells using the concept of Hamaker coefficient. The sense of this coefficient (i.e. is it positive or negative), will indicate the nature of the interaction. Ultimately, a suggestion will be made as to what should be done to the system to block M-TB - T-cell interactions. From available information, this approach has not been pursued hitherto.

CHAPTER THREE

MATERIALS AND METHODS

3.1. Theoretical Considerations

3.1.1. Concept of Interfacial Free Energy

The work done by a force F to move a flat plate along another surface by a distance dx is given, for a reversible process, by:

$$\delta w = Fdx \qquad (3.1)$$

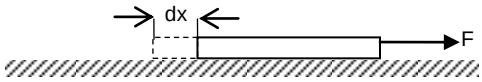

Fig. 3.1: Schematic Diagram Showing Application of a Force on a Surface

(Achebe et al, 2012)

However, the force F is given by; $F = L\gamma$

Where; L is the width of the plate and γ is the surface free energy per unit surface area (interfacial free energy):

Hence; $\delta w = L\gamma dx$

But; $dA = Ldx$

Therefore; $\delta w = \gamma dA \qquad (3.2)$

This is the work required to form a new surface of area dA. For pure materials, γ is a function of temperature (T) only, and the surface is considered a thermodynamic system for which the coordinates are γ, A and T. The unit of γ is J/m^2. In many

processes that involve surface area changes, the concept of interfacial free energy is applicable.

3.1.2. Thermodynamic Approach to Particle-Particle Interaction

Suppose in a certain case, the bacterium, M-TB has been considered as a particle coming in vicinity to the macrophage cell which is further considered as another particle. In the consecutive step one particle (the bacterium) attaches itself on the surface of the other (the macrophage) under a specific condition where the macrophage is dispersed in sputum (follow figure 3.2).

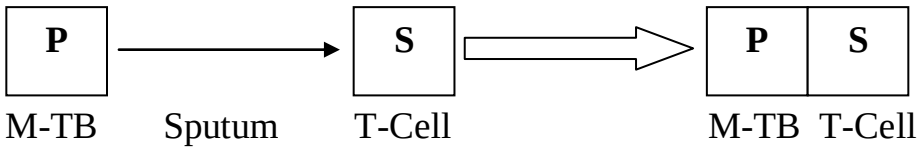

Fig. 3.2: Conceptual representation of M-TB – T-cell macrophage adhesion process

Expression of the thermodynamic free energy associated with adhesion process ΔF_{pls}^{adh} provided in figure (3.2) is represented as follows (Omenyi, 1978):

$$\Delta F_{pls}^{adh}(d_o) = \gamma_{ps} - \gamma_{pl} - \gamma_{sl} \qquad (3.3)$$

In this particular expression, ΔF_{pls}^{adh} represents the integrated free energy of adhesion considered from infinity to the equilibrium where separation distance is d_o. In this equation, P, S represents bacteria and macrophage cell respectively and L signifies the sputum. In the right hand side of the equation, γ_{ps} expresses the interfacial free energy between P and S. γ_{pl} represents the same for P and L, whereas, γ_{sl} provide the same information between S and L.

Successful bacterial infiltration in the macrophage cells will occur through the engulfment of the bacteria requiring net free energy, which is represented as:

$$\Delta F_{NET} = \gamma_{ps} - \gamma_{pl} < 0 \qquad (3.4)$$

In equation (3.4), rejection of the bacteria by the macrophage will be represented, if ΔF_{NET}becomes greater than zero.

For the interaction between the individual components, similar equations can be written also:

$$\Delta F_{ps}^{adh}(d_1) = \gamma_{ps} - \gamma_{pv} - \gamma_{sv} \quad (3.5)$$

$$\Delta F_{sl}^{adh}(d_1) = \gamma_{sl} - \gamma_{sv} - \gamma_{lv} \quad (3.6)$$

$$\Delta F_{pl}^{adh}(d_1) = \gamma_{pl} - \gamma_{pv} - \gamma_{lv} \quad (3.7)$$

For a liquid, the force of cohesion, which is the interaction with itself, is described by:

$$\Delta F_{ll}^{coh}(d_1) = -2\gamma_{lv} \quad (3.8)$$

ΔF^{adh} can be determined by several approaches, apart from the above surface free energy approach. The classical work of (Hamaker, 1937) is very appropriate.

For the four given combinations i.e. Equations (3.5) to (3.8) the equilibrium separation distances, however, are not necessarily the same. When a gap is a vacuum, the equilibrium separation d_1 probably is, but when the gap contains a liquid, a different separation distance d_o may be expected. As a result of this the following becomes true;

$$\left[\frac{A_{132}}{d_0^{\,2}}\right] = \left[\frac{A_{12} - A_{13} - A_{23} + A_{33}}{d_1^{\,2}}\right] \quad (3.9)$$

A system containing two planes could be considered for computing the free energy of interaction. This can be done for semi-infinite, parallel bodies belonging to material 1 and 2 isolated by material 3, bearing thickness d (refer figure 3.3) provided in the following section (Hamaker, 1937). This is calculated by the following equation:

$$\Delta F_{132}(d) = \left[-\frac{A_{132}}{12\pi d^2}\right] \tag{3.10}$$

In this, A_{132}refers to the Hamaker coefficient for a respective system.

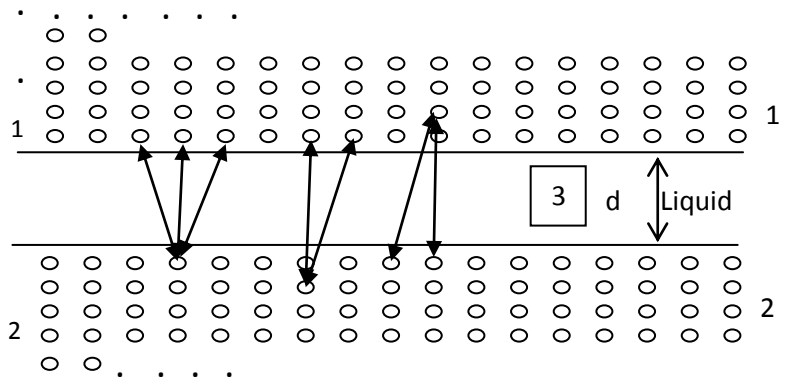

Fig. 3.3: Schematic representation of interaction of two solid bodies, depicted by 1 and 2 which are eventually isolated by d, liquid 3.

Considering nominal isolation distance d_0, and equation (3.10) as valid for such a small distance, the Hamaker coefficient should be expressed as (Hamaker, 1937):

$$A_{132} = -12\pi d_o^2 \Delta F^{adh}(d_o) \tag{3.11}$$

The Hamaker coefficient A_{132} for the interactions between two different bodies in a liquid can be calculated from equation (3.11) once the free energy of adhesion between the two bodies is known or through the pair-wise additivity approach as originally proposed by (Hamaker, 1937) or by the macroscopic approach of (Lifshitz et al, 1961).

Influence of neighbouring atoms remains major hurdle during the pair-wise summation computing between various molecular interactions. In case of highly disperse media such influence is insignificant, for instance, gases whereas for condensed media it is important (Hough and White, 1987).

As the actual material atomic structures are overlooked, the Lifshitz method is suitable in certain cases. In this method, bulk material properties are considered for calculation of interactions between the macroscopic bodies. Properties like refractive indices and dielectric permittivity $\varepsilon(i\zeta)$ are considered for such calculations. Dielectric permittivity represents the microscopic polarizability as a manifested macroscopic property for the constant atoms belonging to certain materials. The Hamaker coefficient represents the macroscopic resultant for the interactions happened due to the atom polarizations in a material (Hough and White, 1987).

Following Lifshitz theory, the Hamaker coefficient is represented as follows:

$$A_{ikj} = \frac{3}{4}\pi\hbar\int_0^\infty \left[\frac{\varepsilon_i(i\zeta)-\varepsilon_k(i\zeta)}{\varepsilon_i(i\zeta)+\varepsilon_k(i\zeta)}\right]\left[\frac{\varepsilon_j(i\zeta)-\varepsilon_k(i\zeta)}{\varepsilon_j(i\zeta)+\varepsilon_k(i\zeta)}\right]d\zeta \qquad (3.12)$$

Where, $\varepsilon_j(i\zeta)$ refers to the dielectric constant of a specific material j, this is considered through the imaginary i, frequency axis ($i\zeta$), ħ is planck's constant. In this context, the evaluation of equation (3.12) should result in equivalent value with the thermodynamic free energy of adhesion, provided in equation (3.3). The molecular contact was maintained at (d=0). Interestingly, constituent molecule numbers are of finite size and for that it is not possible to attain d=0 for two macroscopic surface. Therefore, whenever the surfaces attain a distance d_o, molecular contacts are considered. The divergences according to Lifshitz theory are eliminated by the parameter d_o.

Thus, the Hamaker coefficient or the Lifshitz-van der Waals constant A_{132} may result in negative. In certain condition, the contact between the interacting particles will be hampered due to the repulsive (electrostatic) force originated. The resultant effect in certain cases remains as repulsion instead of attraction for the considered particles. The Hamaker coefficient and the interfacial free energies are connected through the following equation:

$$A_{PLS} = -12\pi d_o^2(\gamma_{PS} - \gamma_{PL} - \gamma_{SL}) \qquad (3.13)$$

This equation has been derived through combining equation (3.11) with equation (3.3).

For the issue of self-interaction of a particle equation (3.12) should be considered;

$$A_{ij} = \frac{3}{4}\pi\hbar\int_0^\infty \left[\frac{\varepsilon_i(i\zeta) - \varepsilon_j(i\zeta)}{\varepsilon_i(i\zeta) + \varepsilon_j(i\zeta)}\right]^2 d\zeta \qquad (3.14)$$

Therefore, the system under consideration follows equations (3.15) and (3.16):

$$A_{PLS} = A_{PS} + A_{LL} - A_{PL} - A_{SL} = \left(\sqrt{A_{PP}} - \sqrt{A_{LL}}\right)\left(\sqrt{A_{SS}} - \sqrt{A_{LL}}\right) \qquad (3.15)$$

$$A_{PLP} = A_{PP} + A_{LL} - 2A_{PL} = \left(\sqrt{A_{PP}} - \sqrt{A_{LL}}\right)^2 \qquad (3.16)$$

3.2. Mathematical Formulation

To be able to use the absorbance data to calculate the Hamaker coefficients using the Lifshitz theorem of equation (3.12), there is a need to evaluate the dielectric constant ε of the equation. Some relevant equations are required as presented below.From the information of light absorbance, reflection and transmittance, it could be seen that:

$$\bar{a} + T + R = 1 \qquad (3.17)$$

Where; ā is absorbance, T is transmittance, and R is reflectance. Also, from the information of light absorbance and transmittance:

$$T = \exp^{-\bar{a}} \tag{3.18}$$

With the values of ā determined from absorbance experimental results, and substituting the values of ā into equation (3.18) to obtain T, R could easily be derived by substituting the values of ā and T into equation (3.17).

To find a value for the refractive index, *n* employing the mathematical relation (Robinson, 1952):

$$n = \left[\frac{1 - R^{1/2}}{1 + R^{1/2}}\right] \tag{3.19}$$

A value for the extinction coefficient, *k* is obtained from the equation:

$$k = \left[\frac{\alpha\lambda \times 10^{-9}}{4\pi}\right] \tag{3.20}$$

Where; α is the absorption coefficient defined as follows:

$$\alpha = \left[\frac{\bar{a}}{\lambda \times 10^{-9}}\right] \tag{3.21}$$

Substituting the value, α of equation (3.21) into equation (3.20):

$$k = \left[\frac{\bar{a}}{4\pi}\right] \tag{3.22}$$

The dielectric constant, ε could thus be given by the formula (Charles, 1996),
For the real part:

$$\varepsilon_1 = n_1^2 - k^2 \tag{3.23}$$

For the imaginary part:

$$\varepsilon_2 = 2n_2k \tag{3.24}$$

With these values, it is possible to determine A_{ij} using the relevant equations to determine A_{11}:

$$A_{11} = 2.5\left[\frac{\varepsilon_{10}-1}{\varepsilon_{10}+1}\right]^2 = 2.5\left[\frac{n_1^{\,2}-1}{n_1^{\,2}+1}\right]^2 \tag{3.25}$$

This gives a value to the Hamaker constant $A_{11,}$ and by extension to other Hamaker constants A_{22} and $A_{33.}$

For combination of two different materials 1 and 2 in approximation:

$$A_{12} = \sqrt{A_{11}A_{22}} \tag{3.26}$$

For a combination of two disimilar materials (i.e. macrophage, 1 and the bacteria, 2) with the gap between 1 and 2 is filled with sputum as the medium 3, the combined Hamaker coefficient will be given by:

$$A_{132} = A_{12} + A_{33} - A_{13} - A_{23} \tag{3.27}$$

$$A_{131} = A_{11} + A_{33} - 2A_{13} \tag{3.28}$$

Rewriting these equations will give:

$$A_{132} = \left(\sqrt{A_{11}} - \sqrt{A_{33}}\right)\left(\sqrt{A_{22}} - \sqrt{A_{33}}\right) \tag{3.29}$$

For a combination of two similar materials, the combined Hamaker coefficient of equation (3.29) will be given by:

$$A_{131} = \left(\sqrt{A_{11}} - \sqrt{A_{33}}\right)^2 \tag{3.30}$$

Equation (3.29) shows that, for a three-component system involving three different materials, 1, 2 and 3, A_{132} can become negative:

$$A_{132} \prec 0 \tag{3.31}$$

When; $$\sqrt{A_{11}} \succ \sqrt{A_{33}} and \sqrt{A_{22}} \prec \sqrt{A_{33}} \quad (3.32)$$

Or; $$\sqrt{A_{11}} \prec \sqrt{A_{33}} \prec \sqrt{A_{22}} \quad (3.33)$$

A_{33} = Hamaker constant for sputum

A_{13} = Hamaker constant between both materials (i.e. macrophage and sputum)

A_{23} = Hamaker constant between both materials (i.e. the M-TB and sputum)

Thus the Hamaker Coefficient A_{132} becomes:

$$A_{132} = \frac{3}{4}\pi\hbar\int_0^\infty \left[\frac{\varepsilon_1(i\zeta)-\varepsilon_3(i\zeta)}{\varepsilon_1(i\zeta)+\varepsilon_3(i\zeta)}\right]\left[\frac{\varepsilon_2(i\zeta)-\varepsilon_3(i\zeta)}{\varepsilon_2(i\zeta)+\varepsilon_3(i\zeta)}\right]d\zeta \quad (3.34)$$

Integrating all the values of the combined Hamaker coefficient, A_{132} gives an absolute value for the coefficient denoted by A_{132abs} (refer to equation 3.34) and applying Lifshitz derivation for van der Waals forces as in equation (3.34).

The absolute value for the Hamaker coefficient could be derived by obtaining the mean of all the A_{132} values got from the Lifshitz relation:

$$A_{132abs} = \frac{\sum_{i=1}^{N}(A_{132})}{N} \quad (3.35)$$

Also $$A_{131abs} = \frac{\sum_{i=1}^{N}(A_{131})}{N} \quad (3.36)$$

And $$A_{232abs} = \frac{\sum_{i=1}^{N}(A_{232})}{N} \quad (3.37)$$

3.3. Research Methodology

To determine the combined Hamaker coefficient using the Lifshitz theorem of equation (3.34), there is a need to evaluate the dielectric constant ε of that equation. This can only be done through the measurement of the absorbance for each sample of infected M-TB sputum, uninfected M-TB sputum and TB/HIV co-infected sputum.

3.3.1. Sample Collection of TB Specimens

This research work involved collection of Sputum samples from twenty TB infected, twenty uninfected and twenty HIV/TB co-infected persons. The collected sputum samples were screened to determine the infection status using GeneXpert thus giving a total of sixty sputum samples from different individuals. The sputum samples were collected from Anambra State University Teaching Hospital (ANSUTH) Awka (formerly General Hospital Awka). Spot Specimens were used to ensure the freshness of the collected Sputum samples and to avoid the samples becoming lysed (spoilt). Storage facilities like refrigerators were also used to ensure that the samples were healthy enough so as to obtain good results.

Sputum collection is the most dangerous procedure in the AFB smear microscopy technique and this must be carried out in the open air at a distance from other people. A fresh sputum container was given to each patient for sputum examination. Good sputum is produced by repeated deep inhalation and exhalation of breath followed by coughing. This is followed by opening the container and carefully spitting and closing it back.

Note: A good specimen should be approximately 3 – 5ml. It is usually thick and mucoid. It may be fluid and may contain pieces of purulent material. Colour varies from opaque white to green. Bloody specimens will appear reddish or brownish. Clear saliva or nasal discharge is not suitable as a TB specimen.

3.3.2. Sample Preparation

A. Direct Sputum for GeneXpert Determination of M-TB Positive/Negative

The collected samples were loaded into GeneXpert Cartridge to determine if the sample is mycobacterium TB positive or negative. This helped to obtain and separate the positive and negative M-TB. The glass slides were prepared and smeared with the samples for absorbance measurements. The slide preparations and sample smearing were done at the same laboratory.

Method:

The lid of sputum container was carefully unscrewed and 2 volumes of sample reagent (SR) was poured directly into 1 volume of sputum in the sputum container (1ml of sputum is the minimum quantity, while 3 - 4ml is the optimal quantity required), then the lid was replaced and was vigorously shook for 10 – 20 times (one back and forth movement is a single shake). The specimen was incubated at room temperature for 10minutes (i.e. for sputum liquefaction and inactivation of the organisms) and after 10 minutes of incubation, it was again shook vigorously for about 10 – 20 times. After additional 5 minutes of incubation, the sample was perfectly fluid before being tested, with no visible clumps of sputum.

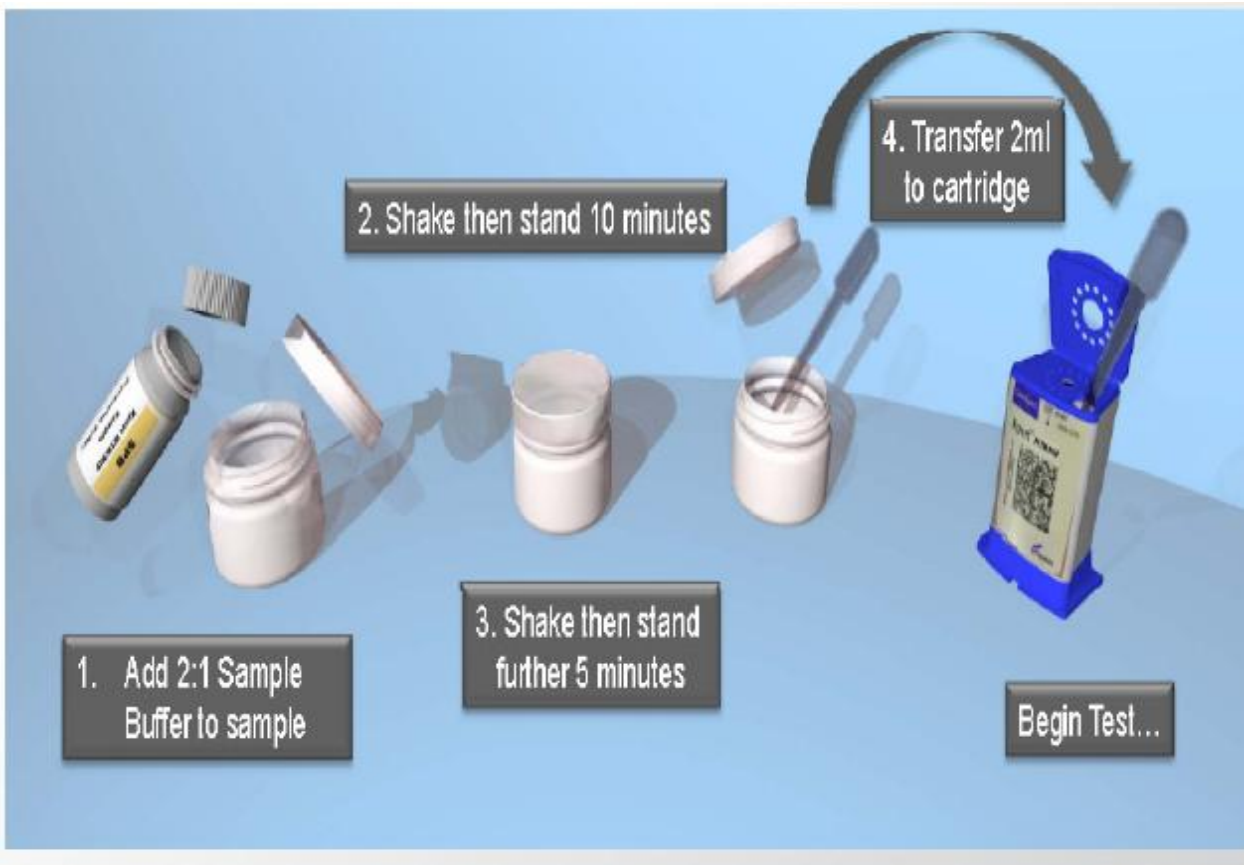

Fig. 3.4: Sample Preparation: direct sputum

The sample reagent (buffer) was poured carefully into the sample to avoid production of aerosols and the sample was pipetted carefully to avoid any solid particles from the sample mix into the cartridge and bubbles when mixed into the cartridge (i.e. to avoid error 5006/5007/5008 "probe check failure" which can occur as a result of pipetting wrong sample volume).

B. Processed Sputum Sediment for GeneXpert Determination of M-TB Positive/negative

Method:

1.5ml of sample reagent was added to 0.5ml of suspended sediment from digested/decontaminated and concentrated sputum specimen and the lid was

replaced, shook vigorously for 10 – 20 times. Then the specimen was incubated at room temperature for 10 minutes (i.e. for sputum liquefaction and inactivation of the organisms) and after 10 minutes of incubation, it was again shook vigorously for about 10 – 20 times and was incubated again for additional 5 minutes, then the sample was perfectly fluid before being tested, with no visible clumps of sputum.

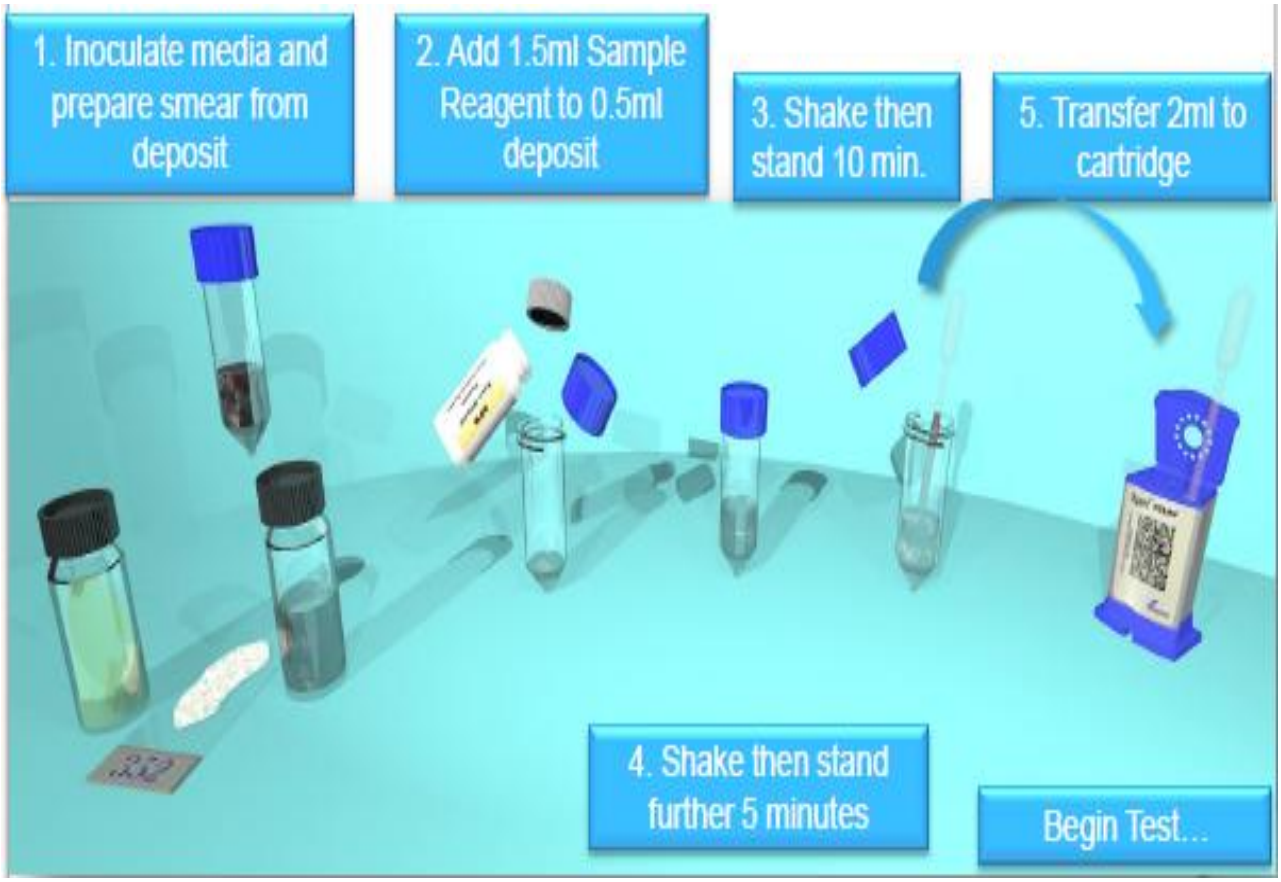

Fig. 3.5: Sample Processed Sputum Sediment

Preparation of Cartridge: Inoculation

2.4ml of prepared sample was pipetted from the cartridge using the plastic transfer pipette, then the sample was pipetted carefully to avoid creating aerosols and bubbles when mixed into the cartridge (i.e. to avoid error 5006/5007/5008 "probe check failure" which can occur as a result of pipetting wrong sample volume) and the lid was firmly closed, then the test was carried out.

Storage of samples and Inoculated Cartridges

Storage of Sputum: Direct or processed (decontaminated/Concentrated) sputum; the specimen was refrigerated at 2 – 28^{o}C for about 10 days maximum (i.e. to avoid reagents deterioration which may inhibit the PCR process during Genexpert screening).

Storage of Specimen in presence of sample reagent: Direct or processed (decontaminated/Concentrated) sputum; the specimen was processed within 12 hours and was kept at 2 – 28^{o}C. When refrigeration was not possible, it was processed within 5 hours.

3.3.3. Slide Preparation

The glass slide of 25.4mm x 76.2mm x 1.2mm was used for the preparation of test surfaces. A dropper was used to draw each of the Sputum samples from the container and smeared carefully on a slide to ensure even distribution of the sputum samples on the slides. Three slides were prepared for each of the twenty sputum samples and smeared with the samples for absorbance measurements. The slide preparations and sample smearing were done at Chest Clinic/Laboratory, Anambra State University Teaching Hospital, Awka). The samples were allowed to dry naturally at room temperature because exposing the prepared slides to the sun is likely to cause oxidation and the surface energy might be increased unconditionally. All the well prepared and dried surfaces were covered with microscopic cover slip, ready for the experiment.

3.3.4. Measurements

Absorbance measurements were done on all the positive and negative sputum components of all sixty samples (TB infected, TB uninfected, TB/HIV co-infected and macrophage sputum samples). A digital Ultraviolet Visible Spectrophotometer (UV/VIS MetaSpecAE1405031Pro) was used for the measurements. The measurements of absorbance and transmittance were done at the department of Mechanical Engineering Laboratory, Nnamdi Azikiwe University, Awka. The absorbance values of the samples were measured over a range of wavelength spanning between 230 and 950 Å. The data collected were used in calculating the Hamaker coefficients using the Lifshitz formula.

3.4. Summary

The application of these thermodynamics theories for M-TB - macrophage interactions and M-TB/HIV interaction were considered. The M-TB was modeled as a particle interacting with another particle, Macrophage T-cell with sputum as intervening medium.

The use of Lifshitz formula to determine the combined Hamaker coefficients was sought since this, to the best of this researcher's knowledge, has not been done. The various variables of that equation [equation (3.34)] were determined and the value of A_{132} calculated where 1 refers to the Macrophage negative sputum smear, 2 refers to the M-TB positive sputum smear (M-TB/HIV positive sputum smear) and 3 to the suspending medium, negative sputum smear.

These processes were repeatedly done to ensure reliability of the collected data. To prevent the collected sputum samples getting lysed (spoilt) especially M-TB/HIV

samples and isolated Macrophage T-cells which are readily susceptible to TB infection adequate refrigeration were employed. Diligence, persistence and determination on the part of the researcher eventually paid off giving rise to the emergence of this work.

CHAPTER FOUR

RESULTS AND DISCUSSION

4.1 Results and Data Analysis

The raw data obtained for both M-TB and M-TB/HIV positive and negative sputum samples were collated. The raw data were collected and presented at appendix on tables A1, B1, C1, D1, E1 and F1. This paved the way for the data analysis. However, since extinction coefficient "*k"*, absorption coefficient "α" and dielectric constant "ε*"* are obtained as functions of wavelength λ, an integration of equation (3.34) will give a more accurate value. The data on absorbance obtained as a function of wavelength as presented at appendix on tables A1, B1, C1, D1, E1 and F1 are plotted on figures (4.1), (4.2), (4.3), (4.4), (4.5) and (4.6). Equation (3.14) was used to obtain for each interacting system, A_{ij} $(A_{11}, A_{22}, A_{33}, A_{12}, A_{13}, A_{23})$ by approximate change of variables. MATLAB computation tools were used. This involved the numerical integration of equation (3.14) for each wavelength from 230 to 950 for all the twenty samples in each category.

Analysis based on the mathematical formulations outlined yielded values for the needed variables and are presented in appendix. Such variables as the transmittance *T,* reflectance *R,* refractive index (real and imaginary) *n,* extinction coefficient *k,* absorption coefficient α, dielectric constants (real and imaginary) ε_{ij}, Hamaker Constants $A_{ij,}$ and Hamaker Coefficients A_{132} were calculated. Various tables and plots as shown depict the results obtained for infected and uninfected sputum samples respectively. The determination of a value for the absolute

combined Hamaker coefficient set the pace for modeling for the zero/negative Hamaker coefficient.

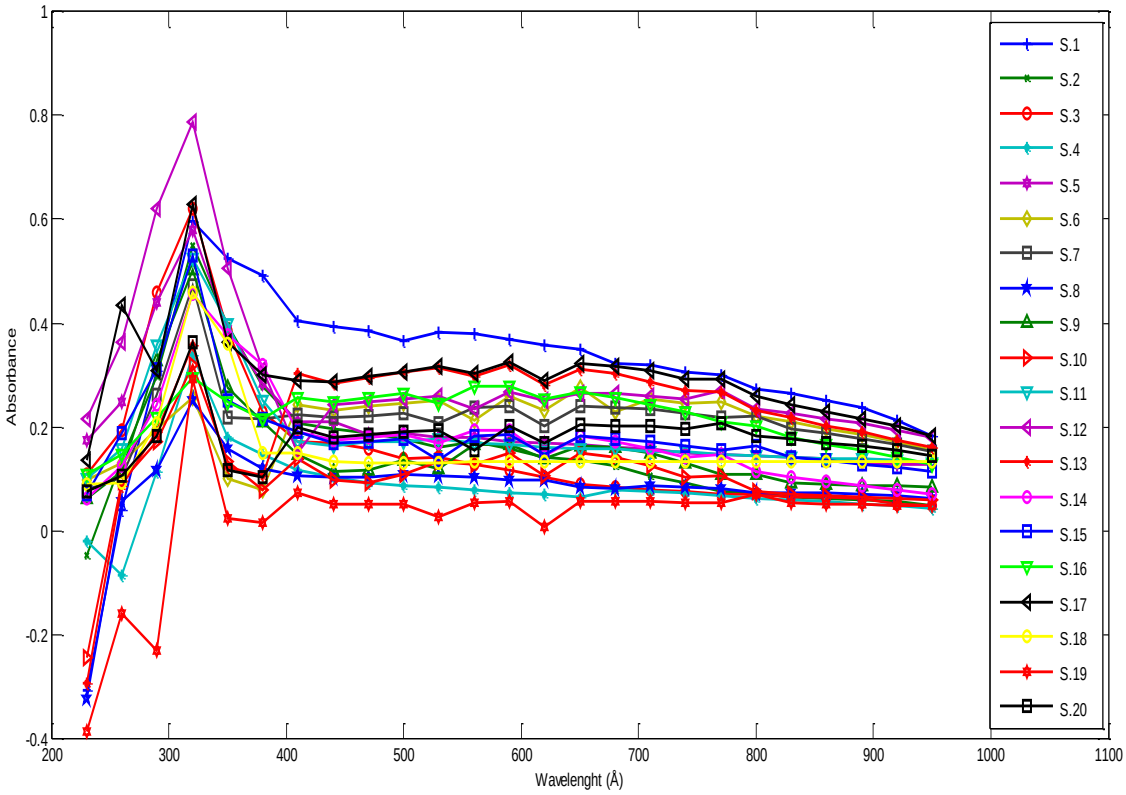

Fig.4.1: Variation of Absorbance, $\bar{a}$ with Wavelength, λ for Twenty Samples of M-TB Infected Sputum

Figure (4.1) shows an interesting pattern for M-TB positive sputum. The absorbance of the individual twenty M-TB infected sputum samples steeply increased as the wavelength increased until a critical wavelength of 320Å, where the peak value was attained. A further increase in the wavelength saw at first a sudden and latter a gradual decrease in the absorbance values. This peak value falls within the visible range of ultraviolet radiation which is between 300 - 600Å. The peak values of absorbance range between 0.2918 and 0.7877 ($0.2918 \leq \bar{a} \leq 0.7877$). These values are listed for each sample in table (4.1). It is interesting

though, that at the lower wavelengths of between 230 – 290Å some negative absorbance values were recorded.

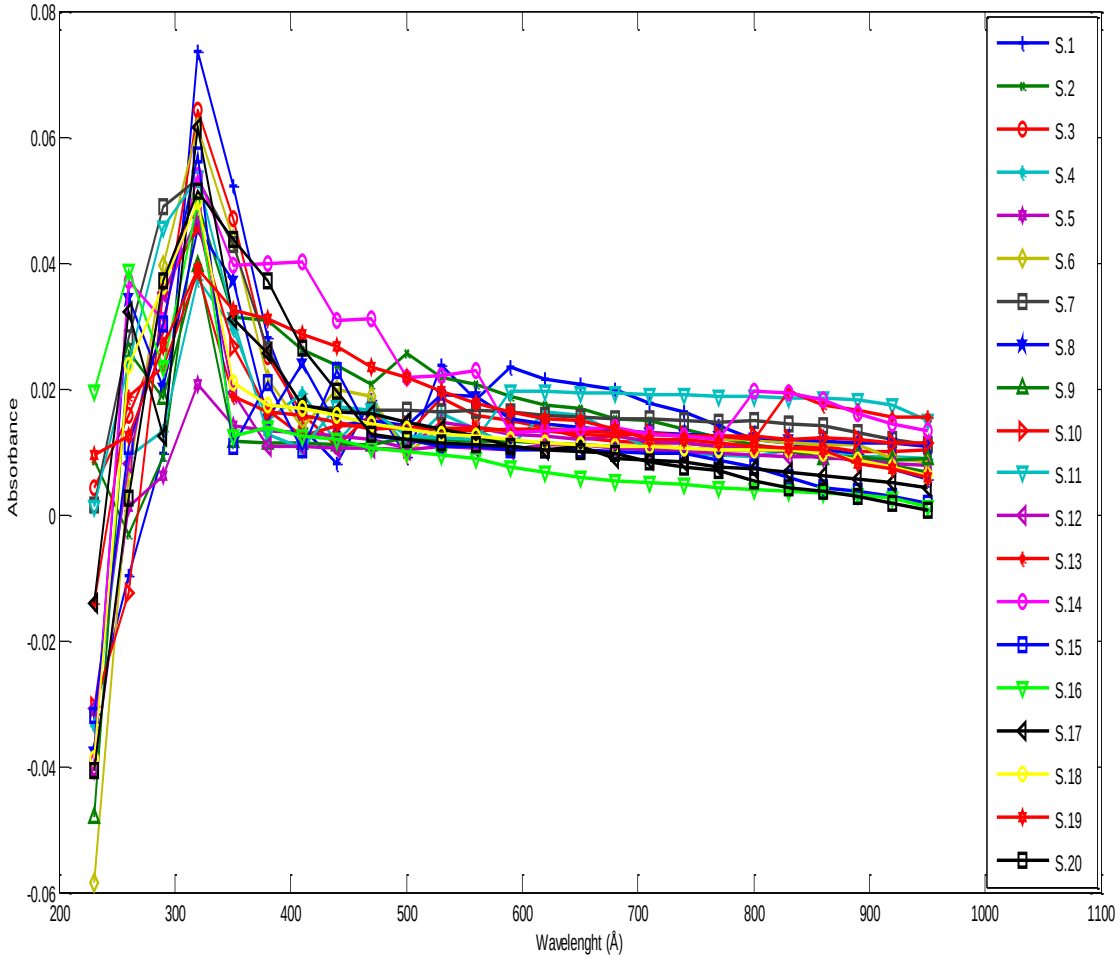

Fig.4.2: Variation of Absorbance, $\bar{a}$ with Wavelength, λ for Twenty Samples of M-TB Infected Macrophage

Figure (4.2) shows a similar pattern as that of figure (4.1) with the peak value occurring at the wavelength of 320Å which corresponds exactly with that of the figure (4.1). However, the peak absorbance values are of the range 0.0206 and 0.0736 ($0.0206 \leq \bar{a} \leq 0.0736$). It is interesting though, that at the lower wavelengths of between 230 – 260Å some negative absorbance values were recorded. (See table 4.1)

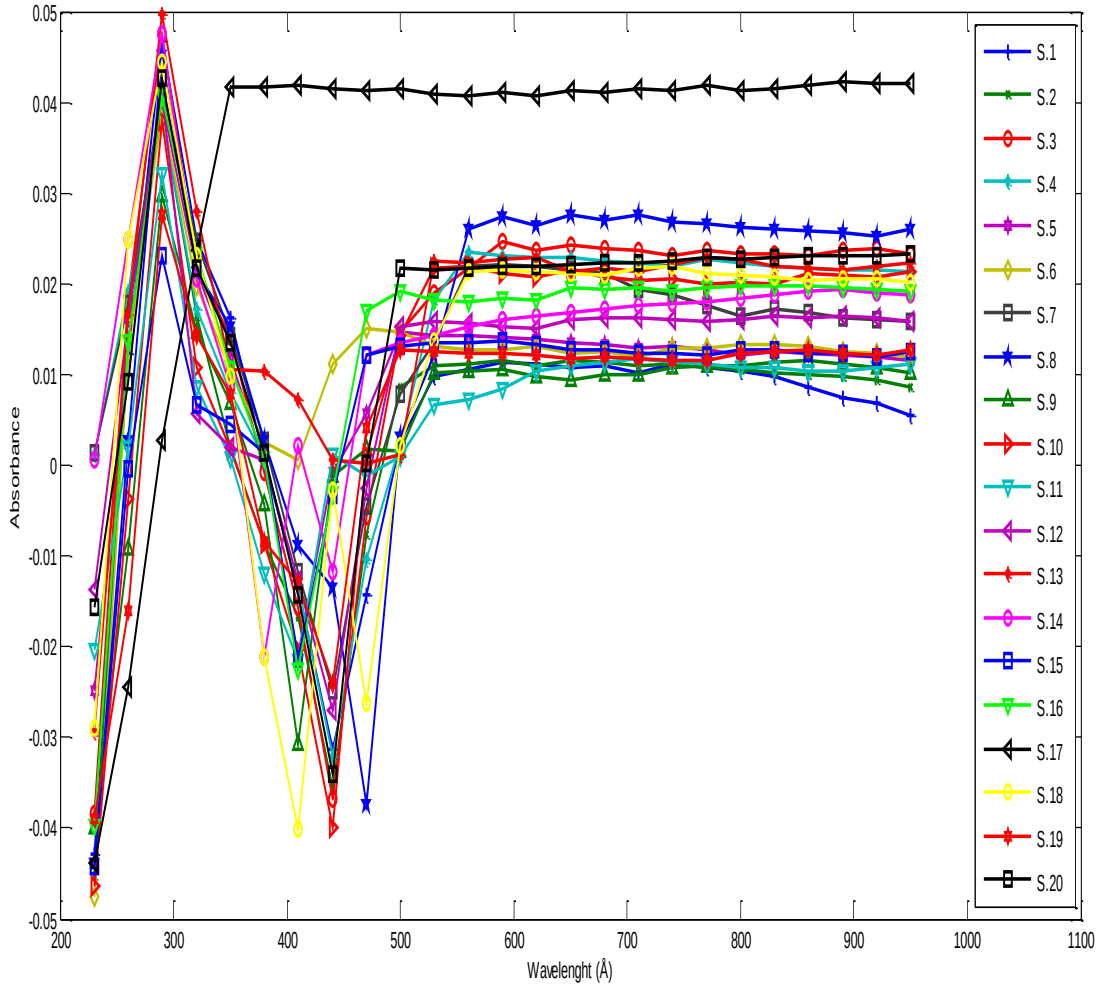

Fig.4.3: Variation of Absorbance, $\bar{a}$ with Wavelength, λ for Twenty Samples of M-TB/HIV Co-infected Sputum

Figure (4.3) reveals an interesting pattern for M-TB/HIV positive Sputum. The absorbance of the respective twenty M-TB/HIV co-infectious sputum samples systematically increased as the wavelength increased until a critical wavelength of 290Å, where a peak value was accomplished. A further increase in the wavelength saw at first a steady decrease in absorbance until a minimum was attained. As wavelength increases, a progressive increase in absorbance values was recorded and latter a gradual decrease follows. These peak values of absorbance fall within

the visible range of the ultraviolet radiation which is between 300 - 600Å. The peak values of absorbance range between 0.0231 and 0.0498 ($0.0231 \leq \bar{a} \leq 0.0498$), (see table 4.1) except sample 17 which showed a steady increase as wavelength increased until 410Å and steeply decreases as wavelength increases; the value of absorbance recorded is obviously a faulty one, this could be explained against the possibility of some experimental error or as a result of some sputum related disease conditions like diabetes, Hepatitis etc. it is interesting though, that at the lower wavelengths of between 230 – 260Å some negative absorbance values were recorded.

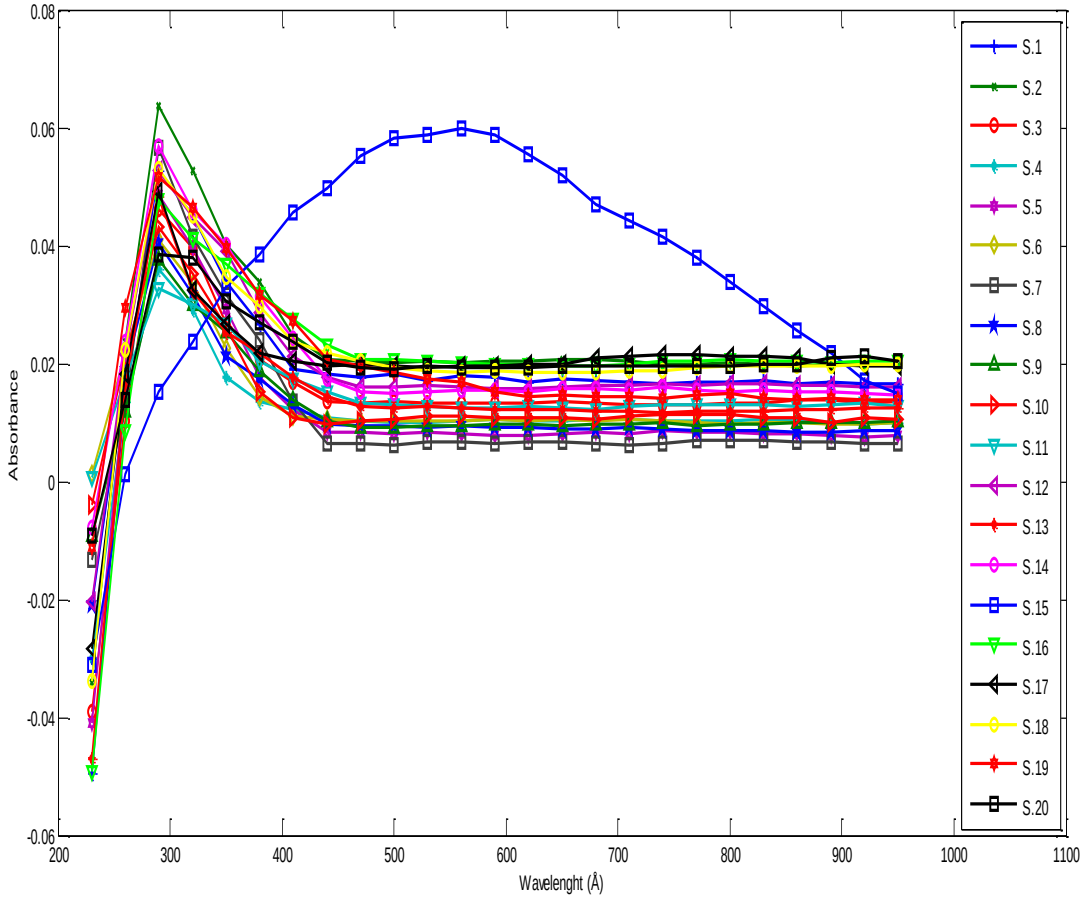

Fig.4.4: Variation of Absorbance, $\bar{a}$ with Wavelength, λ for Twenty Samples of M-TB/HIV Co-infected Macrophage

Figure (4.4) followed similar pattern as that of figure (4.2) with the peak values occurring at the wavelength of 290Å. However, the peak absorbance values are of the range 0.0152 and 0.0637 ($0.0152 \leq \bar{a} \leq 0.0637$) (see table 4.1). Sample 15 showed a marked departure in its response from the rest until the wavelength of 560Å and latter decreased systematically as wavelength increased. The continuous increase and latter decrease in the absorbance value recorded is clearly a defective one. This could be explained against the possibility of some experimental or machine error or as a result of some disease related conditions like diabetes, Hepatitis etc.

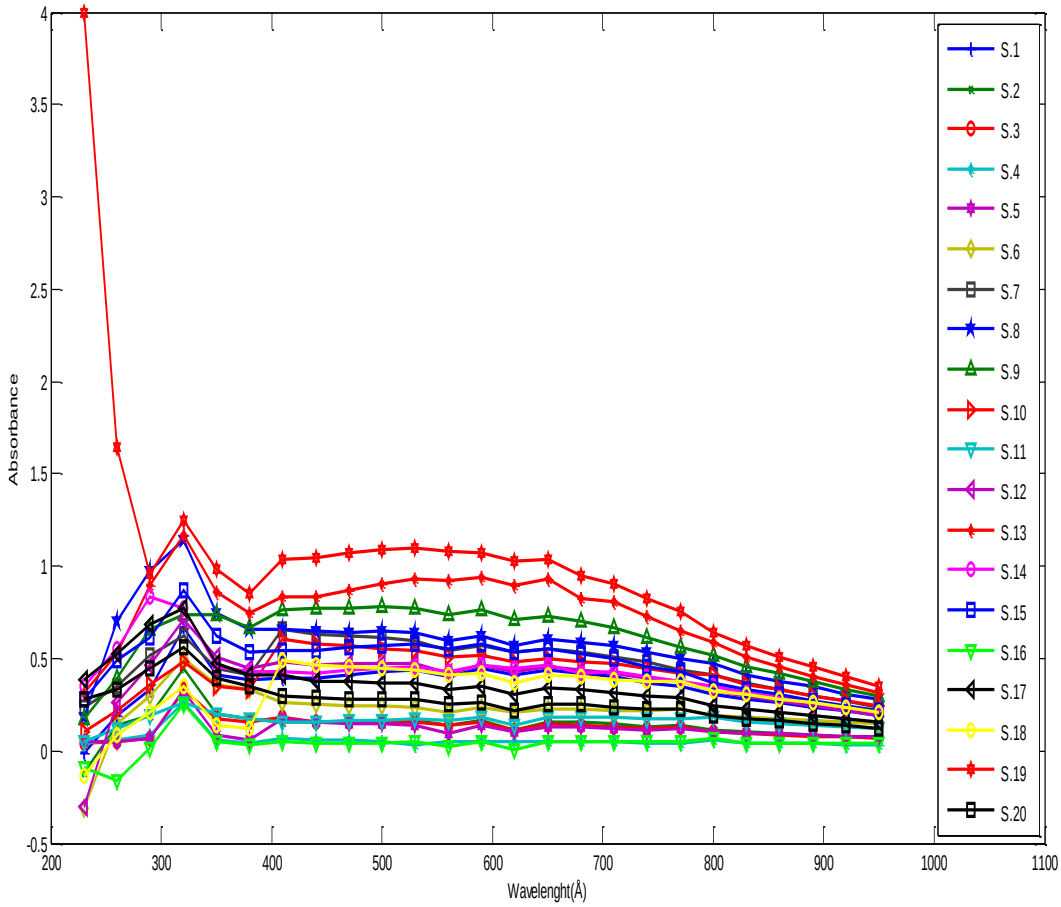

Fig.4.5: Variation of Absorbance, $\bar{a}$ with Wavelength, λ for Twenty Samples of M-TB Negative Sputum

The peak value of the absorbance for M-TB negative sputum of figure (4.5) was obtained at the wavelength of 320Å and ranges as follows $0.2657 \leq \bar{a} \leq 1.2501$ (see table 4.1). The reaction here also follows the earlier patterns with the various twenty samples showing moderately conformed characteristics. An exception to the rule is found with sample 19 which showed a drop down decrease from the pattern exhibited by the rest of the samples. This again could be explained against machine error.

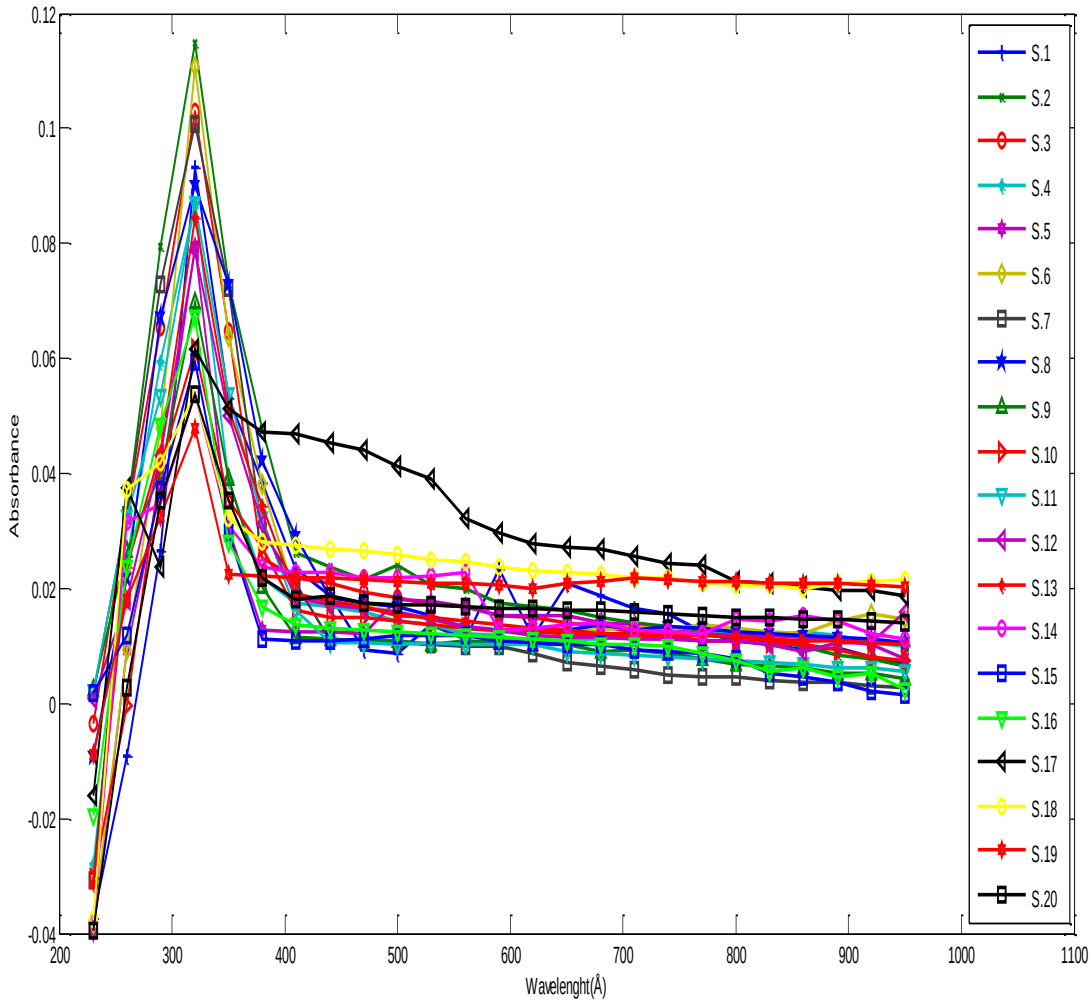

Fig.4.6: Variation of Absorbance, $\bar{a}$ with Wavelength, λ for Twenty Samples of M-TB Macrophage Negative

Figure (4.6) for the samples of M-TB Macrophage negative sputum reveals similar characteristics as their counterparts, however with the peak values occurring at 320Å. The absorbance values at this peak point are of the magnitude between 0.0478 and 0.1148 ($0.0478 \leq \bar{a} \leq 0.1148$) (see table 4.1).

4.2 Comparison between the Peak Absorbance Values of M-TB Positive, M-TB/HIV Positive and Negative Sputum Components

From results presented in Figs.4.1, 4.2, 4.3, 4.4, 4.5, and 4.6 and summarized in table 4.1, it could be seen that the peak absorbance values of the various sputum samples and components vary in magnitude revealing the notable effect of the bacteria on them. The comparison between the positive and negative samples of the macrophages is imperative to this research. This is because Mycobacterium Tuberculosis actually attacks the macrophages by attaching itself to the macrophage cells. Table 4.1 reveals also the degree of variation between similar infected and uninfected sputum components at a glance for a clearer understanding.

Table 4.1: Comparison between Peak Absorbance values of M-TB Positive, M-TB/HIV Positive and Negative Sputum Components respectively

Sample Type	Wavelength, λ(Å) Peak Values	Absorbance, ā Peak Values				
		M-TB Positive	M-TB Negative	M-TB/HIV Co-infected	M-TB/HIV Uninfected	Mean Values
Sputum	320	0.2918 – 0.7877	---	---	---	0.4588±0.1468
		---	0.2657 – 1.2501	---	---	0.6244±0.3545
	290	---	---	0.0231 – 0.0498	---	0.0379±0.0108
		---	---	---	0.2657 – 1.2501	0.6244±0.3545
Macrophage	320	0.0206 – 0.0736	---	---	---	0.0496±0.0116
		---	0.0478 – 0.1148	---	---	0.0784±0.0206
	290	---	---	0.0152 – 0.0637	---	0.0456±0.0106
		---	---	---	0.0478 – 0.1148	0.0784±0.0206

The difference between the peak absorbance values of M-TB positive, M-TB/HIV co-infected and negative sputum components respectively is an indication of how the bacteria affects the properties of the macrophage cells. The trend is such that the mean absorbance peak values of M-TB negative sputum samples are reduced by infection from 0.6244±0.3545 to 0.4588±0.1468 by a factor of about 26.5%. In M-TB macrophage samples, the reduction is from 0.0784±0.0206 to 0.0496±0.0116, a factor of about 36.7%. While in M-TB/HIV co-infected macrophage samples, the reduction is from 0.0784±0.0206 to 0.0456±0.0106 by a factor of about 41.8%. Comparing the mean absorbance peak values of M-TB positive sputum samples and the mean absorbance peak values of M-TB/HIV co-infected sputum samples; the results of the mean absorbance peak values reveal that the mean absorbance peak value of the M-TB/HIV co-infected samples is generally reduced as compared to that of the mean absorbance peak values of the

M-TB positive sputum samples (see table 4.1). The macrophages are of particular interest to this research since the bacteria attacks this T-cells component which serves as receptor cells. Comparing the mean absorbance peak values of M-TB positive macrophage samples and the mean absorbance peak values of M-TB/HIV co-infected macrophage samples; the results of the mean absorbance peak values reveal that the mean absorbance peak values of the M-TB/HIV co-infected samples is generally reduced by infection from 0.0784±0.0206 to 0.0456±0.0106 by a factor of about 41.8% as compared to that of the mean absorbance peak values of the M-TB positive macrophage sample with a factor of about 36.7%. It could be seen that the reduction between the peak values absorbance (mean) of the sputum component is such that the macrophages reduced from M-TB to M-TB/HIV by a factor of about 8.1%. The reduction in the absorbance of the M-TB/HIV infected sputum samples reveals the role of the bacteria in drastically affecting the surface properties of the infected macrophage cells and specimens.

4.3 Computation of the Absolute value of the Hamaker constants

The computation for the absolute value of the Hamaker constants of different interacting systems derived from;

$$A_{ijabs} = \frac{\sum_{i=1}^{N}(A_{ij})}{N} \qquad (4.1)$$

Referring to equation. (3.29); Thus

For $A_{132} < 0$

$\sqrt{A_{11}} > \sqrt{A_{33}}$ and $\sqrt{A_{22}} < \sqrt{A_{33}}$

Or $\sqrt{A_{11}} < \sqrt{A_{33}} < \sqrt{A_{22}}$

Or $A_{11} < A_{33} < A_{22}$ and $A_{11} > A_{33} > A_{22}$ (4.2)

4.4 Computation of the Hamaker Coefficients

The values of the Hamaker constants, A_{11} obtained for the various sputum mechanisms were employed in the derivation of the Hamaker coefficients, A_{132}. The underlying equation here is equation (3.29) with the necessary modifications as shown in equation (4.3):

$$A_{132} = \left(\sqrt{A_{11}} - \sqrt{A_{33}}\right)\left(\sqrt{A_{22}} - \sqrt{A_{33}}\right) \quad (4.3)$$

The modifications are as follows;

A_{11}, $\tilde{A}_{11} = A_{11}$ values for M-TB negative Macrophage.

A_{22}, $\tilde{A}_{22} = A_{11}$ values for M-TB, M-TB/HIV positive Macrophage respectively.

The infected macrophages are used in lieu of the M-TB because there is currently no known means of isolating the disease. The assumption here is that the infected macrophage is an approximation of the actual disease owing to the manner of the infection. The mechanism of the infection is such that it actually attaches its macrophage cells on the lungs while changing the nature of the cells. The important issue is that the disease does not affect the blood cells but actually infuses the cells thereby altering the nature and characteristics of the blood cells. This thus makes the use of the infected macrophage a close replacement for the disease in calculating the Hamaker coefficients.

A_{33}, $\tilde{A}_{33} = A_{11}$ for M-TB, M-TB/HIV positive sputum as the intervening medium respectively.

The results are presented in figures (4.7), (4.8), (4.9) and (4.10).

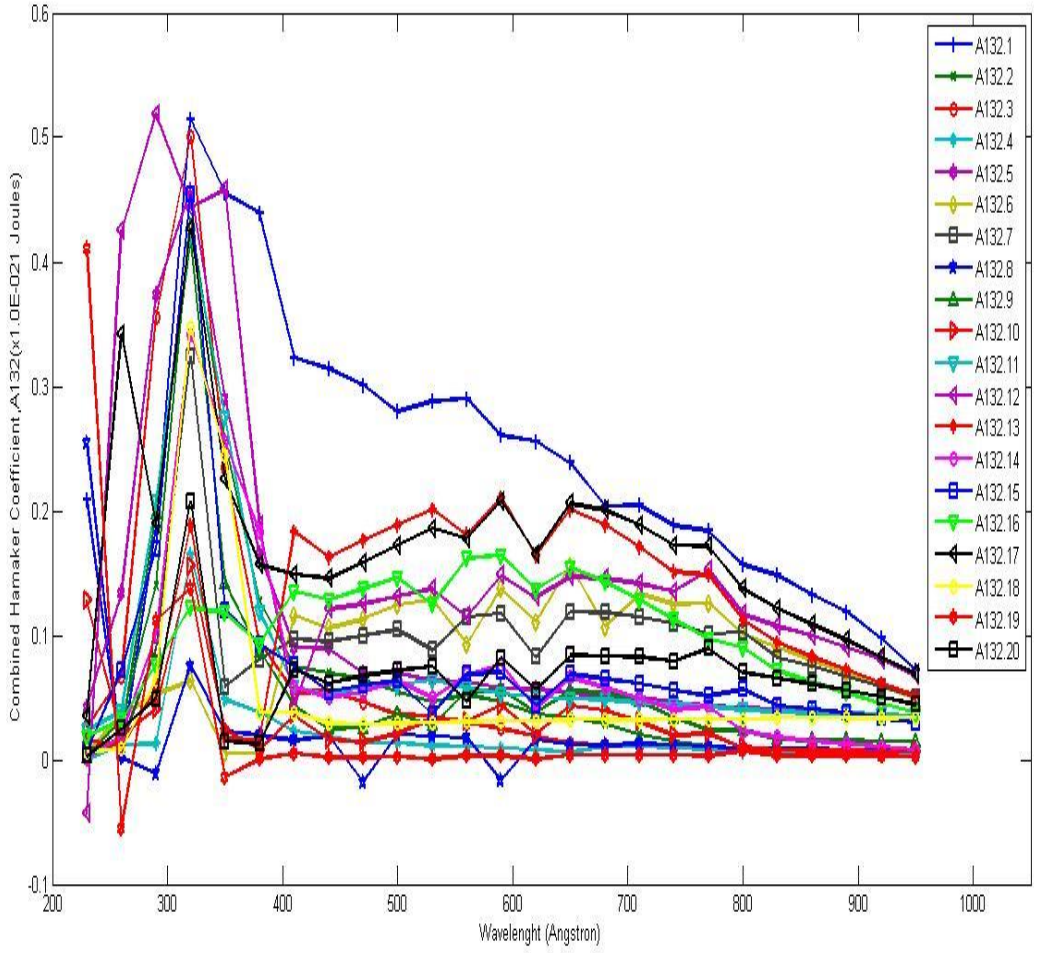

Fig.4.7: Variation of Combined Hamaker Coefficient, A_{132} with Wavelength, λ (Å) for the M-TB infected Sputum Samples

Figure (4.7) reveals the pattern of the combined Hamaker coefficients for the infected sputum samples with clear maxima and minima values occurring at various wavelengths. Harmonized values of the combined Hamaker coefficient became necessary to streamline the findings. This involves the integration of all the Hamaker coefficients first over each wavelength, secondly with each sputum sample in view to give the harmonized combined Hamaker coefficients, A_{132har}. Ultimately a single value of the Hamaker coefficient is essential in determining the

final outcome. This is known as the absolute combined Hamaker coefficient, A_{132abs}. It is obtained by integrating all the values of the Hamaker coefficient to give a single value.

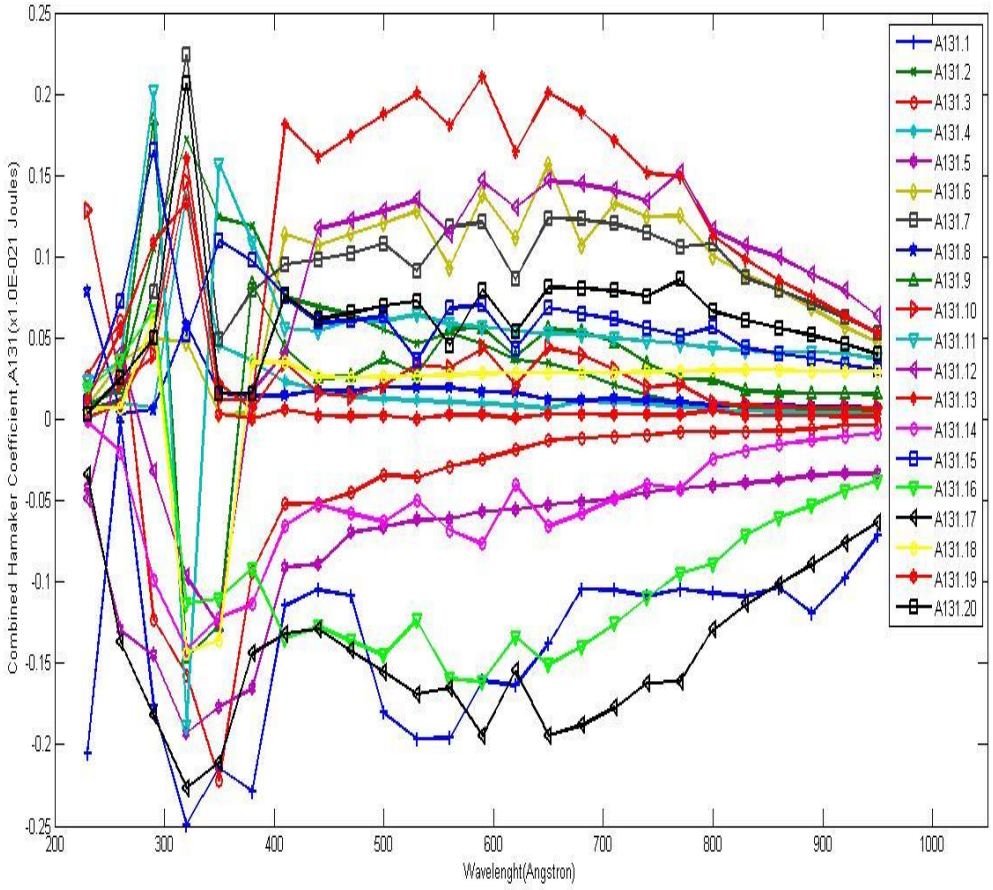

Fig.4.8: Variation of Combined Hamaker Coefficient, A_{131} with Wavelength, λ (Å) for the M-TB uninfected Sputum Samples

Figure (4.8) reveals the pattern of the combined Hamaker coefficients for the uninfected sputum samples with clear maxima and minima values occurring at various wavelengths. Harmonized values of the combined Hamaker coefficient became necessary to streamline the findings. This involves the integration of all the Hamaker coefficients first over each wavelength, secondly with each sputum sample in view to give the harmonized combined Hamaker coefficients, A_{131har}.

Ultimately a single value of the Hamaker coefficient is essential in determining the final outcome. This is known as the absolute combined Hamaker coefficient, A_{131abs}. It is obtained by integrating all the values of the Hamaker coefficient to give a single value.

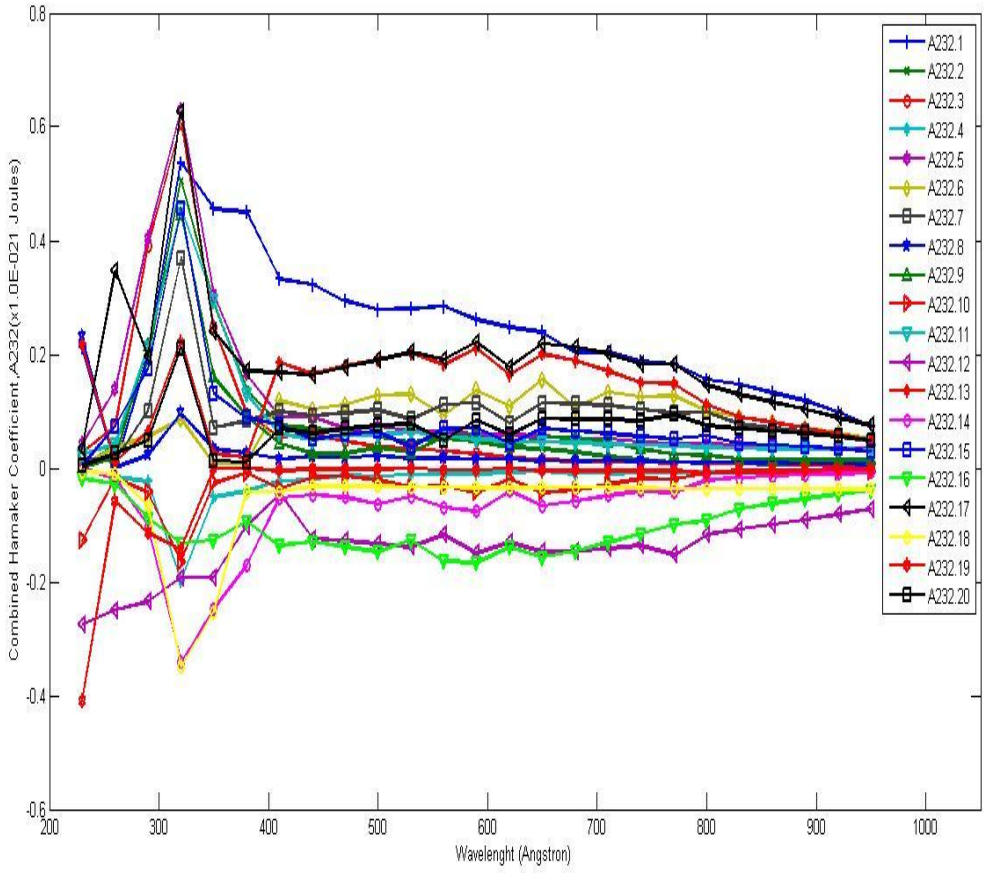

Fig.4.9: Variation of Combined Hamaker Coefficient, A_{232} with Wavelength, λ (Å) for the M-TB infected Sputum Samples

Figure (4.9) reveals the pattern of the combined Hamaker coefficients for the infected sputum samples with clear maxima and minima values occurring at particular wavelengths. Harmonized values of the combined Hamaker coefficient became unnecessary the finding is streamlined. The peak value of the combined

Hamaker coefficients A_{232} for the infected sputum is 0.6298 occurring at wavelength of 320Å. Ultimately this single value of the Hamaker coefficient is essential in determining the final outcome. This is known as the absolute combined Hamaker coefficient, A_{232abs}.

Not much meaning could be made out of figures (4.7) - (4.9). To generate more meaningful plots, average value for the given Hamaker coefficients of a given wavelength was determined from the data for the twenty samples. These results are given in figure (4.10).

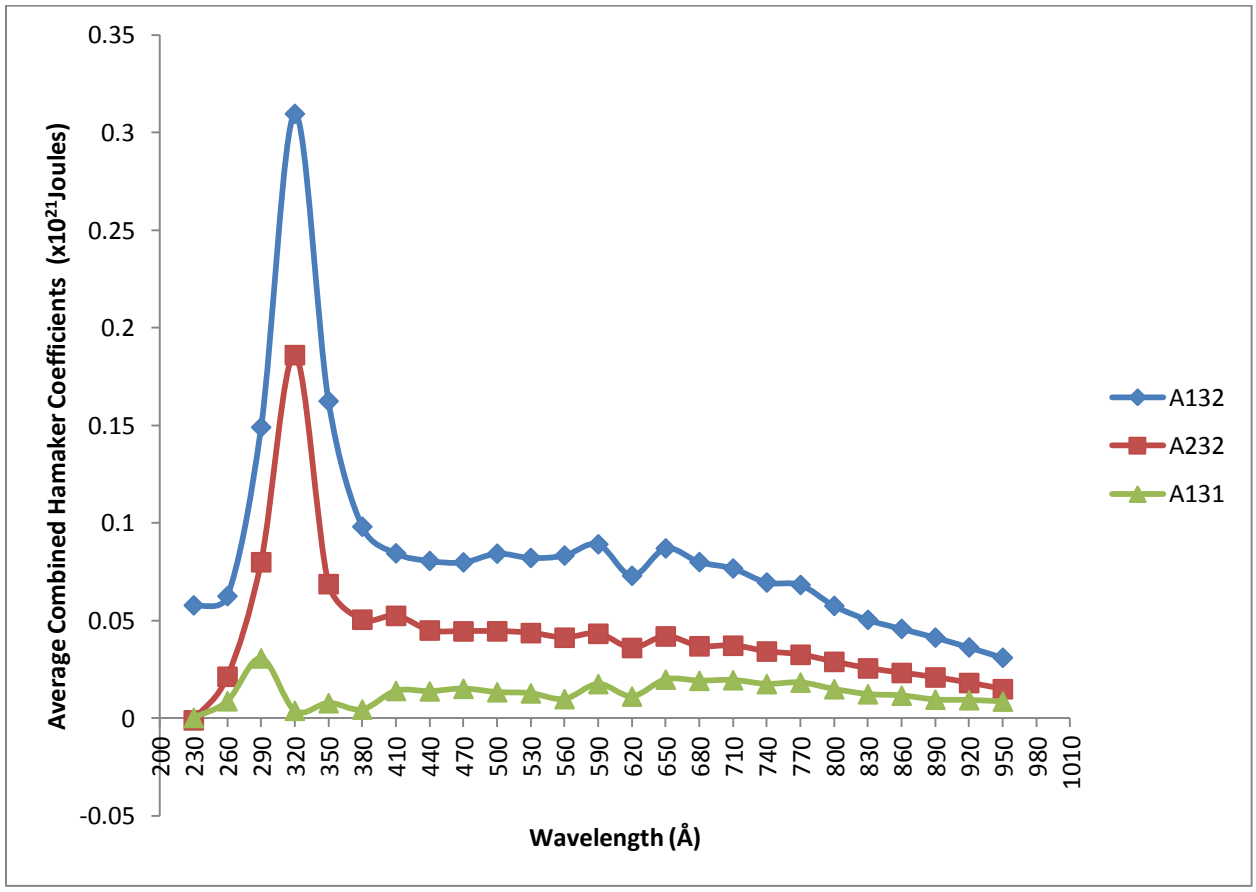

Fig.4.10: Variation of Average Combined Hamaker Coefficients, A_{132} A_{131} and A_{232} with Wavelength, λ (Å) for the M-TB infected Sputum Samples

Figure (4.10) reveals the pattern of the average combined Hamaker coefficients, A_{132}, A_{131} and A_{232} for the sputum samples with clear peak values occurring at various wavelengths. The peak average values of A_{132} and A_{232} occur at wavelength of 320Å with values of 0.30968 $x10^{-21}$J and 0.18609 $x10^{-21}$J respectively, while the peak average value of A_{131} occurs at wavelength of 290Å with value of 0.03074 $x10^{-21}$J. Energy level increases in average combined Hamaker coefficients, A_{132} and A_{232} which is the infected Hamaker coefficients as against the decreased energy level of the uninfected average combined Hamaker coefficient, A_{131}. This is quite a significant phenomenon which explains away the fact of infection.

4.5 Deductions for the Absolute Combined Hamaker Coefficient A_{132abs} and $\tilde{A}_{132abs}$

Applying Lifshitz derivation for van der Waals forces as in equation (3.34), The absolute value for the Hamaker coefficient could be derived by obtaining the mean of all the A_{132} values got from the Lifshitz relation.

Solving the Lifshitz relation as modified in equations (3.35), (3.36) and (3.37), an absolute value of combined Hamaker coefficient could be derived. Table G1 (appendix) shows integrated values of A_{132}, for each infected sputum sample.

A summation of all the values of the Hamaker coefficients and deriving a mean value to obtain a single value known as absolute combined Hamaker coefficient A_{132abs} became necessary and was got using MATLAB with the result as stated:

For M-TB: $A_{132abs} = 0.21631x10^{-21}$Joule

For M-TB/HIV: $\tilde{A}_{132abs} = 0.18825x10^{-21}$Joule

This was done by obtaining a mean of all the values of the Hamaker coefficients for the infected sputum for both M-TB and M-TB/HIV over the whole range of wavelength, λ = 230Å - 950Å, which gave $A_{132abs} = 0.21631 \times 10^{-21}$Joule and $\tilde{A}_{132abs} = 0.18825 \times 10^{-21}$Joule respectively. This value agrees with those obtained by various authors for other biological processes e.g. (van Oss,1988) in hydrophobic chromatography on phenyl-sepharose of human serum (see table 2.3).

Table 4.2: Computation of the absolute values of A_{131} for Uninfected M-TB Sputum and A_{132}, A_{232} for Infected M-TB Sputum

Variable ($\times 10^{-21}$ Joule)	Absolute Value
A_{131}	0.10165
A_{232}	0.24986
A_{132}	0.21631

Table 4.3: Computation of the absolute values of $\tilde{A}_{131}$ for Uninfected M-TB/HIV Sputum and $\tilde{A}_{132}$, $\tilde{A}_{232}$ for Infected M-TB/HIV Sputum

Variable ($\times 10^{-21}$ Joule)	Absolute Value
$\tilde{A}_{131}$	0.10165
$\tilde{A}_{232}$	0.20474
$\tilde{A}_{132}$	0.18825

Tables (4.2) and (4.3), reveals that the surface energy of the macrophages as computed interms of Hamaker coefficients is less than the surface energy of the M-TB, M-TB/HIV. This result also shows that the surface energy of the M-TB/HIV macrophage is less than that of M-TB macrophage. HIV has the tendency to reduce the energy with the consequences of increased viral loads and decreased immune systems. This is because, TB is an opportunistic disease and in prensence of HIV, the consequence is grievious. Hence for $A_{132} > 0$, $A_{131(\text{macropage})} < A_{232(\text{M-TB/HIV})}$.

4.6 Deductions for the Absolute Combined Negative Hamaker Coefficient

To define the condition where the absolute Hamaker coefficient becomes negative will require employing the relations that express that condition. Hence, recalling equations (3.31), (3.32),(3.33), a state where the Hamaker Coefficient, A_{132} is less than zero can be derived. This situation could be possible with the following already stated conditions (refer to equations (3.31 – 3.32);

$$A_{132} < 0$$

When; $\sqrt{A_{11}} > \sqrt{A_{33}}$ and $\sqrt{A_{22}} < \sqrt{A_{33}}$

Or $\sqrt{A_{11}} < \sqrt{A_{33}} < \sqrt{A_{22}}$

Or $A_{11} < A_{33} < A_{22}$; $A_{11} > A_{33} > A_{22}$

The mean of all values of A_{11} and A_{22} could be obtained and substituted into the relation below [equation (3.29)] in order to derive a value for A_{33} at which A_{132} is equal to zero in agreement with the earlier stated reasons.

$$A_{132} = \left(\sqrt{A_{11}} - \sqrt{A_{33}}\right)\left(\sqrt{A_{22}} - \sqrt{A_{33}}\right) \qquad (4.4)$$

Rearranging equation (4.4) and making A_{33} subject of the formula we obtain;

$$A_{33} = \left[\frac{2\sqrt{A_{11}}\sqrt{A_{22}} - A_{132}}{\sqrt{A_{11}} + \sqrt{A_{22}}} \right]^2 \qquad (4.5)$$

The mean of all the values of A_{11} and A_{22} respectively gave the absolute values of the Hamaker constants as shown below;

For mycobacterium Tuberculosis:

$\mathbf{A_{11}} = 0.94188 \times 10^{-21}$ Joule

$\mathbf{A_{22}} = 0.96068 \times 10^{-21}$ Joule

For mycobacterium Tuberculosis/HIV Association:

$\tilde{\mathbf{A}}_{\mathbf{11}} = 0.94188 \times 10^{-21}$ Joule

$\tilde{\mathbf{A}}_{\mathbf{22}} = 0.97862 \times 10^{-21}$ Joule

Thus, inserting these values into equation (3.35) and rendering $A_{132} \leq 0$ will give the critical value of A_{33C} that satisfies the condition for the combined Hamaker coefficient to be equal to or less than zero. Hence any value of A_{33} greater than the critical would be the desired value necessary to attain a negative combined Hamaker coefficient.

Hence, the critical absolute Hamaker constant A_{33C} for the sputum which renders the A_{132} negative is given as;

For mycobacterium Tuberculosis:

$$\mathbf{A_{33C}} = 0.9527\text{x}10^{-21}\text{Joule}$$

For mycobacterium Tuberculosis/HIV Association:

$$\tilde{\mathbf{A}}_{\mathbf{33C}} = 0.9598\text{x}10^{-21}\text{Joule}$$

Thus for negative combined Hamaker coefficient A_{132}, $\tilde{A}_{132}$ of the infected M-TB, M-TB/HIV sputum to be attained respectively, the combined Hamaker constant of the sputum as the intervening medium A_{33}, $\tilde{A}_{33}$ respectively should be of the magnitude;

$$\mathbf{A_{33C}} \geq 0.9527\text{x}10^{-21}\text{Joule and } \tilde{\mathbf{A}}_{\mathbf{33C}} \geq 0.9598\text{x}10^{-21}\text{Joule respectively}$$

Inserting the above values of A_{33}, $\tilde{A}_{33C}$ into equation (3.29) would yield negative values for A_{132}, $\tilde{A}_{132}$ respectively as follows;

$$\mathbf{A_{132}} = -\,0.22669\text{x}10^{-25}\text{Joule (when } \mathbf{A_{33}} = 0.9527\text{x}10^{-21}\text{Joule)}$$

And $$\tilde{\mathbf{A}}_{\mathbf{132}} = -\,0.08786\text{x}10^{-25}\text{Joule (when } \mathbf{A_{33}} = 0.9598\text{x}10^{-21}\text{Joule)}$$

To obtain a value for the combined Hamaker coefficient A_{131} for the uninfected sputum the relation of equations (3.27) and (3.28) are employed.

$$A_{131} = A_{11} + A_{33} - 2A_{13}$$

$$A_{131} = \left(\sqrt{A_{11}} - \sqrt{A_{33}}\right)^2$$

Upon integration of all values of A_{131} for the twenty uninfected sputum samples, an absolute value for both A_{131abs} and $\tilde{A}_{131abs}$ was derived as given below;

$$\mathbf{A_{131abs}} = \tilde{\mathbf{A}}_{\mathbf{131abs}} = 0.10165\text{x}10^{-21}\text{Joule}$$

This value is very nearly equal to zero which is a clear indication of the validity of the concept of Hamaker coefficient to the process and progress of human infection with the M-TB as an opportunistic disease. The near zero value of the A_{131abs} and $\tilde{A}_{131abs}$ shows the absence of infection in the sputum samples thus suggesting the usefulness of the concept of negative Hamaker coefficient in finding a solution to M-TB and M-TB/HIV co-infection. Table (4.4) shows the comparison of the Hamaker constants and coefficients for the infected and uninfected sputum samples for both M-TB and M-TB/HIV.

Table 4.4: Values of the Hamaker Constants and Hamaker Coefficients for the Infected and Uninfected M-TB Sputum Samples

Variable ($x10^{-21}$ Joule)	Infected Sputum		Uninfected Sputum	
	Peak Value	**Absolute Value**	**Peak Value**	**Absolute Value**
A_{11}	---	---	1.1328	0.94188
A_{22}	1.2134	0.96068		---
A_{33}	0.4205	0.23067	0.6701	0.42470
A_{132}	0.5187	0.21631		---
A_{131}	---	---	0.2241	0.10165
A_{232}	0.6298	0.24986		---

Tables (4.4) show the comparison of the Hamaker constants and coefficients for the positive and negative sputum samples. A_{11} is Hamaker constant for the uninfected sputum samples. A_{22} is the Hamaker constant for the M-TB, here represented by the infected macrophage. This is as a result of no known process of isolation of the M-TB at the moment. This is a very close approximation for the

bacteria owing to the manner of the infection mechanism. The Hamaker constants A_{33} for the sputum show greater values for the uninfected samples which regularly indicate a higher surface energy than the infected samples. The higher absolute values of A_{132} and A_{232} as against that of A_{131}, as well as the lower value of the absolute combined Hamaker coefficient A_{131abs} for the uninfected samples is a clear suggestion of the relevance of the concept of Hamaker coefficient in the M-TB infection process. The surface energy A_{131} of the macrophages is less than the surface energy A_{232} of the disease (M-TB).

Table 4.5: Values of the Hamaker Constants and Hamaker Coefficients for the Infected and Uninfected M-TB/HIV Sputum Samples

Variable ($x10^{-21}$ Joule)	Infected Sputum		Uninfected Sputum	
	Peak Value	**Absolute Value**	**Peak Value**	**Absolute Value**
$\tilde{A}_{11}$	---	---	1.1328	0.94188
$\tilde{A}_{22}$	1.0267	0.97862	---	---
$\tilde{A}_{33}$	0.5962	0.28812	0.6701	0.42470
$\tilde{A}_{132}$	0.4253	0.18825		
$\tilde{A}_{131}$			0.2241	0.10165
$\tilde{A}_{232}$	0.5014	0.20474		

Tables (4.5) show the comparison of the Hamaker constants and coefficients for the positive and negative sputum samples. $\tilde{A}_{11}$ is Hamaker constant for the uninfected sputum samples. $\tilde{A}_{22}$ is the Hamaker constant for the M-TB/HIV co-infection, here represented by the infected macrophage. This is as a result of no

known process of isolation of the M-TB/HIV co-infection at the moment. Though, this is a very close approximation for the bacteria owing to the manner of the infection mechanism. The Hamaker constants $\tilde{A}_{33}$ for the sputum show greater values for the uninfected samples which regularly indicate a higher surface energy than the infected samples. The higher absolute values of $\tilde{A}_{132}$ and $\tilde{A}_{232}$ as against that of $\tilde{A}_{131}$, as well as the lower value of the absolute combined Hamaker coefficient $\tilde{A}_{131abs}$ for the uninfected samples is a clear suggestion of the relevance of the concept of Hamaker coefficient in the M-TB/HIV co-infection process. The surface energy $\tilde{A}_{131}$ of the macrophages is less than the surface energy $\tilde{A}_{232}$ of the bacteria (M-TB).

Comparing tables (4.4) and (4.5); A_{33}, which serves as the energy of sputum as an intervening medium, is seen in M-TB data to be reduced by infection from 0.4247 $x10^{-21}$J to 0.23067 $x10^{-21}$J by a factor of about 45.7% (see table 4.4). In M-TB/HIV co-infection, the reduction is from 0.4247 $x10^{-21}$J to 0.28812 $x10^{-21}$J, a factor of about 32.2% (see table 4.5). The reduction is lower in M-TB/HIV co-infection probably because of the interaction between HIV and TB. For the combined Hamaker coefficient, the value is 0.21631 $x10^{-21}$J for M-TB and 0.18825 $x10^{-21}$J for M-TB/HIV. This result is as expected. HIV has the tendency to reduce the energy on the surface of a given material, in this case by about 13%, conforming adverse effects observed in HIV patients with tuberculosis. Note that the values of A_{132} are all positive showing that attraction exists between the macrophage and the M-TB particles. The effect of the infection can only be abated if a drug, in the form of additive is added that can change the value of A_{132} to negative under that condition, mutual repulsion will occur and it will be expected that, in principle, the TB bacteria will not attack the macrophage.

4.7. Computation for Harmonized Hamaker Coefficients

A derivation of a mathematical expression for this relationship was made and the following result was obtained.

$$A_{132har} = \phi_t A_{132\max} \tag{4.6}$$

Where;

$$\phi_t = \int_0^{\infty} \left(A_{132\max} - A_{132har}\right) d\lambda \tag{4.7}$$

Where Φ_t = the integral of the difference between A_{132max} and $A_{132hars}$

Thus, from the deductions made from this work the following result was got;

$$A_{132har} \approx 0.4725\left(A_{132\max}\right) \tag{4.8}$$

Hence;

$$A_{132\max} \approx \frac{1}{0.4725}\left(A_{132har}\right) \tag{4.9}$$

It could easily be seen that in finding a solution for the absolute Hamaker coefficient, the maxima and harmonized values of Hamaker coefficient could be used. This approximate method thus serves as an alternative method for obtaining a reliable value for the absolute combined Hamaker coefficient for human sputum systems and could well be relevant to other biological and particulate systems. This latter statement needs verification and could be taken up as a new research area in this field.

Table 4.6: Comparison of the Values of the Absolute Combined Hamaker Coefficients, A_{132abs}, A_{131abs} and the Harmonized Combined Hamaker Coefficents, A_{132har}, A_{131har} of the M-TB on both Infected and Uninfected Sputum

Infected Sputum		Uninfected Sputum	
A_{132abs} ($\times 10^{-21}$ Joule)	**A_{132har} ($\times 10^{-21}$ Joule)**	**A_{131abs} ($\times 10^{-21}$ Joule)**	**A_{131har} ($\times 10^{-21}$ Joule)**
0.21631	0.24509	0.10165	0.10589

Table 4.7: Comparison of the Values of the Absolute Combined Hamaker Coefficients, $\tilde{A}_{132abs}$, $\tilde{A}_{131abs}$ and the Harmonized Combined Hamaker Coefficents, $\tilde{A}_{132har}$, $\tilde{A}_{131har}$ of the M-TB/HIV on both Infected and Uninfected Sputum

Infected Sputum		Uninfected Sputum	
$\tilde{A}_{132abs}$ ($\times 10^{-21}$ Joule)	**$\tilde{A}_{132har}$** ($\times 10^{-21}$ Joule)	**$\tilde{A}_{131abs}$** ($\times 10^{-21}$ Joule)	**$\tilde{A}_{131har}$** ($\times 10^{-21}$ Joule)
0.18825	0.2010	0.09627	0.10589

The single value of the Hamaker coefficient is necessary in determining the final conclusion. Harmonized values of the combined Hamaker coefficient is required to rationalize the findings. This involves the integration of all the Hamaker coefficients over each wavelength, with each sputum sample in view to give the harmonized combined Hamaker coefficients, A_{132har} for both M-TB and M-TB/HIV co-infection. The harmonized values of the combined Hamaker coefficient for each infected and uninfected sputum samples are shown in tables (4.6) and (4.7) alongside with that of the absolute combined Hamaker coefficient for both M-TB and M-TB/HIV co-infection. The association systems of M-TB with the HIV sputum samples gave a positive absolute combined Hamaker coefficient, A_{132} which entails attractive van der Waals forces. The positive sense

of the absolute combined Hamaker coefficient obtained is in agreement with the statement of (Achebe et al, 2012). However, the positive values of the absolute combined Hamaker coefficient A_{131} for M-TB associating with HIV negative sputum samples as shown in table (4.7) indicate that there is an attraction between the associating bodies. This is so because the positive sense of the absolute combined Hamaker coefficient shows that the van der Waals forces of the associating systems are attractive. A comparison in tables (4.6) and (4.7) of the maxima A_{132max} and the harmonized A_{132har} values of the combined Hamaker coefficient shows a direct association between the two. Difference in terms of the magnitude only was recorded. However, this research work is limited to the role the van der Waals forces play in the process and progress of M-TB/HIV co-infection, the mechanism involved and the contribution its study could offer in the chase for a feasible solution to the overwhelming condition.

4.8 Computation of Surface Free Energy and Change in Free Energy of Adhesion

For all given combinations, it is possible to express the van der Waals force of cohesion which is the force of attraction between similar particles in a substance, just as the surface energy or energy of interaction is a function of van der Waals force of adhesion which is the force of attraction between different particles suspended in a liquid medium.

From equation (2.26) and equation (2.27):

$$A_{ij} = -12\pi d_0^{\,2} \Delta F_{ij}(d_0) \tag{4.10}$$

And

$$\Delta F_{ij}^{coh} = -2\gamma_{iv} \tag{4.11}$$

Combining equation (4.10) and equation (4.11):

$$A_{ij} = -12\pi d_0^{\,2} \times -2\gamma_{sv} \tag{4.12}$$

Hence; $$A_{ij} = 24\pi d_0^{\,2}\gamma_{sv} \tag{4.13}$$

The surface free energy is given thus;

$$\gamma_{sv} = \frac{A_{ij}}{24\pi d_0^2} \tag{4.14}$$

The minimum distance d_o between the same particles is given as: $d_0 = 1.82 Angstrom = 1.82 nm = 1.82 \times 10^{-9} m$ (van Oss et, 1972)

Aij = Hamaker constant measured in ($\times 10^{-14}$ mJ) or ($\times 10^{-21}$ Joule) or ($\times 10^{-14}$ ergs)

γ_{sv} = Surface Free Energy measured in (mJ/m^2) or (J/m^2) or ($ergs/cm^2$)

From equation (3.11): $$\Delta F_{132}^{adh}(d_0) = -\left[\frac{A_{132}}{12\pi d_0^{\,2}}\right] \tag{4.15}$$

Using equation (4.14) and computed values of A_{ij} as shown in tables (4.4) and (4.5), the calculated values of γ_{sv} is given in tables 4.8 and 4.9 for both M-TB and M-TB/HIV respectively.

Table 4.8: Computed values of surface energies γ_{sv} of the M-TB Sputum Interacting Systems

Interacting System	$A_{11}(\times10^{-14}mJ)$ (Macrophage)	γ_{sv} (mJ/m^2) (Macrophage)	$A_{22}(\times10^{-14}mJ)$ (M-TB)	γ_{sv} (mJ/m^2) (M-TB)	$A_{33}(\times10^{-14}mJ)$ (Sputum)	γ_{sv} (mJ/m^2) (Sputum)
Infected Sputum	---	---	0.96068	38.5	0.23067	9.2
Uninfected Sputum	0.94188	37.7	---	---	0.42470	17.0

Since the surface energy is a measure of workdone on the surface. Table (4.8) shows the surface energy of the M-TB is greater than the surface energy of the sputum. Also, the surface energy of the uninfected sputum 17.0mJ/m^2 was apparently reduced to 9.2mJ/m^2 when M-TB attacked the human system. Consequently, the disease incidence lowers the surface energy of the infected sputum. This in effect indicates that M-TB has a surface energy reducing capacity in line with the finding by (Ozoihu, 2014) for HIV-Lymphocytes.

From Table 4.8; the following deductions are made;

- Surface energies of infected sputum components are lower than the uninfected, i.e., they became more hydrophobic.
- M-TB infection has the surface energy reducing capacity (i.e. reduces the work done on the surface).

Table 4.9: Computed values of surface energies γ_{sv} of the M-TB/HIV Sputum Interacting Systems

Interacting System	$\tilde{A}_{11}(\times 10^{-14}mJ)$ (Macrophage)	γ_{sv} (mJ/m^2) (Macrophage)	$\tilde{A}_{22}(\times 10^{-14}mJ)$ (M-TB/HIV)	γ_{sv} (mJ/m^2) (M-TB/HIV)	$\tilde{A}_{33}(\times 10^{-14}mJ)$ (Sputum)	γ_{sv} (mJ/m^2) (Sputum)
Infected Sputum	---	---	0.97862	39.2	0.28812	11.5
Uninfected Sputum	0.94188	37.7	---	---	0.42470	17.0

Table (4.9) shows that the surface energy of the M-TB/HIV is greater than the surface energy of the sputum. Also, the surface energy of the uninfected sputum $17.0mJ/m^2$ was in fact reduced to $11.5mJ/m^2$ when M-TB/HIV co-infection attacked the human system. As a result, the disease incidence lowers the surface energy of the infected sputum as shown in table 4.9. This in effect indicates that M-TB/HIV has a surface energy reducing capacity, tending to make the surface of the bacteria (sputum) more hydrophobic.

From Table 4.9; the following deductions are made;

- Surface energies of infected sputum components are lower than the uninfected.
- M-TB infection has the surface energy reducing capacity (i.e. reduces the work done on the surface).
- It is well identified that M-TB/HIV attacks the macrophage; the reduction (difference on infected and uninfected) in surface free energies of Sputum could be as a result of its presence in the sputum.

Table 4.10: Comparison of the values of Surface Free Energy γ_{sv} of the M-TB and M-TB/HIV Infected and Uninfected Sputum

Variable	Infected Sputum		Uninfected Sputum	
	Hamaker constant, A ($\times 10^{-14}$mJ)	γ_{sv} (mJ/m^2)	Hamaker constant, A ($\times 10^{-14}$mJ)	γ_{sv} (mJ/m^2)
$\mathbf{A_{11}}$	---	---	0.94188	37.7
$\mathbf{A_{22}}$	0.96068	38.5	---	---
$\mathbf{A_{33}}$	0.23067	9.2	0.42470	17.0
$\mathbf{\tilde{A}_{11}}$	---	---	0.94188	37.7
$\mathbf{\tilde{A}_{22}}$	0.97862	39.2	---	---
$\mathbf{\tilde{A}_{33}}$	0.28812	11.5	0.42470	17.0

Table 4.11: Computation of Change in free energy of adhesion, ΔF^{adh} (mJ/m^2)

Variable	Hamaker coefficients, ($\times 10^{-14}$mJ)	ΔF^{adh} (mJ/m^2)
$\mathbf{A_{132}}$	0.21631	-17.3
$\mathbf{A_{131}}$	0.10165	-8.1
$\mathbf{A_{232}}$	0.24986	-20.0
$\mathbf{\tilde{A}_{132}}$	0.18825	-15.1
$\mathbf{\tilde{A}_{131}}$	0.10165	-8.1
$\mathbf{\tilde{A}_{232}}$	0.20474	-16.4

The surface free energies described in tables 4.10 and 4.11 are used to determine the free energy of adhesion. When the change in free energy of adhesion is negative; adhesion is thermodynamically favorable. Adhesion is therefore governed by attractive van der Waal forces. When M-TB or M-TB/HIV co-

infection affixes itself to the surface of the macrophage in a liquid medium, there is the tendency of the bacteria to be engulfed by the macrophage cells. Thus increased adhesion may lead to more depletion of macrophage cells. The adhesion of the bacteria on the cell will lead to penetration into the macrophage. Such a penetration will cause replication of bacteria and destruction of macrophage. What is required is for this attachment not to occur. Results obtained (Table 4.11) give the following deductions:

- The change in free energies of adhesion is all negative indicating that the net van der Waals forces are attractive.
- The change in free energies of adhesion is higher for infected M-TB/HIV than infected M-TB. In order words, presence of HIV increases the change in free energy of adhesion and hence tendency for increased attack.
- Hamaker coefficients are all positive suggesting van der Waals forces are attractive, as negative free energy of adhension.

4.9 Application of Statistical Thermodynamics to the System

4.9.1 Micro-Canonical Ensembles Application

In micro canonical ensemble N, V and E are fixed: since the second law of thermodynamics applies to isolated systems, the first case investigated will correspond to this case. The micro canonical ensemble describes isolated systems.

The system described in this research work is an isolated system thus micro canonical ensemble is employed, because an isolated system keeps a constant energy, the total energy of the system does not fluctuate. Thus, the system can access only those of its micro-states that correspond to the given value of'' E' of

the energy. The internal energy of the system is then strictly equal to its energy (Terrell, 2008):

$$E(S, V) = U(S, V) \qquad (4.16)$$

Let n(E) the number of microstate corresponding to this value of the system energy. The macroscopic state of maximal entropy for the system is the one in which all microstates are equally likely to occur, with probability $\frac{1}{n(E)}$, during the system's fluctuations (Udayanandan et al, 2009; Donald, 2000):

$$S = -K_b \sum_{j-1}^{n(E)} \left[\frac{1}{n(E)} ln \frac{1}{n(E)}\right] = K_b \ln[n(E)] \qquad (4.17)$$

The probability P_i that a macroscopic system is in thermal equilibrium with its environment will be in a given microstate with energy E_i according to the Boltzmann distribution (Uduyanandan et al, 2009):

$$P_i = \frac{e^{-\beta E_i}}{\sum_j^{jmax} e^{-\beta E_i}} \qquad (4.18)$$

Where; $$\beta = \frac{1}{KT} \qquad (4.19)$$

The temperature T arises from the fact that the system is in thermal equilibrium with its environment. The probabilities of the various microstates must add to one, and the normalization factor in the denominator is the canonical partition function (Udayanandan et al, 2009; Donald, 2000):

$$Z = \sum_j^{jmax} e^{-\beta E_i} \qquad (4.20)$$

Where; E_i is the energy of the ith microstate of the system.

Since a microstate is a complete description of every particle in the system and the partition function is a measure of a number of states accessible to the system at a given temperature T.

Then, the probability of finding a system at temperature T in a particular state with energy E_i is given by (Terrell, 2008):

$$P_i = \frac{e^{-\beta E_j}}{Z} \tag{4.21}$$

Where; $$E = \sum_i E_i e^{-\beta E_i} = \frac{1}{Z}\frac{d}{d\beta} \tag{4.22}$$

Since the system does not fluctuate:

$$S = k_b lnN \tag{4.23}$$

Since partition function and fugacity relate (Uduyanandan et al, 2009):

$$\mu = k_b T lnZ \tag{4.24}$$

Where; μ is partition function, Z = fugacity (i.e. the easiness of adding a new particles into the system).

$$S = \frac{\mu}{T} \ln \left(\frac{N}{Z}\right) \tag{4.25}$$

Since T is constant throughout.

Therefore: $$S = \mu_f lnZ_n \tag{4.26}$$

Where; μ_f is the new partition function, Z_n is the number of fugacity.

Equation (4.25) and equation (4.26) shows that S increases as μ_f increased and both are the functions of fugacity Z.

4.9.2 Numerical Application of Statistical Thermodynamics

Applying composite Trapezoidal rule modified with Romberg formula to the system (Jain et al, 2010):

$$A_{abs} = \int_0^{\infty} Ad\lambda = \int_a^b F(x)dx = \frac{h}{2}\left[A_1 + 2(\sum_{i=1}^{n-1} A_i) + A_n\right] \qquad (4.27)$$

Where; $F(x) = A, dx = d\lambda,$ a = minimum limit, a = maximum limit, A_1=Initial Combined value of A and A_n = Final Combined value of A.

$$A_1 = \sum_{\iota=1}^{n} \left(\frac{A}{n}\right)_{\lambda_i} \qquad (4.28)$$

$$A_n = \sum_{\iota=1}^{n} \left(\frac{A}{n}\right)_{\lambda_n} \qquad (4.29)$$

$$h(step\ size) = \sum_{\iota=1}^{n-1} \left(\frac{b-a}{n}\right)_i \qquad (4.30)$$

Applying Regression approach to the system (Engene, 2005):

$$A = A(\lambda) \qquad (4.31)$$

Let the approximating polynomial be given by (Jain etal, 2010):

$$A = \alpha_0 + \alpha_1\lambda + \alpha_2\lambda^2 \qquad (4.32)$$

Define a variable;

$$X = \begin{pmatrix} 1 & \lambda_1 & \lambda_1^2 \\ 1 & \lambda_2 & \lambda_2^2 \\ 1 & \lambda_3 & \lambda_3^2 \\ . & . & . \\ . & . & . \\ 1 & \lambda_n & \lambda_n^2 \end{pmatrix} \quad (4.33)$$

Such that; $A_{abs} = [X] \begin{bmatrix} \alpha_0 \\ \alpha_1 \\ \alpha_2 \end{bmatrix}$ (4.34)

Define a variable;

$$A_{abs} = \begin{pmatrix} 1 & \lambda_1 & \lambda_1^2 \\ 1 & \lambda_2 & \lambda_2^2 \\ 1 & \lambda_3 & \lambda_3^2 \\ . & . & . \\ . & . & . \\ 1 & \lambda_n & \lambda_n^2 \end{pmatrix} \begin{bmatrix} \alpha_0 \\ \alpha_1 \\ \alpha_2 \end{bmatrix} \quad (4.35)$$

Applying combined Hamaker Coefficient values A_{132} (appendix G);

From equation (4.30): h = 1.2

From equation (4.28): $A_{132,i}$ = $0.2022x10^{-21}$Joule

From equation (4.29): $A_{132,n}$ = $0.1420x10^{-21}$Joule

From equation (4.27): A_i = $0.0161x10^{-21}$Joule

Substituting these values into equation (4.27)

$A_{132abs} = \frac{h}{2}\left[A_{132,i} + 2(\sum_{\iota=1}^{n-1} A_i) + A_{132,n}\right] = 0.2258 \times 10^{-21}$Joule

Applying combined Hamaker Coefficient values A_{131} (appendix G);

From equation (4.30): h = 1.2

From equation (4.28): $A_{131,i} = 0.1448x10^{-21}$ Joule

From equation (4.29): $A_{132,n} = 0.0576x10^{-21}$ Joule

From equation (4.27): $A_i = 0.0142x10^{-21}$ Joule

Substituting these values into equation (4.27)

$A_{131abs} = \frac{h}{2}\left[A_{131,i} + 2(\sum_{\iota=1}^{n-1} A_i) + A_{131,n}\right] = 0.1384x10^{-21}$Joule

Applying combined Hamaker Coefficient values A_{232} (appendix G);

From equation (4.30): h = 1.2

From equation (4.28): $A_{232,i} = 0.0296x10^{-21}$ Joule

From equation (4.29): $A_{232,n} = 0.0167x10^{-21}$ Joule

From equation (4.27): $A_i = 0.2037x10^{-21}$ Joule

Substituting these values into equation (4.27)

$A_{232abs} = \frac{h}{2}\left[A_{232,i} + 2(\sum_{\iota=1}^{n-1} A_i) + A_{232,n}\right] = 0.2521x10^{-21}$Joule

The values of absolute combined Hamaker coefficient from numerical computation is summarized in equation (4.36).

$$\begin{bmatrix} A_{132abs} \\ A_{131abs} \\ A_{232abs} \end{bmatrix} = \begin{bmatrix} 0.2258x10^{-21} \\ 0.1384x10^{-21} \\ 0.2521x10^{-21} \end{bmatrix} Joules \quad (4.36)$$

Using MatLab software tools to calculate the values of $\begin{bmatrix} \alpha_0 \\ \alpha_1 \\ \alpha_2 \end{bmatrix}$ from equation (4.35);

For $A_{132(abs)}$; $\begin{bmatrix} \alpha_0 \\ \alpha_1 \\ \alpha_2 \end{bmatrix} = \begin{bmatrix} 0.0001\text{x}10^{-21} \\ 0.0143\text{x}10^{-21} \\ 0.3286\text{x}10^{-21} \end{bmatrix}$ (4.37)

Applying this result to equation (4.32);

$$A = 0.0001x10^{-21} + 0.0143x10^{-21}\lambda + 0.3286x10^{-21}\lambda^2 \quad (4.38)$$

Equation (4.38) is the regression equation for combined Hamaker coefficient for A_{132}

For $A_{131(abs)}$; $\begin{bmatrix} \alpha_0 \\ \alpha_1 \\ \alpha_2 \end{bmatrix} = \begin{bmatrix} 0.0001\text{x}10^{-21} \\ 0.0162\text{x}10^{-21} \\ 0.3725\text{x}10^{-21} \end{bmatrix}$ (4.39)

Applying this result to equation (4.32);

$$A = 0.0001x10^{-21} + 0.0162x10^{-21}\lambda + 0.3725x10^{-21}\lambda^2 \quad (4.40)$$

Equation (4.40) is the regression equation for combined Hamaker coefficient for A_{131}

For $A_{132(abs)}$; $\begin{bmatrix} \alpha_0 \\ \alpha_1 \\ \alpha_2 \end{bmatrix} = \begin{bmatrix} 0.0001\text{x}10^{-21} \\ 0.0113\text{x}10^{-21} \\ 0.2597\text{x}10^{-21} \end{bmatrix}$ (4.41)

Applying this result to equation (4.32);

$$A = 0.0001x10^{-21} + 0.0113x10^{-21}\lambda + 0.2597x10^{-21}\lambda^2 \qquad (4.42)$$

Equation (4.42) is the regression equation for combined Hamaker coefficient for A_{232}

Applying Computational Results to Statistical Thermodynamics

From equation (4.19); $\beta = \frac{1}{KT}$;

Where; k is Boltzmann constant = 1.38x10^{-23}J/K and T = Room temperature = 25^{o}C = 298K.

Therefore; $\beta = 2.4317x10^{-20}Joule$

Substituting the values of β and E_j into equation (4.20); Z = 1.0 Joule.

From equations (4.22), (4.23) & (4.25); E = 0.2022x10^{-21}Joules, S = 4.134x10^{-23}Joules and μ = 4.1122x10^{-21}Joules respectively.

The result above shows the energy level of the system with its corresponding entropy. The unity value of fugacity shows that additive to the system to prevent particle interaction is possible. Since the value of partition function is greater than entropy of the system, particle – particle interaction could be prevented (i.e. bacteria – macrophage could be blocked so that the bacteria will not have access to penetrate and attack the cells).

Table 4.12: Compared Results of Combined Absolute Hamaker Coefficients

Absolute Combined Hamaker Coefficient	Lifshitz Formulation	Statistical Computation	Mean	Variance	Standard Diviation
$A_{132abs} \times 10^{-21}$	0.21631	0.2258	0.22106	0.000045	0.00671
$A_{131abs} \times 10^{-21}$	0.10165	0.1384	0.12025	0.000675	0.02598
$A_{232abs} \times 10^{-21}$	0.24986	0.2521	0.25098	0.000003	0.00158

The values of absolute combined Hamaker coefficients A_{132abs}, A_{131abs} and A_{232abs} obtained as summarized in Table. (4.12) for both statistical computation approaches is in agreement with the values of A_{132abs}, A_{131abs} and A_{232abs} obtained using Lifshitz formula approach. The regression equation (4.38; 4.40; 4.42) shows the correlations among the absorbance and the Hamaker coefficient which increases as wavelength increased. Energy level increases in average combined Hamaker coefficients, A_{132} and A_{232} which is the infected Hamaker coefficients as against the decreased energy level of the uninfected average combined Hamaker coefficient, A_{131}. This is quite a significant phenomenon which explains away the fact of infection mechanisms.

4.10 Deductions

The results obtained are presented in tables (4.8; 4.9; 4.10; 4.11 and 4.12). The table shows an increase in attraction ($-\Delta F^{adh}$) for M-TB infected sputum when compared to uninfected sputum irrespective of the equation used to obtain the change in free energies of adhesion. The negative values suggest that the interaction is driven by attractive forces. Although attraction is more on infected sputum than uninfected sputum, the negative signs on uninfected are an indication that M-TB disease is not the only cause of reduction in immune system.

Table (4.11) shows the values of change in interfacial free energy of adhesion for the infected and uninfected sputum. The table however, shows that attraction is more on infected sputum and less on uninfected sputum. That is to say that M-TB infection increases the van der Waals forces of attraction and this minimizes the surface area at the phase boundary. Here, the particles at the surface will try to reduce the free energy by interacting with the particles at the adjacent phase and hence decrease in surface energy.

The results obtained using Statistical Thermodynamics computational approach is presented in the summarized table (4.12). The tables show the variations in Hamaker coefficients and standard observations obtained from absorbance measurements of infected and uninfected sputum samples.

CHAPTER FIVE

CONCLUSION AND RECOMMENDATIONS

5.1 Conclusion

The absorbance data were suitably measured on M-TB/HIV infected and uninfected sputum using digital Ultraviolet visible metaspecAE1405031Pro Spectrophotometer. The results obtained from absorbance measurements were used to calculate the variables such as transmittance T, reflectance R, refractive index (real and imaginary) n, extinction coefficient K, absorption coefficient α, dielectric constants (real and imaginary) ε_{ij}, Hamaker constants A_{ij} and Hamaker coefficients A_{132}. These results were used to predict the interaction that occurs between M-TB/HIV co-infections. This prediction was based on the concept of van der waals attractive forces and absolute Hmaker coefficient whose negative and positive values respectively indicate attraction. But in a case that van der waals forces become positive and combined absolute Hamaker coefficient becomes negative, the forces repel each other. Therefore, changing the van der waals attractive force to repulsion becomes a traditional method of separation.

The positive values of the absolute combined Hamaker coefficients $A_{132}=0.21631x10^{-21}$Joule (M-TB) and $\tilde{A}_{132} = 0.18825x10^{-21}$Joule (M-TB/HIV) obtained for both the M-TB positive and M-TB/HIV positive samples are a confirmation that the sputum samples were actually infected. The absolute Hamaker coefficient $A_{131}=0.10165x10^{-21}$Joule gives the interaction energy among the macrophage cells in the sputum while A_{232} is the interaction energy among the TB particles in the sputum (i.e. A_{232} is the energy of interaction among the TB particles or among the TB/HIV particles in sputum). A_{232} for TB/HIV co-infection

is less than that for TB alone. Reduction in energy in the presence of HIV confirms the adverse effect when TB and HIV occur simultaneously in a patient. Reduction in energy leads to reduction in CD4 in HIV patient and hence greater prospect for death. This is so since a positive Hamaker value for any interacting system implies an attraction between the interacting bodies or particles while a negative Hamaker coefficient means repulsive van der Waals forces hence the interacting bodies would repel each other.

The first round of calculations of surface free energy and change in free energy of adhesion for both M-TB/HIV infected and uninfected sputum provided an easy approach to the estimation of Hamaker coefficients for the interacting systems. The presence of M-TB/HIV however, reduces the work done on the surface. The surface energy decreases when infected by the M-TB/HIV and thus, M-TB/HIV has the capacity to lower the surface energy. The decrease in surface energy for infected sputum and mostly for macrophage is a confirmation that macrophages are mostly attracted by the M-TB. Absence of M-TB/HIV however, increases the surface energy.

The change in free energy of adhesion increases when M-TB infection affixes itself to the surface of the macrophage. This means that presence of M-TB/HIV increases van der waals attractive force and mostly for infected macrophages. The energies of interactions expressed as Hamaker coefficients are all positive and this also validates the claim that attraction occurs between HIV and blood during infection as observed also by (Ozoihu, 2014). The negative combined Hamaker coefficient ($-0.22669 \times 10^{-19} mJ/m^2$) shows that van der waals attractive force is repulsive.

This research concludes that there is a prospect of finding remedy for the M-TB/HIV epidemic if further work towards defining the conditions of the system that could render the absolute combined Hamaker coefficient negative and the additive(s) to the system (in form of drugs) as the intervening medium that could accomplish this condition. That, as expected, may be the much desired way out for drug resistant strains of the M-TB bacteria.

5.2 Addition to Knowledge

To the best of the available knowledge, no research has studied the M-TB/HIV - Macrophage interactions from the Hamaker coefficient approach. This novel idea has therefore increased the possibility of finding a solution to the M-TB/HIV epidemic through the following research findings.

- The surface energy of M-TB/HIV infected surfaces is known through the Hamaker approach.
- The surface free energies and Hamaker coefficient of the M-TB/HIV were determined using the equation of the thermodynamic free energy of adhesion of a particle on a solid in a liquid at a separation distance.
- M-TB/HIV has the energy reducing capacity. It reduces the surface; M-TB from $17.0mJ/m^2$ – $9.2mJ/m^2$, M-TB/HIV from $17.0mJ/m^2$ – $11.5mJ/m^2$.
- The positive values of Hamaker coefficient imply that attraction occurs between M-TB/HIV and sputum during infection.
- The concept of negative Hamaker coefficient ($-A_{132}$) was establish with the combining rules and this agreed that changing van der waals attractive force to repulsion.

5.3 Recommendations

In other to carry out a further research on this topic, the following recommendations therefore are hereby made:

- Further researches which will include the use of contact angle approach as an alternative means of confirmation of the surface characteristics of sputum be carried out. This is another method of determining the van der Waals forces of interaction between particles in a system.

- Efforts should be made towards the explanation of the characteristics and requirement of the material that would render the combined Hamaker coefficient A_{132} negative as deduced in this research. This should involve a team of medical personnel like pharmacists, pharmacologists, laboratory scientists and doctors in partnership with engineers and physicists. A synergy of this sort cannot be overlooked if a solution to the threat of M-TB/HIV could be in view soonest. This of course is in the spirit of concurrent engineering and technology.

- When properly conducted, such further research should be geared towards seeking for a drug whose surface energies, obtained from the measured Absorbance could render the combined Hamaker coefficient (A_{132}) negative.

REFERENCE

Absolom D. R., Francis D. W., Zingg w., van Oss C. J., Neumann A. W., (1982). "Phagocytosis of bacteria by platelets: Surface thermodynamics", Journal of Colloid and Interface Science, 85: 1, 168 – 177.

Achebe C.H., Omenyi S.N., Manafa O.P., Okoli D., (2012). Human Immunodeficiency Virus (HIV)-Blood Interactions: Surface Thermodynamics Approach. *Proceedings of the International Multi-Conference of Engineers and Computer Scientists* 2012, Hong Kong, 136 – 141.

Achebe C. H., Omenyi S. N., (2013). Mathematical Determination of the Critical Absolute Hamaker Constant of the Serum (As an Intervening Medium) which Favours Repulsion in the Human Immunodefficiency Virus (HIV) - Blood Interaction mechanism. *Proceedings of the world congress on Engineering WCE 2013,* London, UK. *IAENG On-line Journal,* www.iaeng.org/publication/IMECS2012/, 1380 – 1384.

Achebe C. H., Omenyi S. N., (2013). The Effects of Human Immunodeficiency Virus (HIV) Infection on the Absorbance Characteristics of Different Blood Components. *International Journal of Science Invention,* 2(5): 53 – 61.

Achebe C. H., (2014). Surface thermodynamics Approach to HIV- Blood Interactions. LAP Lambert Academic Publishing, 1 – 35.

Adeeb S., Gauhar R., Mazhar U., Waleed A. K., Young S. L., (2013). Challenges in the development of drugs for the treatment of tuberculosis. *The Brazilian journal of infectious diseases,* 17(1): 74 – 81.

Adetunde I. A., (2009). Mathematical models of the dynamical behavior of tuberculosis disease in the upper East Region of the Northern part of Ghana: a case study of Bawku. *Current Research in Tuberculosis,* 1: 15 – 20.

Ait-Khaled N. and Enarson D. A., (2005). Tuberculosis: A manual for medical students. World Health Organization, Geneva, WHO/CDS/TB/99.272.

Alderman, L. M., (1988): On the maintenance of T.-cell populations" Technical report, Los Angeles, University of Califonia, Dept. of Computer Science.

American Thoracic Society and CDC. (2000). Diagnostic standards and classification of tuberculosis in adults and children. *Am. J. Respir. Crit. Care Med.,* 161(4): 1376 – 1395.

American Thoracic Society and Infectious Disease Society of America. (2007). Diagnosis, treatment, and prevention of nontuberculous mycobacterial diseases. *Am. J. Respir. Crit. Care Med.*, 175: 367 – 416.

Aparicio J. P., Carlos C., (2009). Mathematical modeling of tuberculosis epidemics. *Mathematical biosciences and engineering MBE. School of Science and technology, Universidad metropolitan, San Juan 00928-1150, Puerto Rico,* 6(2): 209 – 237.

Aparicio J. P., Capurro A. P., Castillo-chavez C., (2000). Transmission and dynamics of tuberculosis on generalized households. *Journal of theoretical Biology,* 206(3): 327 – 341.

Amy L. Bauer, Ian B. Hogue, Simeone Marino, and Denise E. Kirschner (2008). The Effects of HIV-1 Infection on Latent Tuberculosis. *Math. Model. Nat. Phenom.,* 3(7): 229 – 266.

Badri M., Wilson D., and Wood R., (2002). Effect of highly active antirectroviral therapy on incidence of Tuberculosis in South Africa: a Cohort study. *Lancet,* 359(23): 2059 – 2064.

Baier R. E., (1972). The Role of Surface Energy in Thrombogenesis. *Bull NY., Acad. Med,* 48(2): 257 – 272.

Bauer A. L., Hogue I. B., Marino S., and Kirschner E., (2008). The effects of HIV-1 infection on Latent Tuberculosis. *Math. Model. Nat. Phenom.,* 3(7): 229 – 266.

Beck J. S., Potts R. C., Kardjito T., and Grange J. M., (1985**)**. T4 lymphopenia in patients with active pulmonary tuberculosis. *Clin Exp Immunol*, 60: 49 – 54.

Berthelot D., (1898). Comptes Rendus, *Hebd. Seanc. Acad. Sci. Paris,* 126: 1703 – 1857.

Bezuidenhout J., Roberts T., Muller L., Helden P. Van, and Walzl G., (2009). Pleural tuberculosisin patients with early HIV infection is associated with increased TNF-alpha expression and necrosis in granulomas. *PLos one,* 4: e4228.

Blankson H. K., (2012). Economic Burden of Tuberculosis (TB) in Ghana (Case of Western Region). *KNUSTSpace Institutional Respository for KNUST*.M.Sc Thesis. *http://hdl.handle.net/123456789/4792*.

Blower S. M., and Gerberding J. L., (1998). Understanding, Predicting and Controlling the emergence of drug-resistant tuberculosis: a theoretical framework. *Journal of molecular medicine,* 76(9): 624 – 636.

Blower S., Small P., and Hopwell P. (1996). Control strategies for tuberculosis epidemics: new models for old problems. *Science,* 273: 497 – 500.

Bolger J. C., and Micheals A. S., (1969). Molecular Structure and Electrostatic Interactions: interface Conversion. *P. Weiss and D. Cheevers (Eds), Interface Conversion, Elservier, New York,* Chapter 1. 15 – 30.

Bragardo M., Buonfiglio D., (1997). Modulation of lymphocyte interaction with Endothelium and Homing by HI glycoprotein 120, *Journal of Immunology,* 159(4): 1619 – 1627.

Cao S., Wang f., Tam W., Tse L. A., Kim J. H., Lius Z. (2013). A hybrid seasonal prediction model for turberculosis incidence in China. *BMC Medical Information Decision Making,* 13: 56.

Carney W. P., Rubin R. H., Hoffman R. A., (1981). Analysis of T lymphocyte subsets in CMV mononucleosis. *The Journal of Immunology* 126(6): 2114 – 2116.

Caroline C., Ted C., and Megan M., (2006). Mathematical models of tuberculosis: accomplishments and future challenges. *International Symposium on Mathematical and Computational Biology,* 784 – 791.

Casimir H. B. G and Polder D., (1948). The Influence of Retardation on the London – van der Waals Forces. *Phys. Rev.,* 73: 360.

Chagan-Yasutan H., Saitoh H., Ashino Y., Arikawa T., Hirashima M., Li S., Usuzawa M., Oguma S., Otelan E. F., Obi C. L., and Hattori T., (2009). Persistent Elevation of plasma Osteopontin levels in HIV Patients Despite Highly Active Antiretroviral Therapy. *Tohoku journal of Experimental Madicine,* 218(4): 285 – 292.

Chirenda J., (1999). Low CD4 count in HIV-negative malaria cases, and normal CD4 count in HIV-positive and malaria negative patients. *Cent. Afr. J. Med.,* 45(9): 248.

Chaudhury M. K., (1984). Short Range and Long Range Forces in Colloidal and Macroscopic Systems. Ph.D Thesis, State University of New York at Buffalo. 215.

Charles, Kittel, (1996): Introduction to Solid state Physics, 7^{th} Ed., John Willey and sons Inc. New York. 308.

Claude J. K., Bowong S., Jean J. T., (2011). Stability analysis of the transmission dynamics of tuberculosis models. *Proceedings of World Academy of Science Union,* 107(2): 1 – 5.

Collin R. D., and JoAnne L. E., (2011). HIV-1/Mycobacterium tuberculosis Coinfection Immunology: How does Exacerbate tuberculosis. *Infect. Immune.,* 79(4): 1407 – 1417.

Comas I., Chakravartti J., Small P. M., Galagan J., Niemann S., Kremer K., Ernest J. D., and Gagneux S., (2010). Human T cell epitopes of mycobacterium Tuberculosis are Evolutionarily Hyperconserved. *Nature genetics,* 42(6): 498 – 503.

Corbett E. L., Watt C. J., Walker N., Maher D., Williams B. G., Raviglione M. C., Dye C. (2003). The growing burden of tuberculosis: global trends and interactions with the HIV epidemic. *Arch. Int. Med.*, 163(9): 1009 – 1021.

Corbett E. L., Marston B., Williams B. G., (2006). Tuberculosis in Sub-Sahara Africa: opportunities, challenges and changes in the era of antiretroviral treatment. *Lancert,* 367: 926 – 937.

Crowley T. M., Haring V. R., and Moore R., (2011). Chicken anemia virus: an understanding of the in-vitro host responses over time. *Viral immunology,* 73(10): 6846 – 6851.

Currie C. S. M., Williams B. G., Corbett E. L. (2005). Assessing the impact of HIV on the Annual Risk of TB infection using a mathematical model. *TSRU Progress Rep.*: 13.

Currie C. S. M., Williams B. G., Cheng R. C. H., Dye C., (2003). Tuberculosis epidemics driven by HIV: is prevention better than cure? *AIDS,* 17(17): 2501 – 2508.

Daniel T. M., Ellner J. J., (1994). Cultivation of mycobacterium tuberculosis for research purposes, In Bloom BR, Ed. TB: pathogenesis, protection and control, Washington DC, *American society for microbiology*: 75 – 102.

De Riemer K., and Ampel N. M., (2007). Quantitative Impact of Human Immunodeficiency Virus Infection on Tuberculosis Dynamics. *Am. J. Respir. Crit. Care Med.*, 176(1): 936.

De Souza M. V. N., (2006). Recent patents on Anti-infective. *Drug Discovery,* 1: 33 – 34.

Defay R., Prigogine I., Bellemans A., and Everett D. H., (1966). Surface Tension and Adsorption. *Longmans, Green and Co., London.* 110.

Deryagin, B. V., Zheleznyi B. V., Tkachev A. P., (1972). Dokl. Akad. *Nauk. SSSR,* 206: 1146.

Dietrich J. and Doherty T. M., (2009). Interation of mycobacterium tuberculosis with the host: consequences for vaccine development. *APMIS,* 117: 440 – 457.

Djerassi I., Kim J. S., Suvansri U., Mitrakul C., Cieselka W., (1972). Continuous Flow Filtration-Leukopheresis. *Transfusion,* 12: 75 – 83.

Doellgast G. J. and Fishman W. H., (1974). Purification of Human Pacental Alkaline Phosphatase. Salt effects in affinity Chromatography. *Biochem.* J., 141: 103.

Donald A. M. (2000). Statistical Mechanics. University Science Books, 1 – 8.

Drago R. S., Vogel G. C., Needham T. E., (1971) Four-parameter equation for predictingethalpies of adult formation. *J. Am Chem. Soc.,* 93: 6014 - 6026.

Dupre A., (1869). Theorie Mechanique de la Challeur. *Gauthier - Villars, paris:* 369.

Dye C., Garnett G. P., Sleeman A., Williams B. G., (1998). Prospects for worldwide tuberculosis control under the WHO DOTS strategy. *Lancert,* 352(91): 1886 – 1891.

Dzyaloshinskii, I. E., Lifshitz, E. M., Pitaevskii L. P., (1961). The General theory of Van der Waals forces. *Advanced in Physics,* 10(38): 165 – 209.

Engene A. Avallone (2005). Standard Hand Book for Mechanical Engineering. 4th Ed., 92 – 99.

Fowkes F. M., in K. L., (1983). Mittal (Ed), Physiochemical Aspects of Polymeric Surfaces. *Plenum, New York,* 2: 583.

Fowkes F. M., (1964). Attractive Forces at Interfaces. *Ind Eng .Chem.,* 56: 40.

Fowkes, F.M., (1967): in: Surfaces and Interfaces. *J.J. Burke, ed., Syracuse University Press, New York,* 1: 197, 199.

Gibbs J. W., (1869). Collected Works. *Longman Green - Villars, Paris,* 1: 369.

Girardi E., Antonucci G., Vanacore P., Palmier F., Matteelli A., Lenohi E., Carradori S., Salassa B., Pasticci M. B., Raviglione M. C., Ippolito G., The GISTA-SIMIT Study Group, (2004). Tuberculosis in HIV-infected persons in the context of wide availability of highly active antiretroviral therapy. *European Respiratory Journal,* 24(1): 11 – 17.

Girifalco L. A., and Good R. J., (1957). A theory for the Estimation of Surface and Interfacial. *J. Phys. Chem.*, 64(4): 561 – 565.

Gillman, C. F., and van Oss, C. J., (1971). Thermodynamics of Particle engulfment. *Biophys. J., 251(6): 415 - 423*.

Glynn J. R., Murray J., Bester A., Nelson G., Shearer S., Sonnenberg P., (2008). Effects of duration of HIV infection and secondary tuberculosis transmission on tuberculosis incidence in the South African Gold miners. *AIDS,* 22(14): 1859 – 1867.

Golub E. S., (1977). "The Cellular Basis of the Immune Response", *Sinauer Associates, Sunderland, MA:* 217.

Gonzalez-Juarrero M., Turner O. C., Turner J., Marietta P., Brooks J. V., Orme I. M., (2001). Temporal and Spatial arrangement of lymphocytes within lung granulomas induced by aerosol infection with mycobacterium tuberculosis. *Infect. Immun.* 69: 1722 – 1728.

Good R. J., and Stromberg R. R., (1979). Surface and Colloidal Science. *Plenum,* 11: 1.

Grammack D., Suman G., Simeone M., Jose S., Denise K. E., (2005). Understanding the immune response in tuberculosis using different mathematical models and biological scales. *SIAM Journal on Multiscale Modeling and Simulation,* 3(2): 312 – 345.

Greenwalt T. J., Gajewski M., and McKenna J. L., (1962). A new method for preparing buffy coat-poor blood. *Transfusion,* 2: 221 – 229.

Grossberg A. L., and Pressman D., (1962). Effect of Iodination on the active site of several Antihapten Antibodies. *Biochem.,* 1: 391.

Hamaker, H.C., (1937). The London – Van der Waals attraction between spherical Particles. *Physica*, 4: 1058.

Higby D. J., (1979). in: "Leukopheresis and Granulocyte Transfusions", *E. Cohen and R. B. Dawson, eds., America Assoc. Blood Banks, Washington DC:* 69.

Hough D. H and White L. R., (1987). Adv Colloid Interface. *Sci*ence, 28: 35.

Hraba T., and Dolezal J., (2009). A Mathematical Model and CD4 lymphocyte dynamics in HIV infection. *Emerging Infectious Diseases*, 2(4): 299 – 304.

Isrealachvili J., (1974). Van der Waals Forces in Biological Systems. *Quarterly, Reviews of Biophysics,* 6: 341 – 387.

Israelachivili, J.N., (1992). Adhesion forces between Surfaces in Liquids and Condensable Vapours. *Surface Science Reports*, 14(3): 109 – 159.

Jain M. K., Iyenger S. R. K. and Jain R. K. (2010). Numerical Methods for Scientific and Engineering Computation. 5th Ed., 348 – 352.

Jayaraman P., Sada.Ovalle I, Beladi S, Anderson A. C., Dardalhon V., Hotta C., Kuchroo V. K., and Behar S. M., (2010). Tim3 binding to galectin-9 Stimulates Antimicrobial Immunity. *Journal of Experimental Medicine*, 207(11): 2343 – 2354.

Jean J. T., Samuel B., and Oukouomi N. C. S., (2012). Mathematical analysis of two –patch model of tuberculosis disease with Staged progressions. *Applied mathematical modeling,* 36: 5792 – 5807.

Junker A. K., Ochs H. D., Clark E. A., (1986,). Transient immune deficiency in patients with acute Epstein-Barr virus (EBV) infection. *Clin Immunol Immunopathol,* 40(3): 436 – 446.

Kaeible D. H., (1970). Dispersion-Polar Surface Tension Properties of Organic Solids. *J. of Adhesion,* 2(1): 66 – 81.

Krupp, H., (1967). Particle Adhesion: theory and Experiment. *Advances in Colloid Interface Science,* 1: 111 – 239.

Kumar D., Rao K. V. S., (2011). Regulation between Survival persistence. *Microbes infect*., 13: 121 – 133.

Kua V. H. S., and Wilcox W. R., (1973). Interactions: Their Role in various Speration Methods; Speration and Purification. *Separ. Sci*, 8: 375.

Kwame A. G., Amoakoh G., William O., (2013). Mathematical Modeling of the Epidemiology of Tuberculosis in the Ashanti region of Ghana. *British Journal of Mathematics & Computer Science,* 4(3): 375 – 393.

Langbein, D., (1969): Van der Waals Attraction Between Macroscopic Bodies. *Journal of Adhesion,* 1: 237.

Lawn S. D., Butera S. T., and Shinnick T. M., (2002). Tuberculosis unleashed: the impact of human immunodeficiency virus infection on the host granulomatous response to mycobacterium tuberculosis. *Microbes infect.,* 4: 635 – 646.

Lifshitz E. M., (1961). The Theory of Molecular Attractive Forces between Solids. *Advanced Physics.* 10: 165 – 209.

Lionetti F. J., Hunt S. M., Gore J. M., and Curby W. A., (1975). Cryopreservation of human granulocytes in liquid. *Cryobiology,* 12: 181.

London F., (1930). Van der Waals Forces. *Physics,* 63: 245.

Lonnroth K., Jaramillo E., Williams B. G. (2009). Drivers of tuberculosis epidemics: the role of risk factors and social determinants. *Soc. Sci. med.,* 68: 2240 – 2246.

Lyman D. J., Muir W. M., Lee I. J., (1965). The Effect of Chemical Structure and Surface Properties of Polymers on the Coagulation of Blood: Surface Free Energy Effects. *Trans. Amer. Soc. Artif. Intern. Organs,* 11: 301.

Maartens G., Wilkinson R. J., (2007). Tuberculosis. *Lancert,* 370: 2030 – 2043.

Marchal G., (1993). The Immune response in Tuberculosis. *Annales de l'institut Pasteur,* 4: 216 – 224.

Mclachlan, A. D. (1963). Advances in Chemical Physics, Intermolecular Forces. *Proc. Roy. Soc. London, A271*: 387.

Miller R. G., (1977). In: "The lymphocytes", *J. J. Marchalonis, ed. , part 1, Marcel Dekker, New York:* 69.

Murray M. (2002). Determinants of Cluster distribution in the molecular epidemiology of Tuberculosis. *Proceedings of the National Academy of Sciences of the United States of America,* 99(3): 1538 – 1543.

Murray C. J. L., and Salomon J. A., (1998a). modeling the impact of global tuberculosis control strategies. *Proceedings of the National Academey of Science of the United states of America*, 95(23): 13881 – 13886.

Murray C. J. L., and Salomon J. A., (1998b). Expanding the WHO tuberculosis control strategy: rethinking the role of active case-finding. *Int. J. Tuberc. Lung Dis.,* 2(9): s9 – s15.

Naresh R., Sharma D., and Tripathi A., (2009). Modeling the effect of Tuberculosis on the Spread of HIV Infection in a Population with Density-dependent birth and death Rate. *Mathematical and Computer Modelling,* 50(7-8): 1154 – 1166.

Neumann A.W., Hope C. J., Ward C. A., Herbert M. A., Dunn G. W., and Zingg W., (1975). The Role of Surface Thermodynamics in Thromboresistance of Biomaterials. *J. Biomed. Mater. Res.*,9: 127 – 142.

Neumann A. W., van Oss C. J., Omenyi S. N., Absolom D. R., Viser J., (1983). Measurement of Surface Tensions of Blood Cells and Proteins. Annals New York Academy of Sciences 276 – 298.

Neumann A. W., Good R. J., Hope C. J. and Sejpal M., (1974). An Equation-of-State Approach to Determine Surface Tensions of Low-Energy Solids from Contact Angels. *J. Colloid and Interface Sci*, 49: 291 – 304.

Neumann, A. W., Gillman, C. F., van Oss C.J., (1974). Phagocytosis and Surface free Energies. *Journal of Electroanalytical Chemistry Interfacial Electrochemistry*, 49(3): 393 – 400.

Ninham, B.W., and Parsegian, V.A., (1970). Van der Waals forces across triple-layer films. *Journal of Chemistry and Physics*, 52: 4578.

Nir, S., Robert R., Weiss L., (1972). On the applicability of Certain approximations of the Lifshitz theory to thin films. *Journal of Theoretical Biology*, 34: 135.

Nishijima M. K., Takezawa J., Hosotsubo K. K., (1986). Serial changes in cellular immunity of septic patients with multiple organ-system failure. *Critical Care Medicine*, 14(2): 87 – 91.

Nunes J. E. S., Ducati R. G., Breda A., Rosado L. A., De Souza B. M., Palma M. S., Santos D. S., Basso L. A., (2011). Molecular, kinetic Thermodynamic and Structural analysis of mycobacterium tuberculosis hisD-encoded metal-dependent dimeric histidinol dehydrogenase (EC1.1.1.23). *Archives Biochemistry and Biophysics*, 512: 143 – 153.

Nunn P., Willianms B. et al., (2005). Tuberculosis control in the era of HIV. *Nat. Rev. Immunology,* 5(10): 819 – 826.

Omenyi S. N., Smith R. P., and Neumann A. W., (1980). Determination of Solid/melt Interfacial Tensions and of Contact Angles of Small Particles from the Critical Velocity of Engulfing. *Journal of Colloid and Interface Science,* 75(1): 117 – 125.

Omenyi S. N., (1978). Attraction and Repulsion of particles by Solidification Fronts" PhD Dissertation, University of Toronto, Canada.

Omenyi S. N., Snyder, R. S., (1982). Enhanced Erythrocyte Suspension Layer Stability achieved by Surface Tension Lowering Additives. *J. Dispersion Science and Technology*, 3(3): 307 – 333.

Owens D. K., and Wendt R. C., (1969). Estimation of the Surface Free Energy of Polymers. *J. Appl. Polym. Sci.,* 13: 1741.

Ozoihu, E.M., (2014). Human Immunodefficiency Virus (HIV)-Blood Interactions: Contact Angle Approach, PhD. Dissertation, Nnamdi Azikiwe University, Awka, Nigeria.

Robinson, T.S., (1952). Optical Constants by Reflection. Proceedings of the Physical Society London 65(11): B910.

Safi H., Gormus B. J., Didier P. J., Blanchard J. L., Lakey D. L., (2003). Spectrum of manifestations of mycobacterium tuberculosis infection in primates infected with SIV. *AIDS Res. Hum. Retroviruses*, 19: 585 – 595.

Sandanger O., Ryan L., Bohnhorst J., Iversen A. C., Husebye H., (2009). IL- 10 enhances MD -2 and CD14 expression in monocytes and protein are increased and correlated in HIV – infected patients. *J. Immunol*, 182: 588 – 595.

Schulze, H.J., and Cichos, Chr., (1972). Die Gleichgwichtsdicke sehr dunner, wabriger Flussigkeitsfilme am Ladungsnullpunkt der Quarzoberflache. *Z. Phys. Chemie, Leipzig*, 251: 145 – 151.

Sematimba A., Mugisha J. Y. T., Luboobi L. S., (2005). Mathemical models for thedynamics of tuberculosis in Density-Dependent Populations: The case of Internally Displaced peoples' camps (IDPCs) in Uganda. *Academic journal article from journal of mathematics and statistics*, 1(3): 1 – 6.

Smith, K. (2007). Technological and Economic Dynamics of the World Wine Industry. *International Journal of Technology and Globalisation*, 3: 127 – 137.

Song B. J., Castillo-chavez C., Aparicio J. P., (2002). Tuberculosis models with fast and slow dynamics: the role of close and casual contacts. *Mathematical Biosciences*, 180: 187 – 205.

Sonnenberg P., Glynn J. R., Fielding K., Murry J., Godfrey-Fausselt P., Shearer S., (2005). How soon after infection with HIV does the Risk of Tuberculosis start to increase? A Retrospective Cohort study in South African Gold miners. *Journal of Infecious Diseases,* 191(2): 150 – 158.

Stjernstrom I., Magnusson K. E., Stendahi O. and Tagesson C., (1977). Reduction of Phagocytosis, Surface hydrophobicity and change of Salmonella Typhimurium 395 MR10 by reaction with secretory IgA (SlgA). *Infect.Immun,* 18: 261.

Sumida S., (1973). "Transfusion of Blood Preserved by Freezing". *Lippincolt, Philadephia.* 92:10.

Terrell L. Hill, (2008). Statistical Thermodynamics. Dover Publications, New York (First South Asian Edition), 185.

Toossi Z., Mayanja-Kizza H., Hirsch C. S., Edmonds K. L., Spahlinger T., Hom D. L., Aung H., Mugyenyi P., Elliner J. J., and Whalen C. W. (2001). Impact of Tuberculosis (TB) on HIV-1 activity in dually Infected Patents. Clin. Exp. Immunol. 14: 233 – 238.

Udayanandan K. m., Sathishand R. K., Sethumadhavan P. (2009). Micro-canonical Ensembles – Some case Studies. Physics Education, South Asian Publishers, 207.

van der Esker M. W..J., and Vrij A., (1976). Incompatibility of Polymer Solutions. *J. Polymer Sc.i,*14: 1943.

van der Waals, J.D., (1873): Thesis, Leiden University Press, Leiden.

van Oss C. J., Good R. J., and Neumann A. W., (1972). The connection of interfacial free energies and surface potentials with Phagocytosis and cellular adhesiveness. *J. Electroanal. Chem.,* 37: 387.

van Oss C. J., Absolom D. R., Andres G. A., Albini B. and Neumann A. W. (1979). Surface Thermodynamics of Bacterial Adhension. *Trans. Am. Soc. Artif. Intern. Organs.*25: 152 – 158.

van Oss C. J., Absolom D. R., and Neuman A. W., (1979). Kinetics of Adhesion of the Oral Bacterium Strephococcus. *Separ, Sci. and Technol,* 14(4): 246.

van Oss C. J., Chaudhury M. K and Good R. J., (1988). Monopolar Surfaces. *Advance Colloidal Interface sci., Chem. Rev.,* 88: 927 – 94.

van Oss C. J., Absolom D. R., Grossberg A. L. and Neuman A.W. (1972). Repulsive van der Waals Forces I. Complete Dissociation of Antigen-Antibody Complexes by means of Negative van der Waals Forces. Immunol. Commun, 1: 627, 6.

van Oss C. J., Gillman C. F., and Neuman A. W., (1975). Phagocytic Engulfment and Cell Adhesiveness as Surface Phenomena" *Marcel Dekker Ed., New York.*1975, Chapter 3.

van Oss C. J. and Grossberg A. L., (1979) "Principles of Immunology", *N. R. Rose, F. Milgram and C. J. Van Oss, (Eds), Macmillan, New York,* 1979, Chaper 5.

Velayati A. A., Farnia P., Masjedi M. R., Ibrahim T. A., Tabarsi P., Haroun R. Z., Kuan H. O., Ghanavi J., Farnia P., Varahram M., (2009). Totally drug-resistant tuberculosis strains: evidence of adaptation at the cellular level. *Eur. Resp. J.*, 34: 1202 – 1203.

Velayati A. A., Masjedi M. R., Fernia P., Tabarsi P., Ghanavi J., Ziazarifi A. H., Hoffner S. E., (2009). Emergence of new forms of Totally drug-resistant tuberculosis or Totally drug-resistant Strains in Iran. *Chest.,* 136: 420 – 425.

Visser, J., (1981). Advances in Interface Science, *Elsevier Scientific Publishing Company, Amsterdam,* 15: 157–169.

Visser, J., (1975): in: Surface and Colloid Science, *Editor, E. Matijevic, Wiley, Interscience, New York,* 8: 3.

Vroman, L., and Adams A. L., (1967). Possible Involvement of Fibrinogen and Protcolysis in surface activation. A study with the recording ellipsometer. *Thromb. Diath. Haemorrh.,* 18: 510.

Whalen C. C., Nsubuga P., Okwera A., Johnson J. L., Hom D. L., Michael N. L., Mugerwa R. D., Ellner J. J., (2000). Impact of pulmonary tuberculosis on survival of HIV-infected adults: a prospective epidemiologic study in Uganda. *AIDS,* 14(9): 1219 – 1228.

White P. J., and Garnett G. P., (2010). Mathematical modeling of the epidemiology of tuberculosis. *Adv. Exp. Med. Biol.,* 673: 127 – 140.

Williams B. G., Granich R., Chauhan L. S., Dharmshaktu N. S., Dye C. (2005). The impact of HIV/AIDS on the control of tuberculosis in India. *Proceedings of the National Academy of Sciences of the United states of America,* 102(27): 9619 -9624.

Williams R. C., Koster F. T., Kilpatrick K. A., (1983). Alterations in lymphocyte cell surface markers in various human infections. *Am. J. Med.,* 75: 807 – 816.

World Health Organization (WHO), (2005). Tuberculosis, WHO Information: Fact Sheets. http://www.who.int/mediacentre/factsheets/fs104/en/index. html, Retrieved 24-11-13.

World Health Organization (WHO), (2012). Global tuberculosis report 2012. Geneva, Switzerland. http://www.who.int/tb/publications/global_report/, Retrieved 24-11-13.

World Health Organization (WHO), (2009). Global tuberculosis Control: Epidemiology, strategy, financing, WHO report 2009, Geneva, Switzerland, WHO/HTM/TB/2009.411.

World Health Organization (WHO), (2010). Global tuberculosis control: WHO report 2010, Geneva, Switzerland, WHO/HTM/TB/2010.7.

World Health Organization (WHO), (2011). Global HIV/AIDS Response Epidemic update and Health sector progress towards Universal Access: http://whqlibdoc.who.int/publications/2011/9789241502986-eng.pdf.

World Health Organization (WHO), (2012). Tuberculosis key facts: http://www.who.int/mediacentre/factsheets/fs104/en/.

Wu. S., (1982). Polymer Interface and Adhesion, Marcel Dekker, New York,

Zisman, W. A., (1964). Advances in Chemistry series. *Amer. Chem. Soc.*, Washington D.C., 43: 1.